

2

AD-A224 584

IDA DOCUMENT D-487

PHYSICS OF HIGH-TEMPERATURE AIR  
PART I, BASICS

DTIC  
SELECTE  
AUG 02 1990  
S D CS

Ernest Bauer

May 1990

DISTRIBUTION STATEMENT A  
Approved for public release  
Distribution Unlimited



INSTITUTE FOR DEFENSE ANALYSES  
1801 N. Beauregard Street, Alexandria, Virginia 22311-1772

## DEFINITIONS

IDA publishes the following documents to report the results of its work.

### Reports

Reports are the most authoritative and most carefully considered products IDA publishes. They normally embody results of major projects which (a) have a direct bearing on decisions affecting major programs, (b) address issues of significant concern to the Executive Branch, the Congress and/or the public, or (c) address issues that have significant economic implications. IDA Reports are reviewed by outside panels of experts to ensure their high quality and relevance to the problems studied, and they are released by the President of IDA.

### Group Reports

Group Reports record the findings and results of IDA established working groups and panels composed of senior individuals addressing major issues which otherwise would be the subject of an IDA Report. IDA Group Reports are reviewed by the senior individuals responsible for the project and others as selected by IDA to ensure their high quality and relevance to the problems studied, and are released by the President of IDA.

### Papers

Papers, also authoritative and carefully considered products of IDA, address studies that are narrower in scope than those covered in Reports. IDA Papers are reviewed to ensure that they meet the high standards expected of refereed papers in professional journals or formal Agency reports.

### Documents

IDA Documents are used for the convenience of the sponsors or the analysts (a) to record substantive work done in quick reaction studies, (b) to record the proceedings of conferences and meetings, (c) to make available preliminary and tentative results of analyses, (d) to record data developed in the course of an investigation, or (e) to forward information that is essentially unanalyzed and unevaluated. The review of IDA Documents is suited to their content and intended use.

The work reported in this publication was conducted under IDA's Independent Research Program. Its publication does not imply endorsement by the Department of Defense, or any other Government agency, nor should the contents be construed as reflecting the official position of any Government agency.

This Document has been reviewed by IDA to assure that it meets the high standards of thoroughness, objectivity, and appropriate analytical methodology and that the results, conclusions and recommendations are properly supported by the material presented.

Approved for public release; distribution unlimited

# REPORT DOCUMENTATION PAGE

Form Approved  
OMB No. 0704-0188

Public Reporting burden for this collection of information is estimated to average 1 hour per response, including the time for reviewing instructions, searching existing data sources, gathering and maintaining the data needed, and completing and reviewing the collection of information. Send comments regarding this burden estimate or any other aspect of this collection of information, including suggestions for reducing this burden, to Washington Headquarters Services, Directorate for Information Operations and Reports, 1215 Jefferson Davis Highway, Suite 1204, Arlington, VA 22202-4302, and to the Office of Management and Budget, Paperwork Reduction Project (0704-0188), Washington, DC 20503.

1. AGENCY USE ONLY (Leave blank)		2. REPORT DATE May 1990	3. REPORT TYPE AND DATES COVERED Final--October 1987 to December 1988	
4. TITLE AND SUBTITLE Physics of High Temperature Air: Part I, Basics			5. FUNDING NUMBERS IDA Independent Research Program	
6. AUTHOR(S) Ernest Bauer				
7. PERFORMING ORGANIZATION NAME(S) AND ADDRESS(ES) Institute for Defense Analyses 1801 N. Beauregard St. Alexandria, VA 22311-1772			8. PERFORMING ORGANIZATION REPORT NUMBER IDA Document D-487	
9. SPONSORING/MONITORING AGENCY NAME(S) AND ADDRESS(ES)			10. SPONSORING/MONITORING AGENCY REPORT NUMBER	
11. SUPPLEMENTARY NOTES				
12a. DISTRIBUTION/AVAILABILITY STATEMENT Approved for public release; distribution unlimited.			12b. DISTRIBUTION CODE	
13. ABSTRACT (Maximum 200 words) <p>This document provides an introduction for the non-specialist to the physics of dissociating and ionizing air in the temperature range from 1000-12,000 K. Topics addressed include the equilibrium composition and radiative properties of air under these conditions together with an indication of when and how the assumptions of equilibrium tend to break down. A preliminary discussion is given of applications to missile reentry, to nuclear fireballs, and to the physics of the upper atmosphere.</p>				
14. SUBJECT TERMS High-temperature air, Equilibrium composition, Air radiation, Dissociation, Ionization			15. NUMBER OF PAGES 118	
			16. PRICE CODE	
17. SECURITY CLASSIFICATION OF REPORT UNCLASSIFIED	18. SECURITY CLASSIFICATION OF THIS PAGE UNCLASSIFIED	19. SECURITY CLASSIFICATION OF ABSTRACT UNCLASSIFIED	20. LIMITATION OF ABSTRACT SAR	

IDA DOCUMENT D-487

PHYSICS OF HIGH-TEMPERATURE AIR  
PART I, BASICS

Ernest Bauer

May 1990

Accession For	
NTIS - CRA&I	<input checked="" type="checkbox"/>
ERIC - IAB	<input type="checkbox"/>
Unannounced	<input type="checkbox"/>
Justification	
By	
Distribution/	
Availability Codes	
Dist	Avail and/or special
A-1	



INSTITUTE FOR DEFENSE ANALYSES  
IDA Independent Research Program



## ACKNOWLEDGMENTS

Many people have helped with identifying the specific topics addressed and with critiquing the treatment. I particularly wish to acknowledge Parney Albright, Bohdan Balko, Ronald Finkler, Steven Kramer, Richard Loda, Robert Oliver, and William Jeffrey of IDA. I am also grateful to Forrest Gilmore of R&D Associates, Sol Penner of the University of California, San Diego, and John Zinn of Los Alamos National Laboratory. The thoughtful and detailed comments of all these people have improved the document substantially.

# CONTENTS

Acknowledgments .....	iii
Figures .....	vii
Tables .....	viii
EXECUTIVE SUMMARY .....	S-1
1. INTRODUCTION .....	1-1
2. COMPOSITION OF HIGH-TEMPERATURE AIR .....	2-1
2.1 Introduction .....	2-1
2.1.1 Basic Data for Air .....	2-1
2.1.2 On Thermodynamic Equilibrium .....	2-6
2.1.3 Outline of the Chapter .....	2-6
2.2 Equilibrium Dissociation and Ionization for a Single Species .....	2-8
2.2.1 Introduction .....	2-8
2.2.2 Dissociation of Molecular Oxygen .....	2-8
2.2.3 Ionization of Atomic Oxygen .....	2-10
2.3 Equilibrium Composition of (Dry) Air As Function of Temperature .....	2-11
2.4 Effects of Dissociation Energy on Thermodynamic Properties .....	2-13
2.5 Collisions and Non-Equilibrium Processes .....	2-20
2.6 Some Comments on Heat Transfer in High-Temperature Air .....	2-25
3. RADIATION FROM HIGH-TEMPERATURE AIR .....	3-1
3.1 Introduction .....	3-1
3.2 Blackbody Radiation .....	3-2
3.3 Equation of Radiative Transfer .....	3-8
3.3.1 Without Scattering .....	3-8
3.3.2 With Scattering .....	3-9
3.3.3 Opacities .....	3-11
1. Diffusion Approximation in an Optically Thick Medium .....	3-12
2. Emission Approximation in an Optically Thin Medium .....	3-12

3.4	Atomic Line Radiation: Transitions, f-Number and Absorption Cross Section, Line Shape, Curves of Growth .....	3-15
3.5	Molecular Band Radiation .....	3-23
3.6	Atomic Radiation in General: Free-Free, Free-Bound, Bound-Bound .....	3-30
3.7	Absorption Coefficient of High-Temperature Air .....	3-35
3.8	Radiation From High-Temperature Air .....	3-40
4.	SOME HEATING MECHANISMS .....	4-1
4.1	Introduction .....	4-1
4.2	Reentry Heating .....	4-2
4.3	Nuclear Fireball .....	4-7
4.4	Upper Atmosphere .....	4-12
5.	BIBLIOGRAPHY .....	5-1
Appendix A--	Electronic Structure of Some Air Atoms and Molecules .....	A-1
Appendix B--	Partition Function for the Dissociation of a Diatomic Molecule .....	B-1
Appendix C--	Einstein A- and B-Coefficients, f-Numbers and Band Strengths .....	C-1
Appendix D--	Excerpts from Physical Constants, USAF, 1985, and U.S. Standard Atmosphere, 1962 .....	D-1

## FIGURES

2-1.	Equilibrium Dissociation of Molecular Oxygen .....	2-9
2-2.	Thermal Equilibrium Ionization of Atomic Oxygen .....	2-12
2-3.	Equilibrium Composition of Dry Air as Function of Temperature and Density .....	2-14
2-4.	$\gamma'$ , Effective Specific Heat Ratio .....	2-21
3-1.	Spectral Radiance of a Blackbody as Function of Wavelength .....	3-4
3-2.	Spectral Radiance of a Blackbody as Function of Wave Number .....	3-5
3-3.	Typical Reflectance of Various Natural Surfaces .....	3-7
3-4.	Natural, Collision, and Doppler Line Widths versus Altitude (Calculations Done for Lines in the 4.3 $\mu\text{m}$ Band of $\text{CO}_2$ ) .....	3-20
3-5.	Curves of Growth of Spectral Lines for Combined Doppler and Lorentz Broadening .....	3-22
3-6.	$\text{O}_2$ Absorption Cross Section in the UV .....	3-31
3-7.	$\text{O}_3$ Absorption Cross Section .....	3-32
3-8.	Continuous and Discrete Levels in an Atomic Spectrum.....	3-34
3-9.	Absorption Coefficient of High-Temperature Air.....	3-37
3-10.	Energy Radiated From Hot Air .....	3-41
4-1.	Energy Transfer on Reentry .....	4-3
4-2.	Schematic Air Flow on a Reentry Vehicle .....	4-5
4-3.	keV X-Ray Absorption and Extinction Coefficients for Air.....	4-8
4-4.	Variation of Apparent Fireball Surface Temperature with Time in a 20-kt Explosion.....	4-11
4-5.	Penetration of Radiation into the Atmosphere .....	4-13

## TABLES

2-1.	Composition of Dry Air at 1 Atmosphere Pressure.....	2-2
2-2.	The Atmosphere to High Altitudes .....	2-3
2-3.	Some Properties of Principal Air Atoms and Molecules .....	2-5
2-4.	Mean Free Path and Collision Times as Function of Density .....	2-23
3-1.	Planck Mean Absorption Coefficient and Rosseland Mean Free Path for Air at Different Temperatures and Densities.....	3-14
3-2.	Transition Probabilities $A_{ul}$ , Life Times $\tau_u$ , and Absorption Oscillator Strengths $f_{lu}$ for Low-Lying Atomic States .....	3-18
3-3.	Some Characteristics of Important Molecular Band Systems of Air.....	3-26
3-4.	Continuous Contributors for the Absorption Coefficient of High-Temperature Air.....	3-36
4-1.	Energy Balance Behind a Normal Shock in Air.....	4-6
4-2.	Optical Thickness for keV X-rays in the Atmosphere .....	4-9
4-3.	Fraction of Solar Irradiance in Different Wavelength Intervals .....	4-14
4-4.	O <sub>2</sub> Dissociation in the Thermosphere: Actual and LTE.....	4-14
4-5.	Population Temperatures for Different Degrees of Freedom in the Upper Atmosphere .....	4-15

## EXECUTIVE SUMMARY

This document is a set of notes intended to help a new Ph.D. in physics or chemistry (or person of equivalent training) become familiar with the specialized literature of the applied fields of atmospheric nuclear weapons effects, missile reentry, upper atmospheric physics, or high-energy laser propagation through the atmosphere. The document is not a substitute for a course in high-temperature gas dynamics. It presents a simple overview of some key physical factors, and gives references both to relevant textbooks and to the "gray" literature specific to the field.

Part I consists of a general introduction (Chapter 1), a discussion of equilibrium air at temperatures to approximately 10,000 K (Chapter 2), a discussion of the radiation from high-temperature air (Chapter 3), and--as a bridge to Part II, to be published later, which will address some applications--Chapter 4, which gives a brief discussion of some specific heating mechanisms.

Chapter 2 points out that air starts to dissociate at a temperature of 2000 K to 4000 K (depending on the pressure), even though the mean thermal energy of the molecules at these temperatures is much less than the dissociation energy. The emphasis in the discussion is on equilibrium processes, with an indication of where detailed considerations of non-equilibrium such as chemical kinetics become important. While many current applications deal with non-equilibrium situations, yet those generally start from equilibrium which provides a simple and rigorous limit. It is pointed out that at the higher temperatures  $T$ , radiative energy transfer (which goes as  $T^4$  or faster) tends to predominate over convective heat transfer (which goes as  $\text{grad } T$ ). Chapter 3 treats radiative problems, addressing both radiative transfer and quantitative molecular spectroscopy, and finishes by comparing radiative heat transfer by dissociating air and by other molecules with that from a blackbody in the same temperature range. Chapter 4 addresses the thermal excitation of air by shock and other aerodynamic heating (in spacecraft reentry), by X-ray heating (in the nuclear fireball), and by the absorption of solar ultraviolet radiation (in the earth's upper atmosphere).

Part II, Applications, will be prepared later. It will expand on Chapter 4 with more extensive discussions of reentry physics, atmospheric nuclear weapons effects, and electromagnetic wave propagation within the atmosphere.

## 1. INTRODUCTION

A variety of technical applications require an understanding of the physics of high-temperature air, where "high temperature" is taken to mean 1000 K to 10,000 K . Some applications are to missile or space vehicle entry into the earth's atmosphere, and to nuclear explosions within the atmosphere which lead to the formation of a "fireball." Related applications deal with rocket propulsion and with the propagation of high-energy laser beams in the atmosphere.

When air is heated to 2000 K to 4000 K (depending on pressure) it begins to dissociate; by 10,000 K it is not only fully dissociated but at least singly ionized. To break all these chemical bonds requires a great deal of energy. Thus the physical and chemical properties of high-temperature air are quite different from those of room temperature air because of the presence of reactive molecules (such as oxides of nitrogen), atoms, and (atomic and molecular) ions.

The general training of a Ph.D. physicist or chemist typically does not include the characteristics of air in the 1000 K to 10,000 K temperature range. These properties were elucidated largely between 1950 and 1965, frequently in an applied and often classified context in the "gray literature" of technical reports. Someone who begins working in the field of reentry physics now, in 1989, may be referred to computer codes which were generated originally as much as 25 years ago, have been modified extensively and are probably documented and referenced inadequately. There have been very few atmospheric nuclear tests since 1962, and the literature consists of successively more sophisticated numerical analyses of these very limited test data. In either case, the physical basis of current numerical models is often not readily accessible to the new user.

In much of the current literature, the chemical composition of the relevant gases is based on the solution of systems of coupled chemical reactions rather than on the assumption of Local Thermodynamic Equilibrium (LTE). Such a non-equilibrium description can be more accurate than LTE for times so short that equilibrium is not attained, provided the reaction set used is sufficiently large, appropriate, and correct, which is a non-trivial condition. However, as an introduction to the field it is convenient to

discuss the physics largely in terms of an LTE model which is intuitively simple and provides a starting point for the more detailed non-LTE models.

This document is the first part of a two-part series. Discussed here are the equilibrium composition and radiative properties of high-temperature air (respectively, in Chapters 2 and 3), indicating where non-equilibrium (kinetic) considerations become important. Chapter 4 is a bridge to a planned Part II of this document which will be published later. It presents some examples of how the heated air discussed here can actually be produced: by aerodynamic heating in reentry, where the kinetic energy of hypersonic motion is transformed into random molecular motion or heat, by the absorption of X-rays in the atmosphere that produces nuclear fireballs, or by the absorption of solar ultraviolet radiation in the earth's upper atmosphere, which produces the ionosphere/thermosphere.

Part II will deal in more detail with missile reentry (Chapter 5), with nuclear phenomenology (Chapter 6), and with selected topics in the propagation of visible and infrared radiation from high-temperature sources through the atmosphere (Chapter 7).

This document is a set of notes intended to help a new Ph.D. in physics or chemistry (or person of equivalent training) become familiar with the specialized literature of an applied field such as atmospheric nuclear weapons effects, missile reentry, upper atmospheric physics, or high-energy laser propagation through the atmosphere. It presents a simple overview of some key physical factors, and gives references both to relevant textbooks and to the "gray" literature specific to the field.

While this document has been read critically by a number of people--see the acknowledgments--obscurities and inaccuracies probably remain. The reader should be aware of these limitations in using the material, and is invited to give comments and criticisms to the author to help make the material more useful.

## 2. COMPOSITION OF HIGH-TEMPERATURE AIR

### 2.1 INTRODUCTION

#### 2.1.1 Basic Data for Air

When air at normal pressures (say,  $10^{-6}$  to 1 atmospheres) is heated from room temperature to perhaps 10,000 K, most of the energy absorbed goes into dissociating oxygen molecules rather than into increasing the kinetic energy of the  $O_2$  and  $N_2$  molecules.<sup>1</sup> This fact is a key motivation in preparing the present set of notes, because the physics in the regime discussed involves the excitation of various internal atomic and molecular degrees of freedom, in particular molecular dissociation.

Note that for  $T = 10,000$  K,  $kT/e = 0.86$  eV (where  $k$  = Boltzmann's constant and  $e$  = charge of the electron). The dissociation energy of the  $O_2$  molecule is  $D = 5.11$  eV which corresponds to a characteristic temperature  $\Theta_D = eD/k = 59300$  K, but at normal pressures  $O_2$  is dissociated already at temperatures of 4000-5000 K, in essence because the phase space volume of  $O + O$  is much greater than that of  $O_2$ .<sup>2</sup>

Table 2-1 lists the composition of dry air at sea level. Notice that the chemically and radiatively reactive and therefore most interesting species-- $CO_2$ ,  $CO$ ,  $O_3$ ,  $NO$ , and  $NO_2$  (also  $CH_4$ ,  $NH_3$ , and  $SO_2$  which are not discussed here)--are present in small and typically quite variable concentrations.

Table 2-2 gives some properties of air up to 120 km altitude, where most molecules other than  $N_2$  are significantly dissociated.<sup>3</sup> This table lists the temperature, density, gas-kinetic mean free path (MFP) as well as the mean mixing ratios for the energetically, radiatively, and chemically important minor species  $H_2O$  and  $O_3$ . Note the following:

---

<sup>1</sup> See Section 4.2, in particular Table 4-1.

<sup>2</sup> See the discussion of Section 2.2.2.

<sup>3</sup> Note that this is due to solar photodissociation, not to thermal dissociation. Section 4.4 gives a brief discussion.

**Table 2-1. Composition of Dry Air at 1 Atmosphere Pressure**  
 (From U.S. Standard Atmosphere 1976, pp. 3, 33, 38, 44)

Molecule	Molecular Weight	Volume Fraction
N <sub>2</sub>	28	0.781
O <sub>2</sub>	32	0.209
Ar	39.9	0.0093
CO <sub>2</sub>	44	0.00032 (increasing somewhat after 1980)
Ne	20.2	0.000018
He	4.0	0.0000052
Kr	83.8	0.0000011
CH <sub>4</sub>	16.0	1500 × 10 <sup>-9</sup>
H <sub>2</sub>	2.02	500 × 10 <sup>-9</sup>
CO	28	190 × 10 <sup>-9</sup>
O <sub>3</sub>	48	40 × 10 <sup>-9</sup> (highly variable--see p. 39, op. cit.)
NH <sub>3</sub>	17	4 × 10 <sup>-9</sup>
SO <sub>2</sub>	64	1 × 10 <sup>-9</sup>
NO <sub>2</sub>	46	1 × 10 <sup>-9</sup>
NO	30	0.5 × 10 <sup>-9</sup>

Table 2-2. The Atmosphere to High Altitudes

Altitude (km)	Temperature (K)	Density (kg/m <sup>3</sup> )	MFP (m)	H <sub>2</sub> O (ppmV)	O <sub>3</sub> (ppmV)	Comments
120	360	2.22E-8	3.23	0.20	0.0005	O <sub>2</sub> dissoci. (A)
110	240	9.71E-8	0.815	0.28	0.05	O <sub>2</sub> dissoci. (A)
100	195	5.6E-7	0.163	0.40	0.4	
90	187	3.42E-6	0.0256	0.85	0.7	
80	199	1.85E-5	4.07E-3	2.1	0.3	T min. (B)
70	220	8.28E-5	9.28E-4	3.5	0.3	
60	247	3.1E-4	5.52E-4	4.8	1.1	
50	271	1.03E-3	7.91E-5	5.2	3.1	T max. (C)
40	250	4.00E-3	2.03E-5	5.0	7.3	
30	227	0.0184	4.41E-6	4.7	6.6	
20	217	0.0889	9.14E-7	3.9	2.6	Low H <sub>2</sub> O (D)
10	223	0.414	1.96E-7	70 (E)	0.13	T min. (F)
0	288	1.225	6.63E-8	7800 (E)	0.027	

Notes:

- ppmV = parts per million by volume
  - Temperature, density, mean free path (MFP) from USSA-62--see USAF, 1965, p. 2-19.
  - H<sub>2</sub>O, O<sub>3</sub> from AFGL atmospheric profiles--see Anderson et al., 1986.
- (A) O<sub>2</sub> begins to dissociate above ~ 80 km. By 110-120 km, the number density of atomic O equals that of O<sub>2</sub>. Ozone, water vapor, and carbon dioxide all dissociate at somewhat lower altitudes.
- (B) Temperature minimum (mesopause) near 85 km.
- (C) Temperature maximum (stratopause) near 50 km.
- (D) The atmosphere is very dry above the tropopause (~ 11 km).
- (E) The troposphere (below ~ 11 km) is quite moist, with a highly variable humidity.
- (F) Temperature minimum (tropopause) near 11 km at mid-latitudes.

- The mean free path [defined in Section 2.5--see Eq. (2.13)] is  $7 \times 10^{-6}$  cm = 700 Å at sea level, but 16 cm at 100 km altitude. The MFP is proportional to the inverse of the number density, and normal (~ 1 m ) reentry vehicles will begin to interact with the atmosphere at altitudes below 110 to 100 km.
- The lower atmosphere (troposphere, below the temperature minimum of tropopause near 11 km at mid-latitudes) is quite moist, with highly variable humidity. The minimum temperature of ~ 217 K at the tropopause provides a "cold trap" which reduces the mixing ratio above the tropopause.<sup>4</sup>
- The ozone maximum occurs in the stratosphere as O<sub>2</sub> is photodissociated at higher altitudes while one of the O-atoms produced in this way bonds to another O<sub>2</sub> molecule to produce ozone, which is then photodissociated and reformed repeatedly.

Table 2-3 lists dissociation and ionization potentials and some other information for important air molecules and atoms. This basic information is of importance in the present context. Note in particular:

- The N<sub>2</sub> molecule has a significantly higher dissociation energy (9.76 eV) than any of the other molecules, which explains the persistence of this chemical species.
- The O<sub>2</sub> molecule has the lowest ionization potential of any of the significant species, which explains why this is often the predominant positive ion.<sup>5</sup>
- Vibration frequencies are normally in the range 1000-2000 cm<sup>-1</sup>, which is why the molecular vibration spectra occur in the IR, as the corresponding wavelengths are 10- 5µm.
- Molecular rotation constants B<sub>e</sub> are normally 0.5-2 cm<sup>-1</sup> except for hydrogen-containing species (H<sub>2</sub>O) which have a much lower rotational constant (and larger vibrational frequencies ω<sub>e</sub>).

Some information about the quantum mechanical structure of atoms and air molecules is listed in Appendix A. For more detail, refer to the bibliography.

---

<sup>4</sup> Some numbers are in order. The saturated water vapor pressure over ice at 217 K is 0.018 mb which corresponds to a maximum mixing ratio at 11 km of 80 ppmV. By contrast, the saturated water vapor pressure over water at 288 K is 17 mb which gives a maximum sea level mixing ratio of 17,000 ppmV (cf. Smithsonian Met. Tables, 1949, p. 234 f).

<sup>5</sup> NO and NO<sub>2</sub> have lower ionization potentials, but these molecules are typically present in relatively low concentration.

Table 2-3. Some Properties of Principal Air Atoms and Molecules

Species	D	I	$\omega_e$	$B_e$
O <sub>2</sub> (X <sup>3</sup> Σ <sub>g</sub> <sup>-</sup> )	5.116	12.07	1580	1.446
N <sub>2</sub> (X <sup>1</sup> Σ <sub>g</sub> <sup>+</sup> )	9.76	15.58	2359	1.998
NO (X <sup>2</sup> Π <sub>r</sub> )	6.497	9.26	1904	1.672
CO <sub>2</sub> (X <sup>1</sup> Σ <sub>g</sub> <sup>+</sup> )	5.45 (O-CO)	13.8	1388,667,2349	0.39
O <sub>3</sub> (X <sup>1</sup> A <sub>1</sub> )	1.04 (O-O <sub>2</sub> )	12.5	1103,701,1042	3.55,0.445,0.39
NO <sub>2</sub> (X <sup>2</sup> A <sub>1</sub> )	3.11 (O-NO) 4.50 (N-O <sub>2</sub> )	9.8	1320,750,1618	8.0,0.43,0.41
H <sub>2</sub> O (X <sup>1</sup> A <sub>1</sub> )	5.12 (H-OH)	12.6	3657,1595,3756	27.9,14.5,9.29
O ( <sup>3</sup> P)		13.62		
N ( <sup>4</sup> S)		14.53		
Ar ( <sup>1</sup> S)		15.76		

Notes:

D (eV) = dissociation energy.

I (eV) = ionization potential

$\omega_e$  (cm<sup>-1</sup>) = vibrational frequency.

$B_e$  (cm<sup>-1</sup>) = rotational constant.

For notation on electronic states see Appendix A.

### 2.1.2 On Thermodynamic Equilibrium

Air is made up of a number of chemically reacting species, and thus its composition under given conditions is determined by the detailed balance of different chemical reaction processes. For a complex system, a large number of reactions may have to be considered. While the necessary computations can, in general, be carried out, given present-day computer power, one is sometimes uncertain whether all important reactions have been included, and whether their rate constants are represented correctly.

If we ask for the state of a gas after a sufficiently long time, so that the detailed collisional and radiative energy transfer processes have had an opportunity to establish a balance, then many properties of the gas are characterized simply as functions of temperature and pressure, or of temperature and density, independent of details of reaction mechanisms and rate constants. This is the very useful concept of *Thermodynamic Equilibrium*, which is a very useful limit for high-temperature air in the applications considered here (reentry and nuclear fireballs), and it is a good starting point for more complicated applications.

Even if the limit of thermodynamic equilibrium does not hold universally, it may still apply for some specific processes, such as the excitation of rotational levels of a given molecule or the dissociation of one or another molecule, and thus we can use the concept of *Quasi-Equilibrium* for the particular species to which it applies.

However, if we ask for the changing properties of a medium at times so early that thermodynamic equilibrium has not yet been achieved, it is necessary to consider the details of the *Kinetic Regime* (involving collisional and radiative processes) that underlies the state of the particular medium. While it may be necessary to go to this limit in an actual application, this will not be discussed here, since for our purposes it is better to begin with the simpler case of (near) equilibrium.

### 2.1.3 Outline of the Chapter

In Section 2.2 we discuss the equilibrium dissociation of  $O_2$  and the equilibrium ionization of atomic oxygen, whose ionization potential is 13.62 eV. It is largely ionized by 12,000 K to 15,000 K where  $kT = 1 - 1.3$  eV. This analysis demonstrates how the degrees of dissociation (and ionization) vary with the dissociation (and ionization) energy, temperature, and pressure or density. Because only a single chemical process is considered, the analysis is simple. In Section 2.3 some results are presented on the

equilibrium composition of air at elevated temperatures obtained by minimizing the (Helmholtz) free energy numerically. The basic results which are still in general use are more than 20 years old--newer values of thermodynamic input parameters provide slight improvements<sup>6</sup> which may be important for particular applications. Because the dissociation energy is so important in the regime being considered here, Section 2.4 discusses some of its effects on thermodynamic properties.

The discussion of Sections 2.2 through 2.4 considers thermodynamic equilibrium, but this is not uniformly applicable for chemically and radiatively important species. The concentration of water vapor--while small--is highly variable, and the important species NO is metastable: it is formed in amounts of several percent at temperatures above 2000 K, and at lower temperatures its chemical disappearance rate is so slow that it tends to remain without decomposing ("freezes-in") as the air cools.<sup>7</sup> Thus, Section 2.5 treats some non-equilibrium processes, particularly:

- When kinetics are important (low pressure, uncommon species, short time).
- Some peculiarities of the NO molecule, which is an important radiating species, has a low ionization potential, and is chemically more reactive than N<sub>2</sub> or O<sub>2</sub>.
- Some qualitative factors on radiating species.

Radiative heat transfer tends to dominate over convective heat transfer for gases at very high temperatures, and thus Section 2.6, which sketches some heat transfer issues of importance in high-temperature gases, serves as an introduction to the analysis of radiative processes in Chapter 3.

---

<sup>6</sup> The basic work on the thermodynamic properties of air species was done in the 1950s and 1960s; for more recent work, see, e.g., Moss and Scott, 1985.

<sup>7</sup> The term "freeze-in" is used in the specialized literature of this field to indicate that, as the temperature of a gas parcel falls, its chemical composition no longer follows thermodynamic equilibrium, but rather some high-temperature species (such as NO, O, or OH) may survive for a relatively long time at lower temperatures because the decomposition processes for these high-temperature species may become very slow. See, e.g., Zeldovich and Raizer, 1967, p. 564f.

## 2.2 EQUILIBRIUM DISSOCIATION AND IONIZATION FOR A SINGLE SPECIES

### 2.2.1 Introduction

Here we present the simple expressions and numerical results for the dissociation of the oxygen molecule and for the ionization of the oxygen atom. The results are idealized in that the excited states of O and O<sub>2</sub> listed in Appendix A are not considered. These expressions indicate in parametric form how the dissociation and ionization depend on temperature and density (or pressure), as well as on the effective dissociation or ionization energy. They show that at reasonable pressures (less than 1 atmosphere) the O<sub>2</sub> molecule of dissociation energy  $D = 5.1$  eV is already significantly dissociated at a temperature of 5000 K which is less than 10 percent of the effective dissociation temperature  $\Theta_D = D/k = 59,300$  K; also the O-atom of ionization potential  $I = 13.6$  eV is significantly ionized at a temperature of 12,000 K which is less than 10 percent of the effective ionization temperature  $\Theta_I = I/k = 158,000$  K.

### 2.2.2 Dissociation of Molecular Oxygen

Consider the diatomic molecule O<sub>2</sub> with dissociation energy  $D$  which is made up of two O atoms. At temperature  $T$ , if a total number  $N_{\text{tot}}$  of molecules occupying volume  $V$  are made up of  $N_{\text{O}_2}$  molecules and  $N_{\text{O}}$  O-atoms, then in local thermodynamic equilibrium the respective numbers  $N_{\text{O}}$  and  $N_{\text{O}_2}$  satisfy the following two equations:

$$N_{\text{O}_2} + N_{\text{O}}/2 = N_{\text{tot}} = \text{constant} \quad (2.1)$$

which is the equation of continuity, and the chemical equilibrium condition

$$N_{\text{O}}^2/N_{\text{O}_2} = K_{\text{diss}}(T) = [f_{\text{O}}^2(T)/f_{\text{O}_2}(T)] \exp(-D/kT) \quad (2.2)$$

where  $K_{\text{diss}}(T)$  is the equilibrium constant for the dissociation reaction



and the  $f$ 's are partition functions for the respective atoms and molecules which are proportional to volume  $V$ . The partition function  $f_J(T)$  for a system  $J$  having states  $i = 1, 2, \dots$  of energy  $E_i$  is defined as the sum over all states  $i$  of the factor  $\exp(-E_i/kT)$

$$f_J(T) = \sum_i \exp(-E_i/kT) \quad (2.4)$$

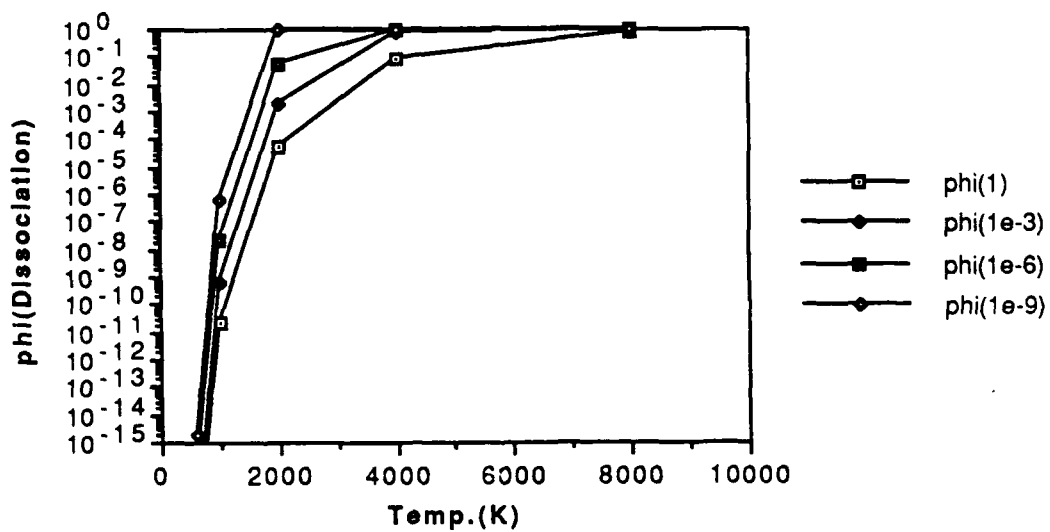


Figure 2-1. Thermal Equilibrium Dissociation of Molecular Oxygen  $O_2$ , as a Function of Temperature  $T$  and of Number Density Ratio  $n/n_0$ . The fractional dissociation  $\phi$  ( $\phi_{diss}$  of Eq.(2.5)) is expressed as a function of the number density ratio,  $n/n_0$ , where  $n_0 = 2.687 \times 10^{19} \text{ cm}^{-3}$ .

The partition function can be written to a good approximation as the product of translational, rotational, vibrational and electronic terms; in Appendix B we give the partition function for the dissociation of a diatomic molecule and the numerical parameters for the dissociation of the oxygen molecule.

In Fig. 2-1 we show the fractional dissociation of oxygen, defined as:

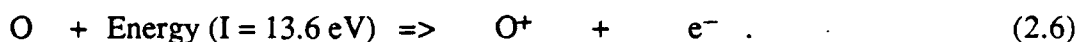
$$\phi_{\text{diss}} = N_{\text{O}}/[N_{\text{O}} + N_{\text{O}_2}] \quad (2.5)$$

for various values of the number density ratio  $n/n_0$ , where  $n_0 = 2.687 \times 10^{19}$  particles/cm<sup>3</sup>, which corresponds to a pressure of 1 atmosphere at a temperature of 273 K for an ideal gas.<sup>8</sup>

The dissociation energy  $D = 5.11$  eV can be expressed as an effective dissociation temperature  $\Theta_D = D/k = 59,300$  K. Note that the temperature dependence of the fractional dissociation  $\phi_{\text{diss}}$  is much stronger than the pressure (or specific volume or density) dependence, and that at  $n/n_0 > 10^{-3}$ , which correspond to a pressure of less than 0.015 atmospheres, the O<sub>2</sub> molecule is already significantly dissociated at 4000 K.<sup>9</sup>

### 2.2.3 Ionization of Atomic Oxygen

For definiteness, consider the single ionization of the oxygen atom:



We begin with  $N_{\text{tot}}$  atoms in a volume  $V$ ; if in equilibrium at temperature  $T$  there are  $N_A$  atoms,  $N_I$  ions and  $N_e$  electrons, the condition of charge neutrality requires that

$$N_I = N_e \quad (2.7)$$

and

$$N_A + N_I = N_{\text{tot}} \quad (2.8)$$

<sup>8</sup> It is appropriate to take  $V = 22.4$  liters/mole and  $N_{\text{tot}} = (n/n_0) N_{\text{Avogadro}}$ . This would give a pressure  $(T/273) (n/n_0) (1 - \phi_{\text{diss}})$  at a temperature  $T$ .

<sup>9</sup> The reason for this strong temperature as against density dependence can be seen from the form of the equation derived for  $N_{\text{O}}$  from Equations (2.1) and (2.2), which is  $N_{\text{O}}^2/(N_{\text{tot}} - N_{\text{O}}) = G V \exp(-\Theta_D/T)$ , where  $G$  has only a weak temperature dependence and no pressure dependence).

The equilibrium constant  $K_i(T)$  for the ionization reaction (2.6) is given by the relation

$$N_I \cdot N_e / N_A = K_i(T) = [f_I(T) f_e(T) / f_A(T)] \exp(-I/kT) , \quad (2.9)$$

where the  $f$ 's are partition functions. For our idealized system, Eq. (2.9) becomes

$$N_e^2 / N_A = V (2\pi k m' / h^2)^{3/2} T^{3/2} [2 g(I) / g(A)] \exp(-I/kT) . \quad (2.10)$$

Here  $m'$  is the reduced mass of the electron in presence of the ion; it is essentially equal to the electronic mass. The factor 2 associated with the statistical weights  $g$  comes from the two spin states of the free electron, and the statistical weights  $g(I)$  and  $g(A)$  are respectively  $g[O^+(^4S)] = 4$  and  $g[O(^3P)] = 3$ . The rest of the partition function comes from the phase space volume term associated with the translational partition function analogous to Eq. (B.1a) of Appendix B.

We define the degree of ionization as

$$\phi_{ion} = N_e / (N_A + N_I) , \quad (2.11)$$

where  $N_A$  and  $N_e$  are determined by solving Eqs. (2.8) and (2.10). The resulting values for  $\phi_{ion}$  as a function of temperature and density are plotted in Fig. 2-2 where again  $N_{tot} = (n/n_0) N_{Avogadro}$ . Note that once again the temperature dependence of  $\phi_{ion}$  is much stronger than the density dependence, and that at temperatures above  $\Theta_I/10 = 16,000$  K the atomic gas is largely ionized at pressures below 1 atmosphere.

### 2.3 EQUILIBRIUM COMPOSITION OF (DRY) AIR AS FUNCTION OF TEMPERATURE

Air is made up of  $O_2$  of dissociation energy 5.12 eV, which is largely dissociated at "normal" pressures by 4,000 K to 6,000 K, and of  $N_2$ , whose dissociation energy of  $D = 9.76$  eV corresponds to  $\Theta_D = eD/k = 113,400$  K, and which does not begin to dissociate at temperatures below  $\sim 8000$  K. Also, some NO is formed at temperatures above 2000 K, and the small fraction of  $CO_2$  and  $H_2O$  will dissociate in the range 1,000 K to 4,000 K. To calculate the composition of equilibrium air under conditions when the chemical composition changes, one either solves a set of equilibrium conditions analogous to Eq. (2.2) or (2.10) for each of the reactions considered, or equivalently minimizes the free energy at constant pressure (using the Gibbs free energy) or at constant density (using the Helmholtz free energy). This is done with a computer program, using as input the atomic composition and the thermodynamic parameters for the various species, some of which are given in Table 2-3. The following points should be noted:

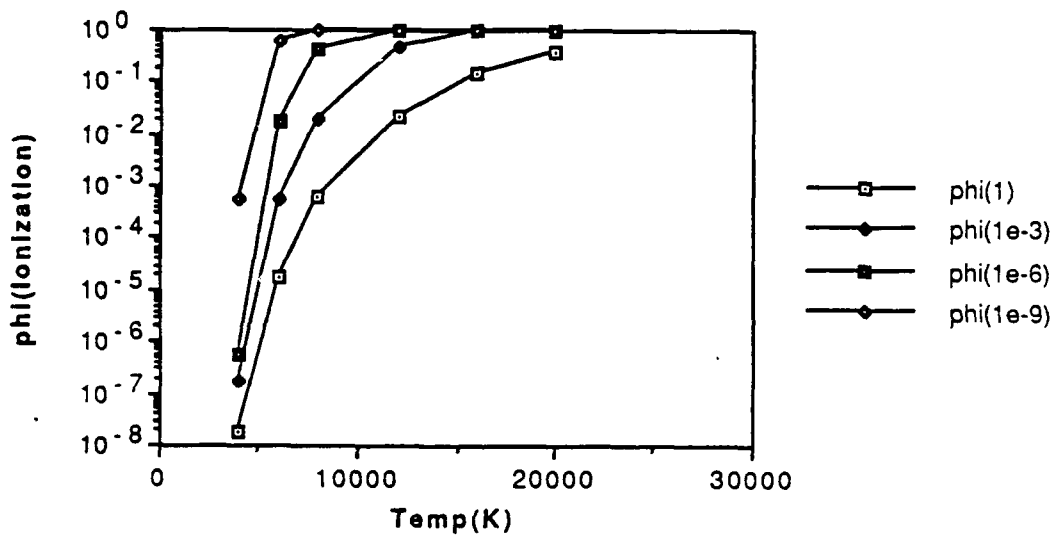


Figure 2-2. Thermal Equilibrium Ionization of Atomic Oxygen as a Function of Temperature  $T$  and of Number Density Ratio  $n/n_0$ . The fractional ionization of  $\phi_i$  ( $\phi_{ion}$  of Eq.(2.11)) is expressed as a function of the number density ratio,  $n/n_0$ , where  $n_0 = 2.687 \times 10^{19} \text{ cm}^{-3}$ .

1. Most calculations have been done for dry air because the atmospheric water vapor concentration is small and highly variable.
2. For a review of thermodynamic calculations in the 1950s and early 1960s, see Hochstim, 1964 (which is reprinted as an appendix to Hilsenrath and Klein, 1965).
3. The "classic" calculations of the early 1960s are still generally accepted, but see, e.g., Moss and Scott, 1985, for references to current work in this field.

Some representative results for the composition of high-temperature dry air (from Hilsenrath and Klein, 1965) are shown in Fig. 2-3. These calculations are done at constant density, i.e., with  $\rho/\rho_0 = 10^{-n}$ , where  $\rho_0 = 1.293 \text{ kg/m}^3$ , which corresponds to STP.<sup>10</sup> The results are inevitably complex, but some general conclusions that can be drawn are the following:

- The air triatomics dissociate below 2,000 K to 3,000 K, depending on density or pressure.
- $\text{O}_2$  ( $D = 5.12 \text{ eV}$ ) dissociates in the 3,000 K to 6,000 K temperature range, while  $\text{N}_2$  ( $D = 9.76 \text{ eV}$ ) dissociates in the 9,000 K to 15,000 K range.
- There is little ionization below 6,000 K where  $\text{NO}^+$  (which has the lowest ionization potential of any of the air species,  $I = 9.25 \text{ eV}$ ) is the principal positive ion; above 9,000 K there are very few molecules left, while above 12,000 K, air is largely ionized [with  $\text{O}^+$  ( $I = 12.1 \text{ eV}$ ) as principal positive ion].
- Metastable molecules or "free radicals" such as  $\text{NO}$ ,  $\text{CO}$ ,  $\text{CN}$ ,  $\text{OH}$ , etc., which are both chemically and radiatively active, form above room temperature but normally decompose above 3,000 K to 5,000 K.

## 2.4 EFFECTS OF DISSOCIATION ENERGY ON THERMODYNAMIC PROPERTIES

The characteristic behavior of air in the temperature range from 1,000 K to 10,000 K which is under discussion here is principally due to the fact that a large amount of energy is required to dissociate the  $\text{O}_2$  and  $\text{N}_2$  molecules. We can write the change in internal energy  $\Delta E$  as

$$\Delta E = -P \Delta V + S \Delta T + \mu \Delta n \quad , \quad (2.8)$$

---

<sup>10</sup>  $\rho_0$  corresponds to  $n_0$  of the previous Section.

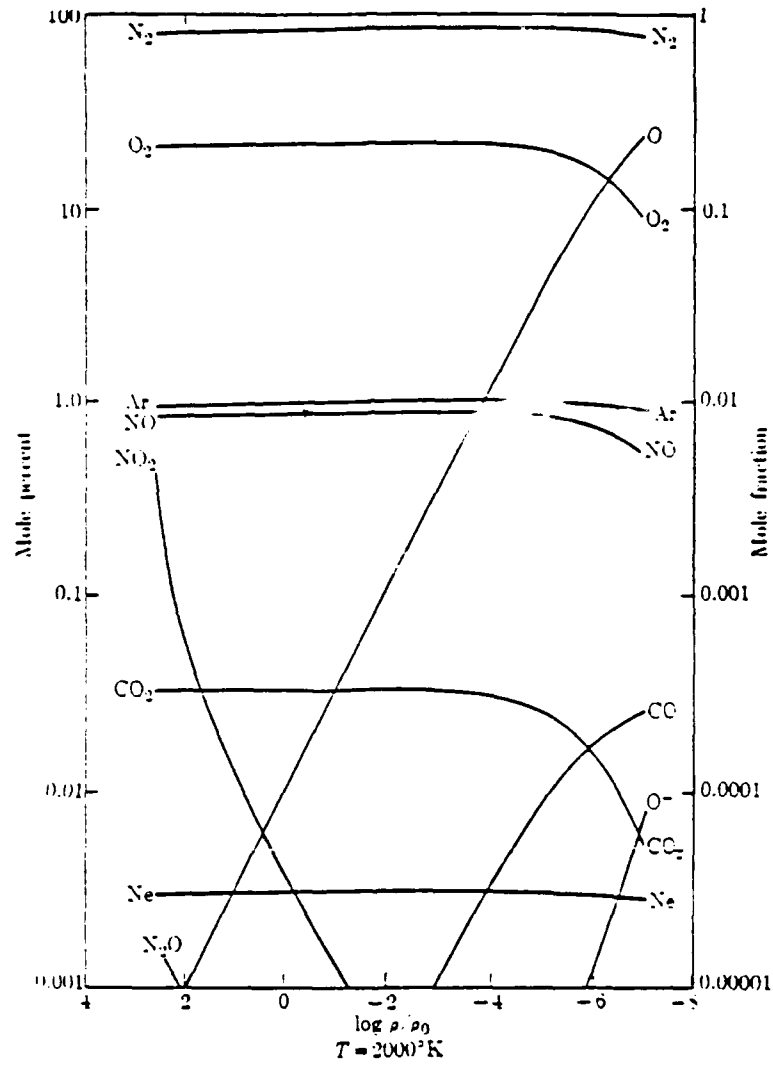


Figure 2-3. Equilibrium Composition of Dry Air as Function of Temperature and Density. Source: Hilsenrath and Klein, 1965.

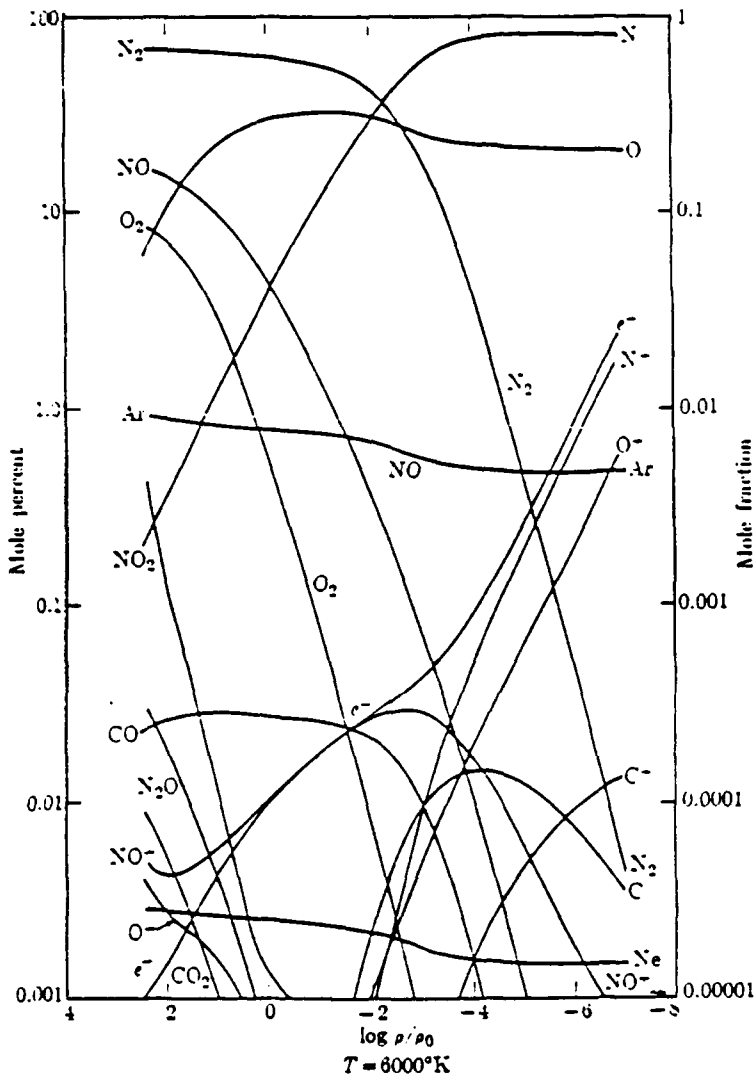


Figure 2-3. (continued)

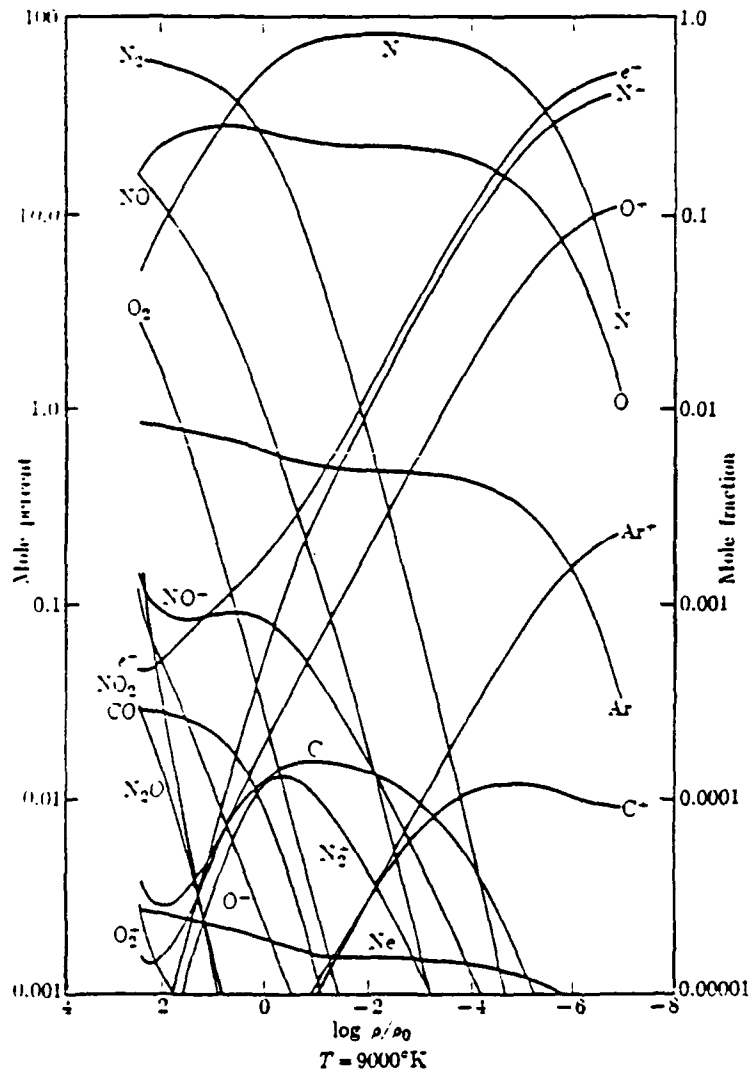


Figure 2-3. (continued)

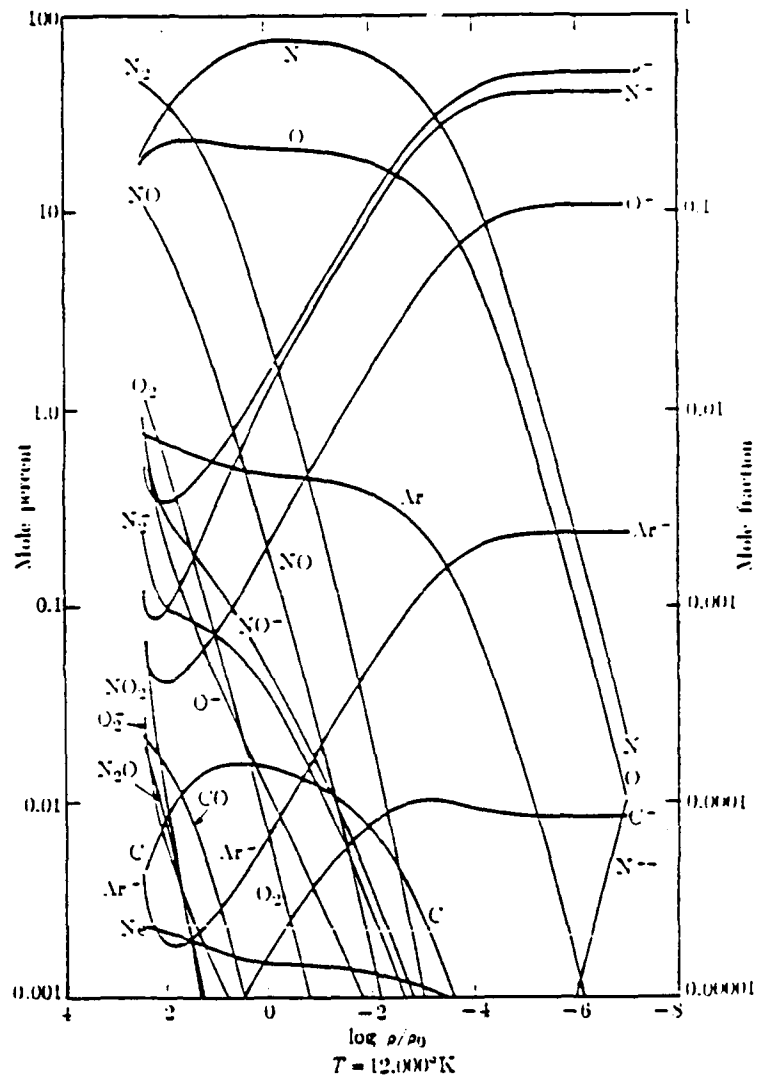


Figure 2-3. (continued)

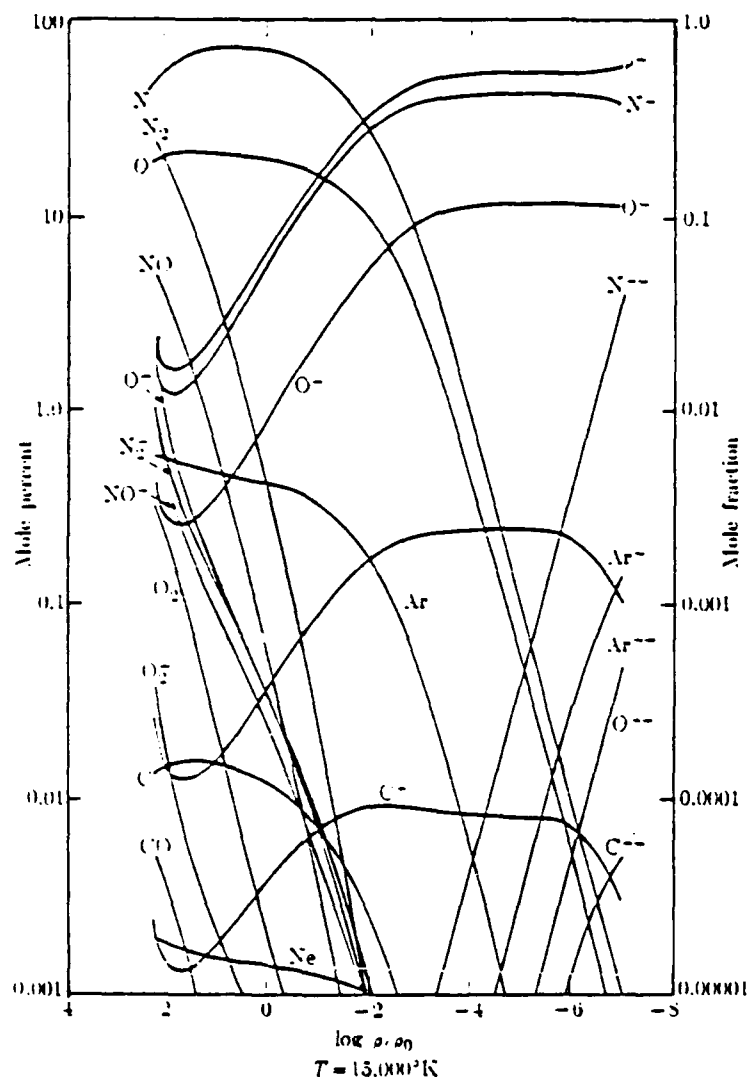


Figure 2-3. (continued)

where  $\mu$  is the "chemical potential" and  $\Delta n$  is the change in chemical species concentration, so that the term  $\mu \Delta n$  corresponds to the change in internal energy due to dissociation. At constant volume, we can simply write the change in internal energy per unit mass as

$$\Delta E = \int c_{v,eff} dT = c_{v,eff} \Delta T \quad , \quad (2.9)$$

by absorbing the chemical energy and entropy in the effective specific heat,  $c_{v,eff}$ .

Note that for a monatomic gas of molecular weight  $M$ , the specific heat at constant volume per unit mass is

$$c_{v,monatomic} = (3/2) (R/M) \quad , \quad (2.10a)$$

where  $R$  ( $= 8.31$  Joule/mole-K) is the gas constant. For a diatomic gas (with the rotation excited classically and the vibration not excited) we have

$$c_{v,diatomic} = (5/2) (R/M) \quad , \quad (2.10b)$$

while for a polyatomic gas or a dissociating diatomic gas,

$$c_{v,polyatomic} = q (R/M) \quad , \quad (2.10c)$$

where  $q$  is appropriately large:  $q = 7/2$  for a triatomic molecule with the vibration not excited or for a diatomic gas with the vibration fully excited.

For a chemically reacting gas such as air at elevated temperatures, the degree of dissociation varies with temperature (and pressure), and thus the specific heat ratio

$$\gamma = c_p/c_v \quad (2.11)$$

is no longer a constant, and thus Gilmore (1955) introduced an "effective specific heat ratio for shock waves"

$$\gamma' = 1 + PV/E \quad (2.12)$$

whose value reverts to  $\gamma$  in the limit of a non-reacting ideal gas. For air at elevated temperatures, the degree of dissociation and thus the values of  $\gamma'$  depend on density as well as on temperature.

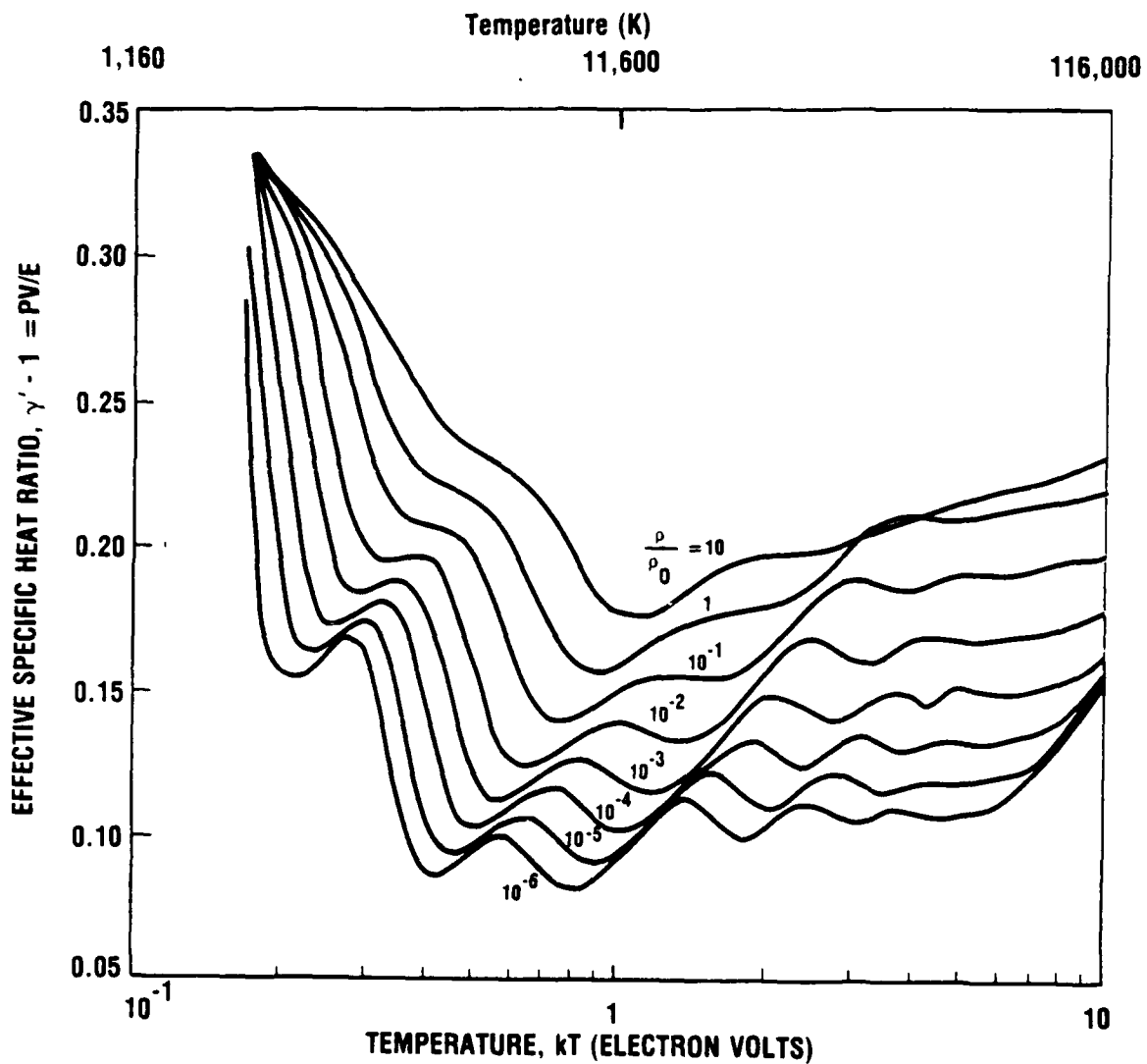
Figure 2-4 shows values of  $\gamma'$  for various values of  $\rho/\rho_0$ . Note that in the region where the  $O_2$  and  $N_2$  molecules dissociate,  $c_{v,eff}$  is particularly large so that  $\gamma'$  is quite small;  $\gamma' = 1.1$  to  $1.2$  corresponds to  $c_{v,eff} = (10.0$  to  $5.0) (R/M)$  as against the much smaller values for non-reacting mono- or diatomic gases.

The structure shown in Fig. 2-4 arises because the various degrees of freedom are excited at increasing temperatures and dissociation and ionization occur first at lower densities. Thus, starting at the lowest temperatures, the initial decrease in  $\gamma'$  is due partly to excitation of  $N_2$  and  $O_2$  vibrational modes, but even more to  $O_2$  dissociation, which causes large increases in internal energy as the temperature is increased only moderately. This dissociation occurs more abruptly and at a lower temperature when the air density is lower. After the  $O_2$  dissociation is essentially completed, these curves level off or even rise slightly, in the region where  $PV$  increases relatively faster with increasing temperature than  $E$  does. At slightly higher temperatures, a second set of dips occurs due to  $N_2$  dissociation. Since the  $N_2$  dissociation energy is about twice that of  $O_2$ , these dips occur at about twice the temperature of the  $O_2$  dips. At still higher temperatures, further dips occur due to first ionization, second ionization, etc.

## 2.5 COLLISIONS AND NON-EQUILIBRIUM PROCESSES

When energy is suddenly deposited in a gas, it is usually absorbed in a non-equilibrium fashion, and it takes a finite amount of time for this energy to be redistributed among the various molecular modes, to approach thermal equilibrium. For example, when a shock passes through air, the energy goes initially into translational energy of the molecules, and later is redistributed successively to the rotational, vibrational, electronic and chemical degrees of freedom. When air is bombarded by a pulse of X-rays from a nuclear burst, or by a pulse of light from a laser, the energy initially goes primarily into electronic excitation and ionization, and later into the other modes.

This energy redistribution is carried out by collisions between the molecules (and atoms and electrons, if present in significant amounts), and also perhaps by radiation. The molecular collision rate increases with the gas density. Consequently, near sea level the duration of the nonequilibrium period is often so short that it can be neglected, and equilibrium assumed in most (though not all) situations. In contrast, at high altitudes equilibrium tends to be the exception rather than the rule. However, even at low altitudes non-equilibrium can persist if the energy deposition process continues, as in the case of delayed beta irradiation from a nuclear burst.



1-23-89-3

Figure 2-4.  $\gamma'$ , Effective Specific Heat Ratio. (Source: Gilmore, 1955)

To make quantitative estimates of the equilibration rate, it is necessary to look at details of the collisional interaction processes. The gas-kinetic collision cross section of an air molecule,  $\sigma(\text{gk})$  is in the range of 1 to  $3 \times 10^{-15} \text{ cm}^2$ . It is customary to define a gas-kinetic mean free path  $l(\text{gk})$  which is related to the particle number density  $n$  and the gas-kinetic collision cross section  $\sigma(\text{gk})$  by the relation<sup>11</sup>

$$l(\text{gk}) = 1/[\sqrt{2} \pi n \sigma(\text{gk})] \quad (2.13)$$

(cf. Jeans, 1982, pp. 135, 145, 159).

For room temperature air at sea level,<sup>12</sup>  $n_0 \sim 2.55 \times 10^{25} \text{ m}^{-3}$  and  $l(\text{gk}) \sim 6.63 \times 10^{-8} \text{ m}$ , which gives  $\sigma(\text{gk}) \sim 1.33 \times 10^{-15} \text{ cm}^2$ .

Table 2-4 gives some representative orders of magnitude for the gas-kinetic mean free path and also the time between collisions in air as a function of density and thus of effective altitude in the atmosphere. Considering that reaction may occur on the average once in  $10^3$  to  $10^6$  collisions, we see that while equilibrium will tend to be established relatively rapidly (fraction of a second) at densities greater than  $10^{-3} \times$  ambient, corresponding to altitudes below 50 km, yet at densities below  $10^{-6} \times$  ambient, which correspond to altitudes above 100 km, non-equilibrium effects will predominate to relatively long times (tens of seconds).

The upper atmosphere ( $> 100 \text{ km}$ ) tends to be in *Photochemical Steady State*<sup>13</sup> rather than in *Local Thermodynamic Equilibrium* (LTE) which is discussed here. However, at the higher densities or pressures (lower altitudes) that apply to missile reentry peak heating (15 to 45 km) or low-altitude nuclear fireballs (say, below 40 km where the pressure is 2.9 mbar versus 1000 mbar at the surface), LTE is often a good first approximation, although it fails for *slow* processes involving species present in *very small* concentration.

---

<sup>11</sup> Note that there are somewhat different definitions for the mean free path and also for the molecular collision diameter which give slightly different numerical values.

<sup>12</sup> See, e.g., U.S. Standard Atmosphere, 1962, reproduced in the listing of Physical Constants in Appendix D.

<sup>13</sup> *Photochemical Steady State* is defined as follows. Solar (or other) ultraviolet radiation incident on the upper atmosphere produces significant dissociation and ionization, but does not raise the kinetic temperature to the LTE value associated with the ambient dissociation and ionization. See Section 4.4 for a discussion.

**Table 2-4. Mean Free Path and Collision Times as Function of Density**

\* We begin with Sea Level Atmosphere (USAF, 1965, p. 2-19) where  $T = 288 \text{ K}$  and  $\rho_r = 1.225 \text{ kg/m}^3$  and go down in density at constant temperature:

Density ratio $\rho/\rho_r$	Particle Number Density, $\text{m}^{-3}$	Mean Free Path $l(\text{gk}), \text{m}$	Time Between Collisions, $\text{s}^{(a)}$
1	$2.55 \times 10^{25}$	$6.63 \times 10^{-8}$	$1.45 \times 10^{-10}$
$10^{-3}$ (b)	$2.55 \times 10^{22}$	$6.63 \times 10^{-5}$	$1.45 \times 10^{-7}$
$10^{-6}$ (c)	$2.55 \times 10^{19}$	$6.63 \times 10^{-2}$	$1.45 \times 10^{-4}$
$10^{-9}$ (d)	$2.55 \times 10^{16}$	66.3	0.145

Notes:

- (a) 1/collision frequency.
- (b) 49 km altitude.
- (c) 96 km altitude.
- (d) 155 km to 165 km, depending on solar activity--this has to be corrected for temperature ( $\sim 530 \text{ K}$  to  $950 \text{ K}$ ).

For a chemical reaction, say



typically not every gas-kinetic collision between the reactants  $A + B$  leads to the products,  $C + D$ , so that  $\sigma(\text{react}) < \sigma(\text{gk})$ . In a "near-LTE" situation in which it is possible to define a temperature  $T$ , at least approximately, it is appropriate to write down a reaction rate coefficient for reaction (2.14) which is normally expressed in the form

$$k(\text{react}) = P v(\text{gk}) \sigma(\text{gk}) \exp\{-\Delta E/kT\} \quad , \quad (2.15)$$

where  $v(\text{gk})$  is a thermal mean molecular velocity [ $\sim 10^5 \text{ cm/sec}$ , so that  $v(\text{gk}) \sigma(\text{gk}) \sim 10^{-10} \text{ cm}^3/\text{sec}$ ].  $P$  is a probability factor, frequently much less than one, while the exponential factor represents an energy barrier  $\Delta E$  that has to be overcome before reaction occurs. The temperature dependence of the reaction rate coefficient comes mainly from the exponential term.

For the reaction (2.14), where species concentrations are  $n_X$  (mol./cm<sup>3</sup>;  $X = A, B, C, D$ ) and the forward and backward rate coefficients are respectively  $k_f(T)$  and  $k_b(T)$ , in a steady state the number of forward reactions per unit volume and unit time,  $k_f(T) n_A n_B$ , is equal to the number of back reactions per unit volume and unit time,  $k_b(T) n_C n_D$ . This is the *Principle of Detailed Balancing*, which states that when equilibrium is reached in a reaction system, any particular chemical reaction and its exact reverse must, on the average, be occurring at the same rate. It gives a useful relation between the equilibrium constant  $K_{eq}(T)$  for reaction (2.14) and the rate constants  $k_f(T)$  and  $k_b(T)$

$$K_{eq}(T) = n_C n_D / n_A n_B = k_f(T) / k_b(T) \quad (2.16)$$

An interesting and important example of a non-equilibrium process in high-temperature air is provided by the *Nitric Oxide Freeze-In* (see footnote 4 on p. 2-4). Reference to Fig. 2-3 or other standard sources shows that at temperatures above 2000 K, equilibrium air contains significant quantities of NO (1 to 10 mole-percent, or half that in units of particles per air atom). The NO is produced by a variety of chemical reactions, with an important contributor being  $O + N_2 + M$  (= some third body); it disappears largely by the reaction



which is exothermic by 1.9 eV, but has a large activation energy  $\Delta E = 5.9$  eV (135 Kcal/mole), and thus becomes exceedingly slow at temperatures below 2000 K.<sup>14</sup> Accordingly, when high-temperature air cools, the NO remains for a long time in above-equilibrium concentrations. It forms NO<sub>2</sub> which is an irritating oxidant itself, and which also reacts photochemically with ambient atmospheric hydrocarbons to form ozone and other oxidants, so that this process is an important source of photochemical smog arising from the products of combustion.<sup>15</sup> This freeze-in process is important in the combustion products from heat engines, in the wakes behind reentering objects, and in nuclear fireballs.

If the chemical composition in a given situation cannot be described by near-equilibrium, in terms of an effective temperature, the following points should be noted:

---

<sup>14</sup> Because the rate constant  $\sim \exp -(\Delta E/kT) = \exp -(5.9/0.18) = e^{-33} \sim 5 \times 10^{-15}$ .

<sup>15</sup> In the stratosphere, due to the lower hydrocarbon concentration and greater ultraviolet intensity than near the ground, NO usually destroys rather than produces ozone.

1. One improvement which is frequently useful is to describe different degrees of freedom (e.g., molecular vibration, dissociation, or electronic excitation) in terms of their own effective temperature(s)  $T_{int}$  which may not always be equal to the gas-kinetic (i.e., translational) temperature.
2. For high-temperature rate constants, see the evaluated data collections of Baulch et al., 1972, 1973, 1976, for near-ambient temperatures, Baulch et al., 1984, and for charged species, DNA, 1972.
3. Sets of coupled chemical reactions are numerically frequently difficult to analyze because as the system approaches a steady state, small fluctuations in concentration about the steady-state value tend to be amplified by numerical techniques. This "stiff" behavior can be avoided by using a procedure originally due to Gear, 1971.

## 2.6 SOME COMMENTS ON HEAT TRANSFER IN HIGH-TEMPERATURE AIR

In the present high-temperature regime, heat transfer is a particularly complex subject. For a discussion, see, e.g., Bond et al., 1965, Penner and Olfe, 1968, and Zeldovich and Raizer, 1966, 1967, and on the aerodynamics, see Anderson, 1982, 1984, Gazley, 1961, and Martin, 1966.

Heat transfer occurs by conduction (molecular transport), by convection and by radiation. Convective heat transfer is normally faster than conductive transfer in gases, and predominates at temperatures below several thousand K. At higher temperatures radiative heat transfer is much more rapid. Typically, in reentry, convection dominates radiation up to several thousand degrees K; thus, for ordinary earth satellite or ICBM entry where the entry velocity is typically 7 km/sec and the maximum temperature is  $\sim 7500$  K, the effects of radiative heat transfer are normally not very important, but at temperatures of 12000 K or higher, which correspond to entry velocities of perhaps 11 km/sec, radiative heat transfer dominates. In nuclear fireball problems also convection dominates radiation up to a few thousand degrees.

Note that :

1. In the temperature regime considered here, a large fraction of the thermal energy is transported as heat of dissociation of the  $O_2$  and  $N_2$  molecules rather than as kinetic and rotational energy of the molecules.
2. Convective heat transfer increases very much when the flow goes turbulent. The determination of when a flow goes turbulent and how large the heat transfer then becomes is, in general, complex and very much dependent on the

detailed character of the flow, so that a simple and useful account of this subject cannot be presented here.<sup>16</sup>

3. Air does not radiate at all like a black body because there are many absorption bands interspersed by transmissive regions. Under reentry conditions ( $T \sim 5000-7000$  K) radiative heat transfer sometimes increases very much more rapidly with temperature than blackbody radiation: S.S. Penner (private communication) mentions that under certain conditions the radiative heat transfer is proportional to  $T^7$  as against  $T^4$  for blackbody radiation.

---

<sup>16</sup> See Ch. 5 in Part II of these Notes.

### 3. RADIATION FROM HIGH-TEMPERATURE AIR

#### 3.1 INTRODUCTION

The radiation from air and from other gases at high temperatures is highly specific spectrally, and one frequently needs some very detailed information about the particular chemical species and radiating systems that are important. At one atmosphere pressure and below, atomic spectral lines of the atmospheric gases tend to have a very narrow spectral line width ( $< 1 \text{ cm}^{-1}$ ), so that a given air mass is likely to be optically thick at the centers of the stronger lines and optically thin in other spectral regions. This gives rise to deviations from Beer's Law, in that the attenuation at wavelength  $\lambda$  in path length  $x$  cannot always be written as  $\exp(-k_\lambda x)$  where  $k_\lambda$  depends on  $\lambda$  but not on  $x$ .<sup>17</sup> Molecular transitions involve bands made up of hundreds or thousands of spectral lines, but conceptually they are not too difficult to describe. In a diatomic molecule, either one, two, or all three of the quantum parameters designating the rotational, vibrational, and electronic state of the molecule can change. These changes typically cause emission or absorption in the microwave, infrared, and visible-ultraviolet spectral regions, respectively.<sup>18</sup>

For orientation, note that a 1 cm thick layer of air at 4000 K and 1 atmosphere pressure, such as in a reentry vehicle boundary layer, is quite thin optically and thus radiates very much less<sup>19</sup> than a blackbody at this temperature, but a 1000-m layer of air at this temperature and pressure, as in a nuclear fireball, is optically thick and radiates like a blackbody.<sup>20</sup>

---

<sup>17</sup> This issue is discussed in more detail in Part II, Section 7.2.3 in the context of the LOWTRAN code.

<sup>18</sup> Triatomic molecules behave similarly, except that (if linear) they have one (doubly-degenerate) rotational mode and three vibrational modes (one doubly-degenerate), while if nonlinear they have three rotational and three vibrational modes, all nondegenerate.

<sup>19</sup> By a factor  $10^{-4}$ --see, e.g., Fig. 3-10.

<sup>20</sup> At temperatures in the 1000 K to 10,000 K range both a near-gray body and an air parcel emits most of its radiation in the "near-visible" spectral range, say 0.2  $\mu\text{m}$  to 2  $\mu\text{m}$ . This is so because many absorption bands are located in this spectral range in which most of the energy of a Planck (blackbody) spectrum lies in the temperature range under consideration. In general, this spectral range or the visible is considered here.

We begin in Section 3.2 by discussing blackbody radiation (which gives the maximum radiance at a given temperature) from the standpoint of applications to the radiation from solid surfaces. Then, in Section 3.3, we discuss the equation of radiative transfer, including effects of scattering as well as of emission and absorption. The limits of optically thick and optically thin media are discussed, and Rosseland and Planck means (which are appropriate for these two limits) are introduced. Section 3.4 treats atomic line radiation to point out some generic characteristics of absorption cross sections, line width and line shapes, and saturation in terms of "Curves of Growth." Section 3.5 analyzes molecular band radiation for the particular example of high-temperature air where six molecular band transitions ( $O_2$  Schumann-Runge,  $NO$   $\beta$  and  $\gamma$ ,  $N_2$  First Positive and Second Positive and  $N_2^+$  First Negative) have frequently been used to describe the bulk of the near-visible thermal radiation which predominates in the temperature range of concern here. Section 3.6 discusses the continuum ("free-free" and "free-bound") radiation which contributes especially at the higher temperatures.

Section 3.7 uses these results to present the absorption coefficient of high-temperature equilibrium air. Section 3.8 applies these results, indicating in quantitative terms that in the present temperature range (1,000 K to 10,000 K) radiation from the air is much less than blackbody radiation at the same temperature.

It must be stressed that the present discussion is not a substitute for a course in atomic and molecular spectroscopy and quantum mechanics, which would explain how the electronic structure is built up<sup>21</sup> and how one calculates the transition probabilities of the various transitions. For this, see for instance Condon and Shortley, 1935, Goody, 1964, Herzberg, 1937, 1944, 1945, 1950, 1966, etc., Penner, 1959, Slater, 1960, 1963, and Zeldovich and Raizer, 1966, 1967. Here we try to sketch out the underlying structure in qualitative terms to explain how the various pieces of the problem fit together, present some key analyses, and show numerical values for some key optical transitions to give the reader a feeling for the orders of magnitude.

### 3.2 BLACKBODY RADIATION

A blackbody is defined as a medium that absorbs all the incident radiation that falls on it. Since, in equilibrium, the amount of energy absorbed must equal the amount emitted, the equilibrium radiant energy emitted from unit area of a blackbody in unit time

---

<sup>21</sup> Appendix A gives a very brief discussion of spectroscopic notation, which is used extensively here.

represents an upper limit for the emission of radiant energy from any substance which is at the same temperature as the blackbody. The radiation from a blackbody at a given wavelength  $\lambda$  or frequency  $\nu$  depends only on  $\lambda$  (or  $\nu$ ) and on  $T$ , and gives the maximum radiance from any source at this temperature. The blackbody spectral radiance  $B(\lambda, T)$  is given by the following expression:

$$B(\lambda, T) = C_1 \lambda^{-5} [\exp(c_2/\lambda T) - 1]^{-1} \quad (\text{W/m}^2\text{-sr-}\mu\text{m}) \quad , \quad (3.1)$$

where (for  $\lambda$  in  $\mu\text{m}$ ,  $T$  in K):

$$C_1 = 2hc^2 = 1.191 \times 10^8 \text{ (W-}\mu\text{m}^5/\text{m}^2\text{-sr-}\mu\text{m)}$$

$$c_2 = hc/k = 14390 \text{ (K-}\mu\text{m)} \quad .$$

Figures 3-1 and 3-2 show the spectral radiance at different temperatures as functions of wavelength  $\lambda$  ( $\mu\text{m}$ ) and wavenumber  $\nu$  ( $\text{cm}^{-1}$ ). Note that the symbol  $\nu$  is sometimes used for frequency (Hz) and sometimes for wavenumber ( $\text{cm}^{-1}$ ). In the present document we normally use wavelength rather than frequency or wavenumber as spectral variable, except in some particular discussions such as that in Section 3.3.3 and in Appendix C. Overall, the notation used in the literature is very confusing. For instance, many people refer to  $\text{W/cm}^2$  rather than to  $\text{W/m}^2$ . See, e.g., *IR Handbook*, 1985, Ch. 2. A good, concise summary is given in USAF, 1965, Appendix B, which is the source of Figs. 3-1 and 3-2.

If one integrates the spectral radiance,  $B(\lambda, T)$ , one obtains the total radiant energy density

$$u = a T^4 \quad (a = 8\pi^5 k^4 / 15c^3 h^3) \quad (\text{J/m}^3) \quad (3.2a)$$

or the radiant exitance of a blackbody

$$E = (c/4\pi)aT^4 = \sigma T^4 \quad , \quad (\text{W/m}^2) \quad (3.2b)$$

where the Stefan-Boltzmann constant  $\sigma = 5.670 \times 10^{-8} \text{ W/m}^2\text{K}^4$ .

Differentiating Eq. (3.1) with respect to wavelength and equating  $\partial B(\lambda, T)/\partial \lambda$  to zero gives *Wien's displacement law*, which states the relation between  $\lambda_{\text{max}}$ , the wavelength at which the spectral radiance  $B(\lambda, T)$  is a maximum, and temperature

$$\lambda_{\text{max}} T = 2.898 \times 10^3 \text{ (}\mu\text{m K)} \quad . \quad (3.3)$$

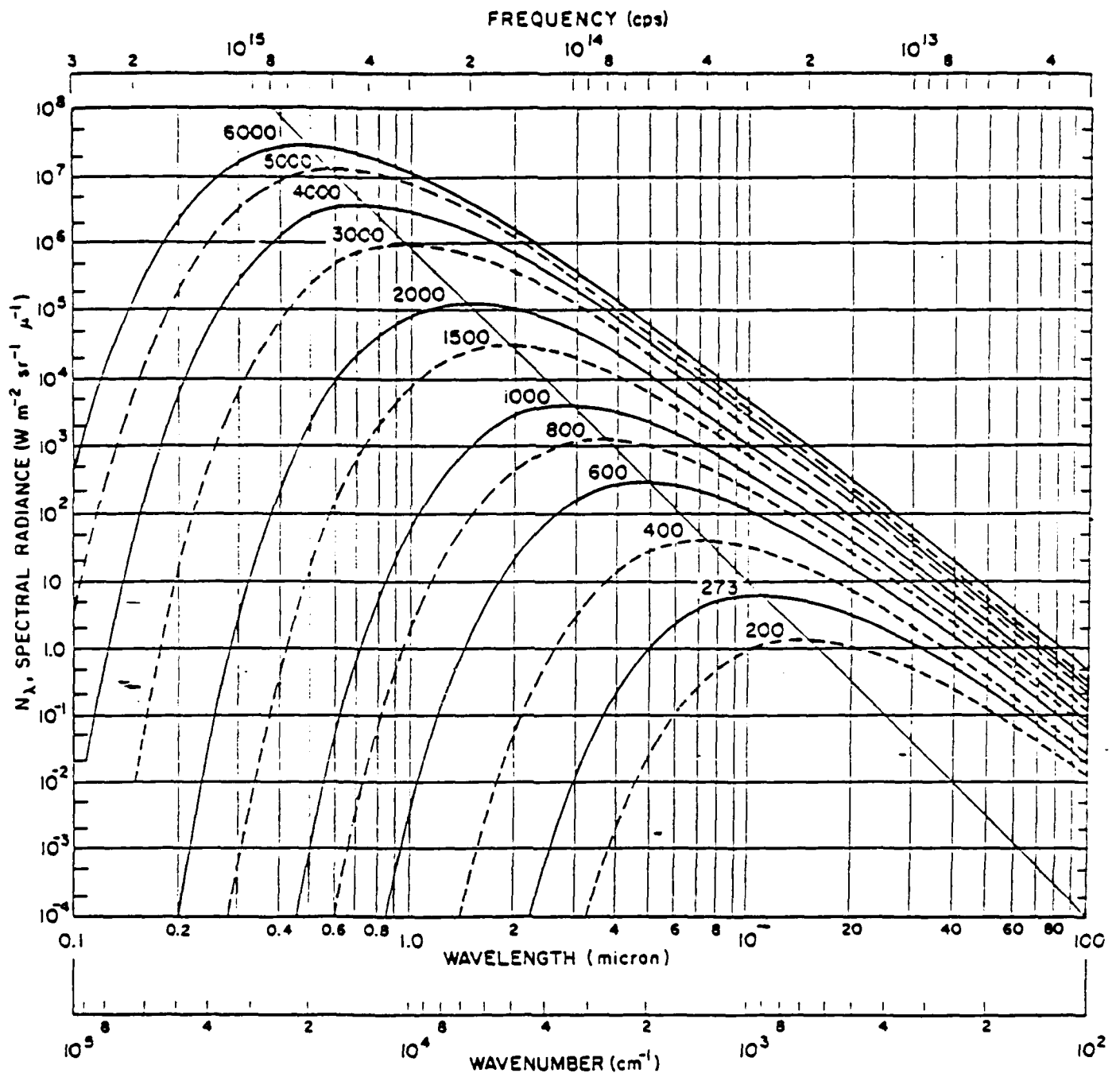


Figure 3-1. Spectral Radiance of a Blackbody as Function of Wavelength.  
 (Source: USAF, 1965, Appendix B)

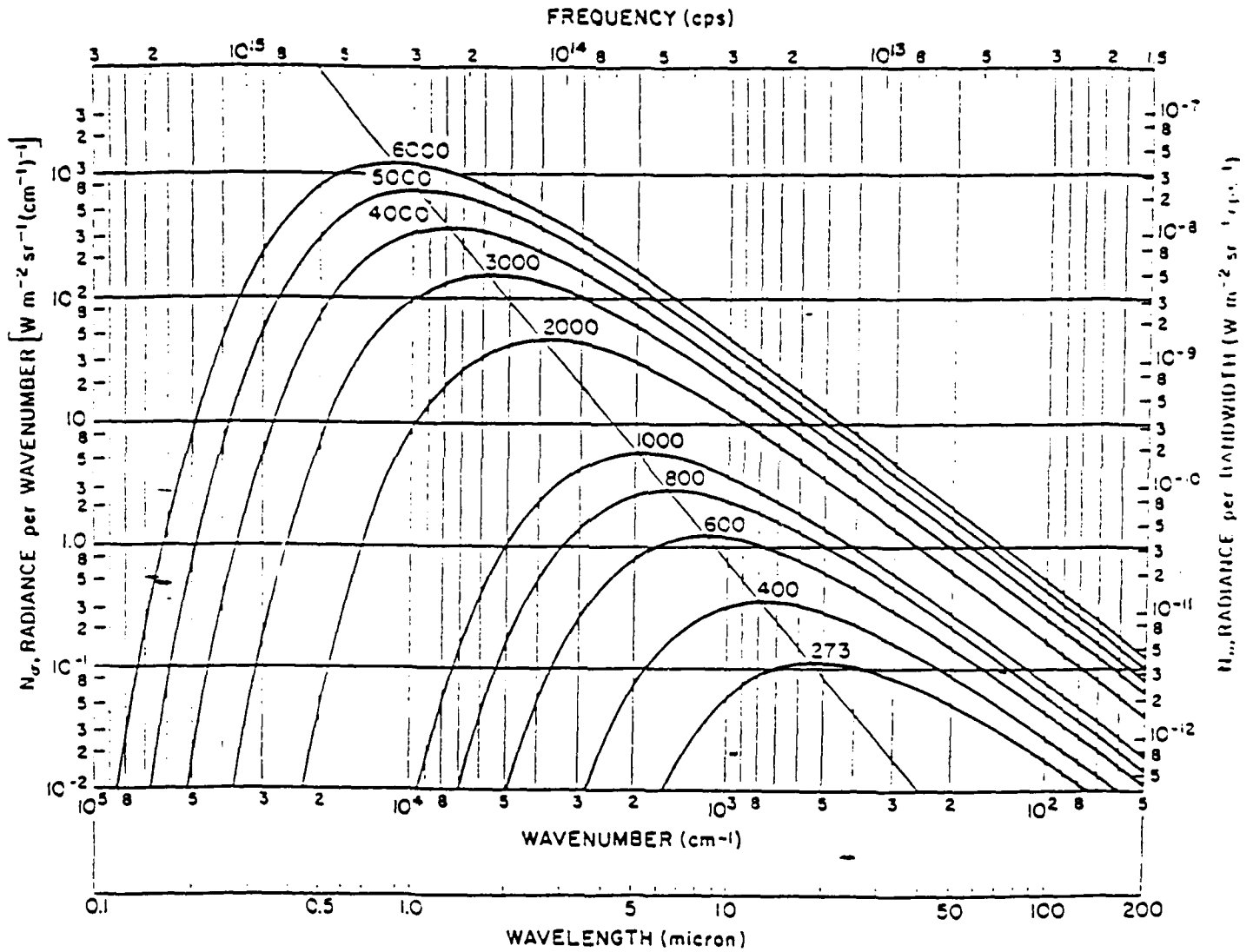


Figure 3-2. Spectral Radiance of a Blackbody as Function of Wavenumber.  
 (Source: USAF, 1965, Appendix B)

Actual solid surfaces often radiate proportionally to a blackbody with an effective emittance<sup>22</sup>  $\epsilon = \epsilon(\lambda)$ , so that the spectral radiance  $L(\lambda, T)$  ( $\text{W}/\text{m}^2\text{-sr}\cdot\mu\text{m}$ ) from a solid "Lambertian" surface<sup>23</sup> is given by the expression<sup>24</sup>

$$L(\lambda, T) = \epsilon(\lambda, T) B(\lambda, T) \quad . \quad (3.4)$$

Figure 3-3 gives the reflectance

$$\text{reflectance} = 1 - \text{emittance} \quad (3.5a)$$

of various natural (solid or liquid) materials at room temperature as a function of wavelength. If there is a general rule, it is that many condensed phase materials have a large emittance (small reflectance) at wavelengths above  $5 \mu\text{m}$  to  $10 \mu\text{m}$ , i.e., at frequencies below the Debye frequency of lattice vibrations. In the visible, transparent materials have a very low emittance, but in the UV the emittance sometimes increases again due to atomic transitions. The temperature dependence of the emittance of most materials is not strong, except when there is a phase change or other structural transition.

An important principle is Kirchoff's Law: at each wavelength

$$\text{emittance} = \text{absorptance} = 1 - \text{reflectance} \quad (3.5b)$$

which is universally applicable.

---

<sup>22</sup> If  $\epsilon = \text{constant}$ , independent of  $\lambda$ , this defines a gray body.

<sup>23</sup> A Lambertian surface is one which reflects and emits energy diffusely.

<sup>24</sup> Some authors use "spectral irradiance"  $E(\lambda, T)$  ( $\text{W}/\text{m}^2\cdot\mu\text{m}$ ) which is the integral of  $L(\lambda, T)$  over solid angle--see, e.g., *IR Handbook*, 1985, Ch.1.

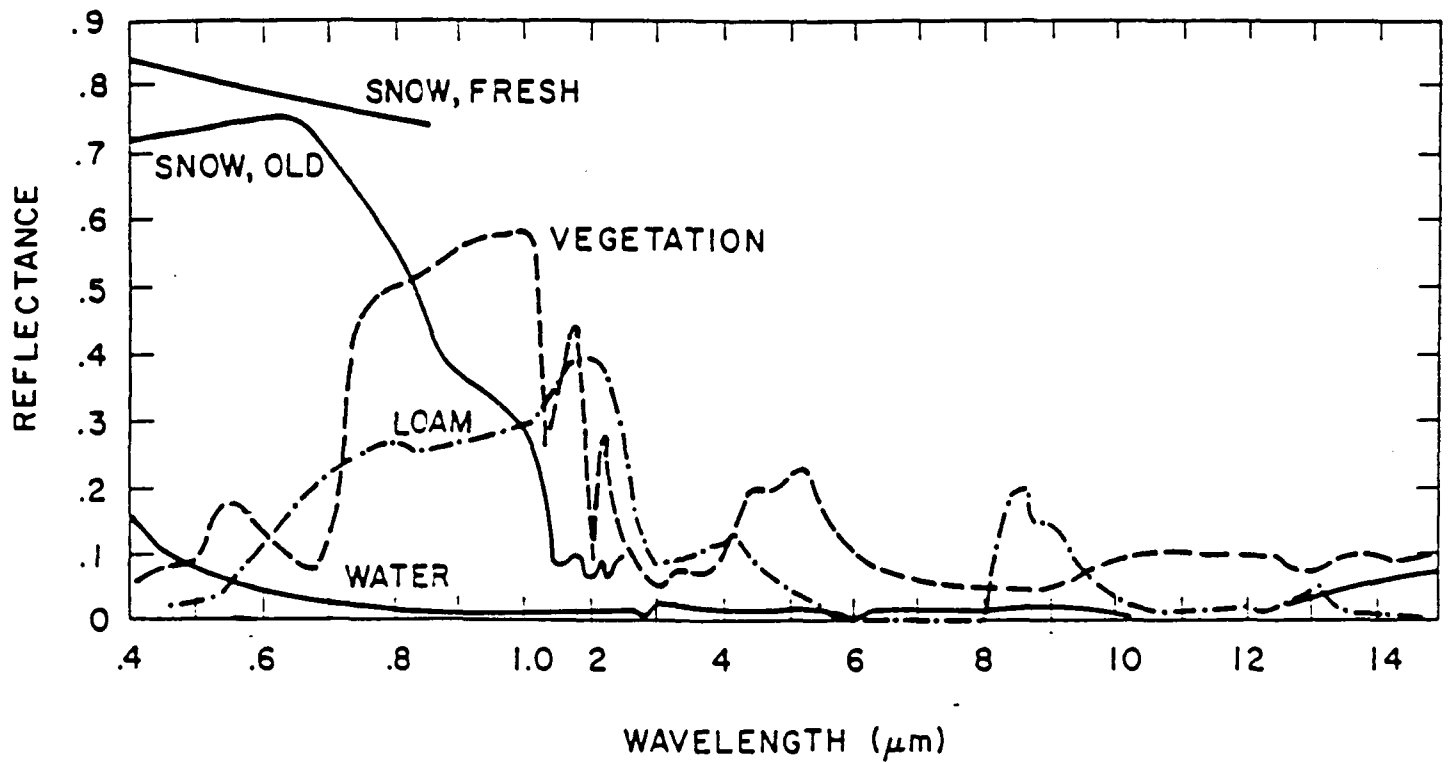


Figure 3-3. Typical Reflectance of Various Natural Surfaces.  
 (Source: McClatchey et al., 1972)

### 3.3 EQUATION OF RADIATIVE TRANSFER

#### 3.3.1 Without Scattering

The equation of transfer describes the change in the intensity function  $I = I(\lambda, x)$  where  $x$  = distance, in a medium characterized by an absorption coefficient  $k_a(\lambda)$  ( $m^{-1}$ ):

$$k_a(\lambda) = \sum_j n_j \sigma_a(j; \lambda) \quad . \quad (3.6)$$

Here  $n_j$  = number density of absorbers of species  $j$ , whose absorption cross section at wavelength  $\lambda$  is  $\sigma_a(j; \lambda)$ . In fact, this expression for the absorption coefficient  $k_a$  has to be corrected for stimulated emission (see Appendix C) to give

$$k'_a(\lambda) = k_a(\lambda) [1 - \exp(-c_2/\lambda T)] \quad (3.7)$$

(recall that  $c_2/\lambda T = hv/kT$ ).

For the transport of radiant energy, it is customary to write down the *Equation of Transfer*. This gives the radiant intensity  $I = I(\lambda, x)$  as a function of an appropriate source function  $S^*(\lambda, x)$  and of the absorption coefficient  $k'_a(\lambda)$  (see, e.g., Aller, 1963, Ch.4 and Ch.5) as

$$dI(\lambda, x)/dx + k'_a(\lambda) I(\lambda, x) = k'_a(\lambda) S^*(\lambda, x) \quad (3.8)$$

and for a medium in which we define a temperature at each point,  $T = T(x)$ , we have

$$S^*(\lambda, x) = B[\lambda, T(x)] \quad , \quad (3.9)$$

so that

$$dI(\lambda, x)/dx = k'_a(\lambda) \{B[\lambda, T(x)] - I(\lambda, x)\} \quad . \quad (3.10)$$

Let us now demonstrate how blackbody radiation relates to the radiation from a uniform layer of gas at temperature  $T$  and of thickness  $x$ . If one uses

$$u = k'_a x \quad (3.11)$$

as an independent variable and suppresses  $\lambda$ , the transfer equation (3.10) becomes

$$dI/du + I = B \quad \text{or} \quad (d/du)(Ie^u) = B e^u \quad . \quad (3.12)$$

Now, with the boundary condition

$$I(x = 0) = 0 \quad , \quad (3.13)$$

i.e., no incident radiant from outside our volume of interest, we find

$$I(x) = B(1 - e^{-k'_a x}) \quad , \quad (3.14)$$

so that for the two limits  $k'_a x \ll 1$  and  $\gg 1$  we have

Optically thin,  $k'_a x \ll 1$ ,<sup>25</sup>

$$I(x) = B k'_a x \quad , \quad (3.15)$$

so that the radiation is proportional to number of atoms, and

Optically thick,  $k'_a x \gg 1$ ,<sup>26</sup>

$$I(x) = B(\lambda, T) \quad , \quad (3.16)$$

i.e., the gas radiates like a blackbody.

The next problem is to determine  $k_a(\lambda)$ , the absorption coefficient, and this is done in the next three sections, respectively, for atomic line radiation (Section 3.4), molecular band radiation (Section 3.5), and continua (Section 3.6). In these three sections 3.4 to 3.6 we evaluate  $\sigma_a(j; \lambda)$ ; the effects of number density or of optical thickness are taken up in Section 3.7 thereafter. However, before we do this, let us write down the equation of transfer in the presence of scattering particles in Section 3.3.2, and set this discussion of radiative transfer in context with a general discussion of opacity coefficients in Section 3.3.3.

### 3.3.2 With Scattering

If one deals only with atoms and molecules at reasonably low density and at relatively long wavelengths, there is very little scattering and thus the equation of transfer in the form (3.8) is satisfactory. However, if there are particles of radius  $a$  such that the Mie parameter<sup>27</sup>

$$q = 2\pi a/\lambda \quad (3.17)$$

---

<sup>25</sup> Which is good to 10% for  $k'_a x < 0.2$ .

<sup>26</sup> Which is good to 10% for  $k'_a x > 1.5$ .

<sup>27</sup> In 1908 G.Mie gave a rigorous solution for the diffraction of a plane electromagnetic wave by a homogeneous sphere--see, e.g., Born & Wolf, 1980, or Van de Hulst, 1957.

is not very much less than unity, then scattering may be as important as absorption or even more so. In general,  $q \ll 1$  defines the Rayleigh scattering regime.<sup>28</sup>  $q \sim 1$  is called the Mie region, and  $q \gg 1$  is the domain of Geometrical Optics. Scattering effects will be discussed in some detail in Chapter 7 of Part II, to be prepared later.

If there are  $n$  particles per unit volume, each of absorption cross section  $\sigma_a$  and of scattering cross section  $\sigma_s = \sigma_s(\theta)$ , then we can define an absorption coefficient  $k_a(\lambda)$  from Eq. (3.6) and a scattering coefficient

$$k_s(\theta) = n \, d\sigma_s/d\theta \quad (3.18)$$

where  $d\sigma_s/d\theta$  is the differential scattering cross section.<sup>29</sup>

The equation of transfer describes conservation of total radiant intensity in a volume element, when account is taken of absorption and emission (terms in  $k'_a$  and  $B(\lambda, T)$ ) as well as of scattering (terms in  $k_s$ ). We write down the equation of transfer for the intensity function  $I = I(x, \mu, \varphi)$  in a semi-infinite slab of uniform material, characterized by  $x > 0$ , in a direction  $(\theta, \varphi)$ :<sup>30</sup>

$$(k_s + k'_a) I - \mu dI/dx = (1/4\pi) \iint d\mu' d\varphi' k_s(\Theta) I(x, \mu', \varphi') + k'_a B(T) \quad (3.19a)$$

$$k_s = (1/4\pi) \iint d\mu' d\varphi' k_s(\Theta) \quad (3.19b)$$

$$\cos \Theta = \cos \theta \cos \theta' + \sin \theta \sin \theta' \cos(\varphi - \varphi') \quad (3.19c)$$

$$\mu = \cos \theta ; \mu' = \cos \theta' \quad (3.19d)$$

This equation is written down here to indicate that absorption and scattering enter in somewhat different ways.<sup>31</sup> By comparing Eq. (3.19) with (3.8) we see that scattering and absorption/emission enter in somewhat different ways. Thus  $k'_a$ --but not  $k_s$ --is corrected for stimulated emission. The difference in sign of the term  $dI/dx$  depends on the

<sup>28</sup> Lord Rayleigh explained the blue of the sky as due to the scattering of sunlight by air molecules. Molecules are, of course, extremely small ( $a \sim 3 \times 10^{-8}$  cm) so that  $q \ll 1$  and thus the scattering per molecule is very small, but the optical thickness of a path through the atmosphere is large because there are so many molecules in the path. If  $q \ll 1$ , the scattering cross section per particle is proportional to  $1/\lambda^4$ , so that blue light is scattered much more than red light, which explains why the sky is blue. (This is a great oversimplification--see, e.g., Minnaert, 1954, p. 238f, and Van de Hulst, 1957, p. 414.). Also, the sun is red at sunrise and sunset because it is seen through a long path in the dusty lower atmosphere, which preferentially removes the blue from the path.

<sup>29</sup> Note that  $\sigma_s$  and  $k_s$  depend on wavelength  $\lambda$  as well as on angle  $\theta$ .

<sup>30</sup> See, for instance, Chandrasekhar, 1960, Ch.1, or Bond, Watson and Welch, 1965, Ch.10.

<sup>31</sup> Conventionally,  $\mu = \cos \theta$  is defined so that  $\mu > 0$  corresponds to radiation coming out of the material and  $\mu < 0$  to radiation going into the material.

sign convention used for  $\mu$ . The right-hand side of Eq. (3.19a) contains an emission term  $k'_a B$  and a scattering term  $(1/4\pi) \int d\mu' \int d\phi' k_s(\Theta) I(x, \mu', \phi')$ , while the scattering term  $k_s$  has been integrated over all scattering angles. We shall not discuss the solution of the equation of radiative transfer (3.19), which becomes very complicated (see, e.g., Aller, 1963, Chandrasekhar, 1960, Goody, 1964, or Kondratyev, 1969), but merely present it here to indicate how the introduction of scattering effects complicates the problem.

### 3.3.3 Opacities<sup>32</sup>

In an optically thin ("transparent") medium we ask how much the intensity of a beam of incident radiation is reduced, i.e., we want to know the (relatively small) absorption coefficient for a situation in which Beers' Law generally holds. By contrast, in an optically thick ("opaque") medium the critical question is how far a photon travels, or what is the mean free path. This concept of optically thin versus optically thick media is straightforward, but its evaluation is not, because of the complications arising from the various physical factors in the equation of transfer.

As has been shown above, in the presence of scattering as well as absorbing particles, the equation of transfer is an integro-differential equation which is normally solved in a number of approximations. It is customary (see, for example, Bond, Watson and Welch, 1965, Chapter 10) to distinguish between the following:

- a. Diffusion approximation, obtained by setting  $I \sim B$  in the transfer equation (3.10). This is valid for optically thick regions where photons emitted in the region have a high probability of reabsorption. Here one introduces the *Rosseland mean opacity*, and because we are talking about an optically thick region, it is useful and customary to use the *Rosseland mean free path*.
- b. Emission approximation, obtained by setting  $I \ll B$  in the transfer equation (3.10). This is valid for optically thin regions from which photons emitted in the region can escape freely, so that scattering is not important. Here one introduces the *Planck mean opacity*.
- c. In the absence of emitters, there is a cold non-radiating medium through which radiation simply diffuses. We shall not discuss this case further here, but Chapter 7 in Part II will treat various applied problems relevant to the earth's atmosphere.

---

<sup>32</sup> The term "opacity" is used technically for the absorption coefficient integrated over the whole spectrum with a blackbody weighting, either  $B(\nu, T)$  or  $B(\lambda, T)$ .

## 1. Diffusion Approximation in an Optically Thick Medium

In an optically thick region one introduces an absorption mean free path<sup>33</sup>

$$l_a(\nu) = 1/k_a(\nu) \quad , \quad (3.20)$$

where the absorption coefficient  $k_a(\nu)$  is defined by Eq. (3.6), and a total mean free path<sup>34</sup>

$$1/l'(\nu) = k'_a(\nu) + k_s(\nu) \quad , \quad (3.21)$$

where the correction for stimulated emission only occurs in the absorption, not the scattering coefficient. To introduce a frequency-averaged form of the transfer equation (3.10) or (3.19), we introduce the Rosseland mean free path  $l_R$  (or Rosseland mean absorption coefficient "opacity"  $k_R$ ) as

$$l_R = 1/k_R = \left\{ \int l'(\nu) \frac{\partial B(\nu, T)}{\partial T} d\nu \right\} / \left\{ \int \frac{\partial B(\nu, T)}{\partial T} d\nu \right\} \quad . \quad (3.22)$$

The physical meaning of this is the following. In an atmosphere with a spatial gradient  $dI(\nu)/dx$ , we define a Rosseland mean opacity as<sup>35</sup>

$$1/k_R = \left\{ \int l'(\nu) [dI(\nu)/dx] d\nu \right\} / \left\{ \int [dI(\nu)/dx] d\nu \right\} \quad , \quad (3.23)$$

replace  $I(\nu)$  by  $B(\nu)$  (hypothesis for case 1) and put

$$dB(\nu, T)/dx = [dB(\nu, T)/dT] \cdot [dT/dx] \quad , \quad (3.24)$$

which leads to the result (3.22).

## 2. Emission Approximation in an Optically Thin Medium

In an optically thin medium, the temperature will often be uniform so that  $dI/dx$  or  $dB/dT$  is not an appropriate quantity, and indeed scattering is unimportant (because the medium is optically thin). In this case  $I(\nu) \ll B(\nu)$ , and one asks for the total flux from the surface,  $J_P$ , which in this ("Planck") limit is given by the multiple integral

$$J_P = \int_0^\infty \int_\Omega \int_0^{\Delta x} B(\nu, T) k'_a(\nu) d\nu d\Omega dx \quad , \quad (3.25)$$

<sup>33</sup> As is conventional, in the present theoretical discussion we describe the spectral dependence in terms of frequency  $\nu$  rather than wavelength  $\lambda$ .

<sup>34</sup> The scattering coefficient  $k_s$  used here is the total scattering coefficient, integrated over all scattering angles  $\theta$ . (The confusing notation is conventional!).

<sup>35</sup> The Rosseland mean is frequently used, but "it has little obvious physical significance throughout the upper visible layers of stellar atmosphere" (Aller, 1963, p. 239).

where  $dx = ds \cos\theta$  is distance normal to the surface of the slab<sup>36</sup> and the integration over the solid angle  $\Omega$  is over outward directions only. In an optically thin medium the temperature is essentially constant, so that if one evaluates the spatial integral over  $d\Omega$  and  $dx$  in Eq. (3.25), one obtains the result

$$J_P = (2\pi a) \Delta x \int k'_a(\nu) B(\nu) d\nu = 2\pi a k_P \Delta x \sigma T^4 \quad , \quad (3.26)$$

where "a" is a numerical factor<sup>37</sup> and the Planck mean opacity  $k_P$  is given by<sup>38</sup>

$$k_P = \int k'_a(\nu) B(\nu, T) d\nu / \int B(\nu, T) d\nu \quad . \quad (3.27)$$

Note that the expression (3.27) for  $k_P$  looks rather different from the expression (3.23) for  $k_R$ , but if we express the Rosseland mean in terms of  $J(\nu)$ , the actual net flux,<sup>39</sup> then since

$$J(\nu) = [1/k'(\nu)] dB(\nu, T)/dT \quad , \quad (3.28)$$

we have, in analogy to Eq. (3.26),

$$1/l_R = k_R = \int k'(\nu) J(\nu) d\nu / \int J(\nu) d\nu \quad . \quad (3.29)$$

The difference in weighting of Planck and Rosseland means can give significantly different numerical values at a given temperature and density, and--as has been indicated at the beginning of this Section--they are used under different conditions.

Table 3-1 lists numerical values for  $k_P$  ( $\text{cm}^{-1}$ ) and  $l_R$  (cm) for high-temperature dry air, for a range of temperatures and densities of interest in the present application. Note that frequently  $k_P$  and  $1/l_R$  do not vary monotonically with the density ratio  $\rho/\rho_0$  and the temperature. While this comes in part from the fact that different species, of different absorption coefficients, are present at different density ratios at the same temperature, yet in part this non-linear behavior comes from the saturation of the curves of growth of the individual spectral lines which is discussed in Section 3.4 below--see in particular Fig. 3-5.

---

<sup>36</sup>  $s$  = distance along the path of the radiation and  $\theta$  = angle relative to normal.

<sup>37</sup> Note that the slab is not optically thin for angles  $\theta$  such that  $k_a(\nu) \Delta x / \cos\theta > 1$ , and thus the numerical factor  $a$  in Eq. (3.26) is equal to 1.8 rather than 2, as the direct analysis would suggest.

<sup>38</sup> Recall that  $\int B(\nu, T) d\nu = \sigma T^4$ .

<sup>39</sup> In an optically thick medium the temperature varies, so that  $J(\nu)$  depends on the temperature profile within the medium.

**Table 3-1. Planck Mean Absorption Coefficient and Rosseland Mean Free Path for Air at Different Temperatures and Densities (Source: Landshoff and Magee, 1969)**

**A. Planck Mean Absorption Coefficient,  $k_p$  ( $\text{cm}^{-1}$ )**

$\rho/\rho_0$	1	$10^{-3}$	$10^{-6}$
T= 2000 K	1.17E-4	1.15E-7	1.01E-10
4000 K	8.04E-4	4.70E-8	3.27E-12
6000 K	5.79E-3	4.83E-7	1.11E-11
9000 K	3.51E-5	1.13E-5	3.74E-9
12000 K	5.25E-1	3.37E-4	2.72E-9

**B. Rosseland Mean Free Path,  $l_R$  (cm)**

$\rho/\rho_0$	1	$10^{-3}$	$10^{-6}$
2000 K	2.06E+12	2.06E+15	2.05E+18
4000 K	1.45E+4	2.75E+8	3.63E+12
6000 K	6.41E+2	1.03E+7	5.00E+11
9000 K	5.41E+1	9.07E+5	3.98E+9
12000 K	1.29E+1	5.14E+4	5.63E+9

### 3.4 ATOMIC LINE RADIATION: TRANSITIONS, f-NUMBER AND ABSORPTION CROSS SECTION, LINE SHAPE, CURVES OF GROWTH

Line radiation provides a good introduction to a number of physical concepts that are very important in their application to the radiation from high-temperature air.

As a simple example, consider sodium vapor at low pressure. As the temperature increases, the vapor looks yellow because it radiates strongly in the Na doublet 589 nm to 589.6 nm. This is the transition: (cf., Radzig and Smirnov, 1985, p. 225)

		$\lambda$ (nm)	$A_{ul}(10^8 \text{ s}^{-1})$	$f_{lu}$	$g_u/g_l$
$3^2S_{1/2}$	- $3^2P_{1/2}$	589.6	0.61	0.32	2/2
	- $3^2P_{3/2}$	589.0	0.61	0.64	4/2

Here  $\lambda$  is the wavelength of the transition,  $A_{ul}$  is the Einstein transition probability ("A- coefficient") for the transition,  $f_{lu}$  is the "f-number" or oscillator strength, and  $g_u/g_l$  is the ratio of statistical weights of upper and lower states for this multiplet transition. These quantities will be defined and explained below. By adding the *f-numbers*,  $f_{lu}$ , of these two transitions we find  $f = 0.96 \cong 1$ .<sup>40</sup>

Electronic transitions involve changes in quantum numbers, and there are selection rules which determine the relative probability of a given transition. In atoms, the most probable transitions are those for which the total orbital angular momentum  $L$  changes by one unit, i.e.,  $\Delta L = \pm 1$ , while the spin angular momentum  $S$  does not change. These are called dipole-allowed transitions and are traditionally characterized by an oscillator strength or f-number,<sup>41</sup>  $f_{lu}$ . For such a dipole-allowed transition, first-order perturbation theory gives the result

$$f_{lu} = (16\pi^3 mc/3e^2 h) \nu(\text{Hz}) |(ulr)|^2, \quad (3.30a)$$

where the quantity  $(ulr)$  is the dipole transition matrix element for the electron coordinate  $r$ . In terms of the more general Einstein A-coefficient, we have

$$f_{lu} = 1.349 \times 10^{21} A_{ul} / \nu(ul)^2. \quad (3.30b)$$

<sup>40</sup> This means that in terms of the Old Quantum Theory (Bohr, 1914 pre-Quantum Mechanics) the Na D-line corresponds to the unique, deterministic jump of the valence electron outside the closed L-shell in Na into a lower orbit.

<sup>41</sup> In the old (Bohr) quantum theory, an atom is interpreted as radiating like an oscillating dipole, and from the "Correspondence Principle,"  $\sum_l f_{lu} = \sum_u f_{lu} = 1$ .

The formula (3.30) is discussed in Appendix C, which presents the relation between the Einstein A- and B-coefficients for spontaneous and stimulated radiation and the f-number.

For a dipole-forbidden transition we have

$$|\langle u|r|l\rangle|^2 = 0 \quad , \quad (3.31)$$

so that higher-order terms have to be used in Eq. (3.30b) rather than (3.30a). In this case, the  $A_{ul}$  coefficient is evaluated quantum mechanically for all lower states  $l$  accessible from a given excited upper state  $u$ , whose lifetime  $\tau_u$  is defined as

$$\tau_u = 1/\sum_l A_{ul} \quad . \quad (3.32)$$

Now we can define an effective f-number  $f_{\text{eff}}$  for the forbidden transitions by the analog to Eq. (3.30b) as

$$f_{\text{eff},lu} = 1.349 \times 10^{21} A_{ul} / \nu(u|l)^2 \quad . \quad (3.33)$$

For a dipole-forbidden transition of the type considered here, the standard relation (3.30a) between the dipole matrix element and the f-number does not hold, although formally Eq. (3.30b) can always be used to define an effective f-number  $f_{\text{eff}}$ , given an A-coefficient. Note that for the dipole-forbidden transitions of Table 3-2B the effective transition probabilities  $A_{ul}$  or  $f_{\text{eff}}$  are much smaller than for allowed transitions.

If there are  $n_l$  atoms per unit volume, each of absorption cross section  $\sigma_{lu}$ , then the absorption coefficient  $k_a(\nu) = n_l \sigma_{lu}(\nu)$ , when integrated over all frequencies contributing to this particular transition, gives the following result. The *line strength*  $S_{lu}$ , which in the integral of the absorption coefficient  $k_a(\nu)$  over the whole of a particular spectral line is defined in Appendix C by the relation

$$S_{lu} = \int k_a(\nu) d\nu = (\pi e^2/mc) n_{\text{abs}} = (\pi e^2/mc) n_l f_{lu} \quad , \quad (3.34a)$$

where  $\nu$  is frequency (Hz). In other words, the effective number of absorbing atoms is  $n_{\text{abs}} = n_l f_{lu}$ , so that  $f_{lu}$  is the fraction of atoms corresponding to absorption in the  $l \Rightarrow u$  transition. We can of course write Eq. (3.34a) in the equivalent form

$$\int \sigma_{lu}(\nu) d\nu = \pi c r_0 \int g(\nu) d\nu f_{lu} = \pi c r_0 f_{lu} \quad , \quad (3.34b)$$

where  $r_0 = e^2/mc^2 = 2.82 \times 10^{-13}$  cm = "classical radius of electron," and  $g(\nu)$  is a normalized spectral shape function for our transition, defined so that

$$\int g(\nu) d\nu = 1 \quad . \quad (3.34c)$$

The form of  $g(\nu)$  under different conditions will be discussed below .

Table 3-2(a) lists transition probabilities for some dipole-allowed transitions of H, N and O atoms, which all correspond to  $\Delta L = \pm 1$  (i.e., S  $\leftrightarrow$  P, P  $\leftrightarrow$  D, etc., but not S  $\rightarrow$  S or S  $\rightarrow$  D) and to  $\Delta S = 0$  (i.e., the multiplicities are the same for initial and final states). Table 3-2(b) lists transition probabilities for some dipole-forbidden transitions, for which either  $\Delta L = \pm 2$  (S  $\leftrightarrow$  D, etc.) or  $\Delta S$  changes (e.g.,  $^1D\text{-}^3P$ ,  $^2D\text{-}^4S$ , etc). Note that the well-known and important auroral red and green lines of atomic oxygen correspond to dipole-forbidden transitions. The point is that the allowed transitions of N and O are either in the VUV or in the NIR, while these forbidden transitions of N and O are in fact quite important because of the large column densities of N and O atoms along reasonable lines of sight, although their transition probabilities are much smaller than those of optically allowed transitions.<sup>42</sup>

Now we ask for the character of the shape function  $g(\nu)$ , which is typically large near the line center and falls off very rapidly to either side.

There are three principal contributors to the line width:

- a. *Natural line width.* As a result of the natural lifetime  $\tau_N$  of the upper state of the transition and the uncertainty principle, there is an energy width  $\Delta E_N = h/\tau_N$ , and thus a natural line width

$$\alpha_N = \Delta E_N/h = 1/2\pi\tau_N \quad . \quad (3.35)$$

- b. *Collision line width.* The upper state  $k$  of the transition is deactivated by collisions with other particles  $j$ , with number density  $n_j$ , collision cross section  $\sigma_j$ , and velocity  $u_j$

$$\alpha_{\text{Coll}} = (1/2\pi) \sum_j n_j \sigma_j u_j \quad . \quad (3.36)$$

---

<sup>42</sup> The intensity of a given transition is characterized either in terms of the Einstein A-coefficient or the oscillator strength or f-number.

**Table 3-2. Transition Probabilities  $A_{ul}$ , Lifetimes  $\tau_u$ , and Absorption Oscillator Strengths  $f_{lu}$  for Low-Lying Atomic States**

(a) Allowed Transitions (Data from Radzig and Smirnov, 1985, p. 225)

Atom (ground state)	Transition (l-u)	Wavelength $\lambda$ (nm)	$A_{ul}$ ( $10^8 \text{sec}^{-1}$ )	$f_{lu}$	$g_u/g_l$
H( $1^2S$ )	1S-2P	121.57	6.26	0.416	6/2
	3P	102.57	1.67	0.0791	6/2
	4P	97.25	0.681	0.0290	6/2
	2S-3P	656.27	0.225	0.435	6/2
	4P	486.13	0.0967	0.103	6/2
	2P-3S	656.29	0.0631	0.0136	2/6
	3D	656.28	0.647	0.696	10/6
	4S3	486.14	0.0258	0.00305	2/6
4S	486.13	0.206	0.122	10/6 sic	
N( $2p^3\text{-}4S_{3/2}$ )	$2^4S_{3/2}$ - $3s^4P$	120	4.2	0.27	12/4
	$2p^4$ $4P$	113.4	1.36	0.080	12/4
	$2p^3$ $2D$ - $3s$ $2P$	149.3	3.4	0.07	6/10
	$3s'$ $2D$	124.3	3.6	0.08	10/10
O( $2p^4\text{-}3P_2$ )	$2p^4$ $3P$ - $3s^3S$	130.4	6.0	0.05	3/9
	$3d$ $3D$	102.7	0.4	0.01	15/9
	$3s$ $5S_2$ - $3p$ $5P$	777.4	1.0	2.7	15/5
	$3s$ $3S_1$ - $3p$ $3P$	844.7	0.28	0.9	9/3

(b) Dipole-Forbidden Transitions

Atom	Transition	$\lambda$ (nm)	Life Time (sec)	$A_{ul}$ ( $\text{sec}^{-1}$ )	$f_{\text{eff},lu}$
O( $2p^4$ )	$1S$ - $1D$	557.7	0.74	1.35	$6.3 \times 10^{-9}$
	$1D$ - $3P$	630.0	110	$9.09 \times 10^{-3}$	$5.5 \times 10^{-11}$
		636.4			
N( $2p^3$ )	$2D$ - $4S$	520.0	$9.4 \times 10^4$ (26 hrs)	$1.07 \times 10^{-5}$	$4.3 \times 10^{-14}$
	$2P$ - $2D$	1040.0	12	$8.33 \times 10^{-2}$	$1.4 \times 10^{-9}$

- c. *Doppler line width.* Because the radiating atom moves with thermal velocity  $(2kT/M)^{1/2}$ , there is a mean width

$$\alpha_D = (v_0/c) (2kT/M)^{1/2}, \quad (3.37)$$

where  $v_0$  is the center line frequency, T the temperature, and M the appropriate atomic mass.

Representative values for  $\alpha_N$ ,  $\alpha_{Coll}$  and  $\alpha_D$  as a function of altitude in the earth's atmosphere are given in Fig. 3-4. (These calculations were actually done for vibrational CO<sub>2</sub> lines in the 4.3  $\mu$ m band, rather than for electronic transitions.) Note that  $\alpha_N$  is typically very small, while  $\alpha_{Coll}$  is large at high densities and predominates in the earth's upper atmosphere at altitudes below 18 km; at higher altitudes (lower densities) Doppler broadening determines the line width. Goody (1964, p. 99) examines line shapes in more detail, and concludes that for different spectral lines the altitude above which Doppler broadening predominates over collision broadening ranges from 7 km to 37 km.

These different mechanisms lead to different line shape function  $g(\nu)$  of Eq. (3.34). Natural and collision broadening lead to a *Lorentz line shape*

$$g_L(\nu) = (\alpha_L/\pi) / [(\nu-\nu_0)^2 + \alpha_L^2], \quad (3.38a)$$

where  $\alpha_L = \alpha_N + \alpha_{Coll}$ , while Doppler broadening leads to a *Gaussian shape*

$$g_D(\nu) = (1/\alpha_D\pi^{1/2}) \{ \exp - [(\nu-\nu_0)^2 / \alpha_D^2] \}. \quad (3.38b)$$

The combination of Doppler and Lorentz broadening gives rise to a "Voigt" line shape--see e.g., Unsoeld, 1955, p. 258f, or Arnold et al., 1969, esp. p. 783.

What is of considerable interest is how the effective absorption coefficient changes with optical thickness, the so-called *Curve of Growth*<sup>43</sup>. Let us define a mean absorptance  $A_{av}$ <sup>44</sup> for a representative spectral line in a band by the relation

$$A_{av} = (1/\delta) \int [1 - e^{-k(\nu, d)}] d\nu, \quad (3.39)$$

where  $\delta$  = mean line spacing in band and  $d$  = geometrical thickness of radiating medium.

<sup>43</sup> This discussion is very sketchy: what is important is the result given in the final paragraph of this section. A more detailed discussion is given, e.g. in Aller, 1963, pp. 359-376.

<sup>44</sup> The absorption coefficient A must not be confused with the Einstein A-coefficient.

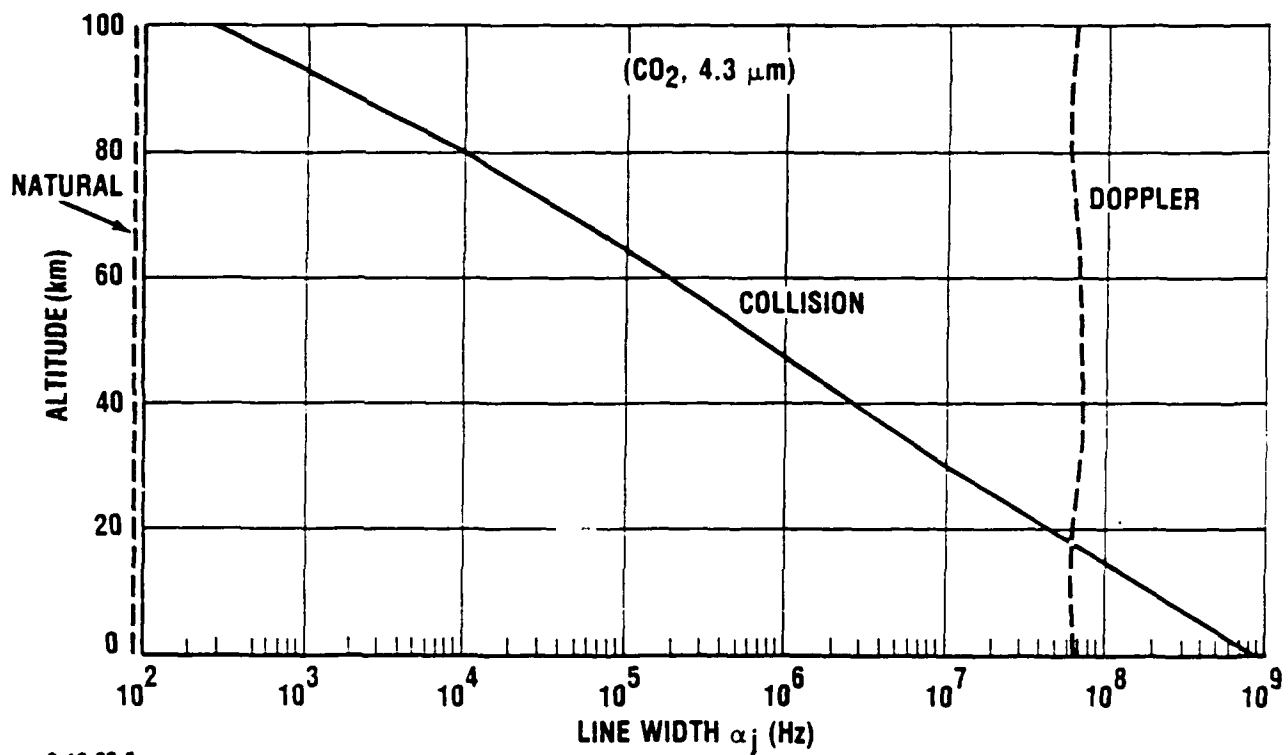


Figure 3-4. Natural, Collision, and Doppler Line Widths versus Altitude  
(Calculations Done for Lines in the 4.3 μm Band of CO<sub>2</sub>)

We now ask for the variation of  $A_{av}$  with the integrated optical thickness<sup>45</sup>

$$X = S d = \int k_a(\nu) d \nu = n_l f_{lu} d \pi r_0 c \quad , \quad (3.40)$$

where there are  $n_l$  atoms per unit volume in the lower (absorbing) state. Figure 3-5 shows the curve of growth, which is the general character of the absorption coefficient as a function of integrated optical thickness  $S d/\alpha_D$  and of the ratio  $2\alpha_L/\alpha_D$  of Lorentz broadening to Doppler broadening. Branch QA corresponds to the optically thin case for which

$$A_{av}(\text{opt. thin}) \sim S d \sim n_l f_{lu} d \quad . \quad (3.41a)$$

Branch QB corresponds to the Doppler limit. Because of the Gaussian line shape the absorption saturates rapidly and increasing  $(S d)$  changes  $A_{av}$  very little, only

$$A_{av}(\text{Doppler}) \sim \sqrt{\log(n_l f_{lu} d)} \quad . \quad (3.41b)$$

Branch QC corresponds to the Lorentz case. Because of the wider wings for this line shape,  $A_{av}$  increases relatively rapidly with  $S d$  or  $n_l f_{lu} d$

$$A_{av}(\text{Lorentz}) \sim (n_l f_{lu} d)^{1/2} \quad . \quad (3.41c)$$

Note, however, that the limit QD, with  $A_{av} \sim (n_l f_{lu} d)$  for large optical thickness, is not physically realistic.

The discussion should be referred to Section 3.3.1 [see in particular Eqs. (3.11) and (3.12)] for the two limits of optically thick and optically thin gas parcels. Typically, for optically thin parcels the spectral radiance is proportional to the optical thickness or to the total number of atoms in the path, while for optically thick parcels the spectral radiance tends to a black-body radiance. *Note that the total absorption and radiance due to a Doppler-broadened line increases extremely weakly with increasing optical depth because a Gaussian profile has such extremely small absorption in the line wings. By contrast, a Lorentz line has very broad wings and so the spectral radiance increases far more rapidly with increasing optical depth.* In either case, the blackbody limit is evidently attained only asymptotically.

---

<sup>45</sup> The optical thickness  $X$  is equal to  $k_a' x$  of Section 3.3.1.

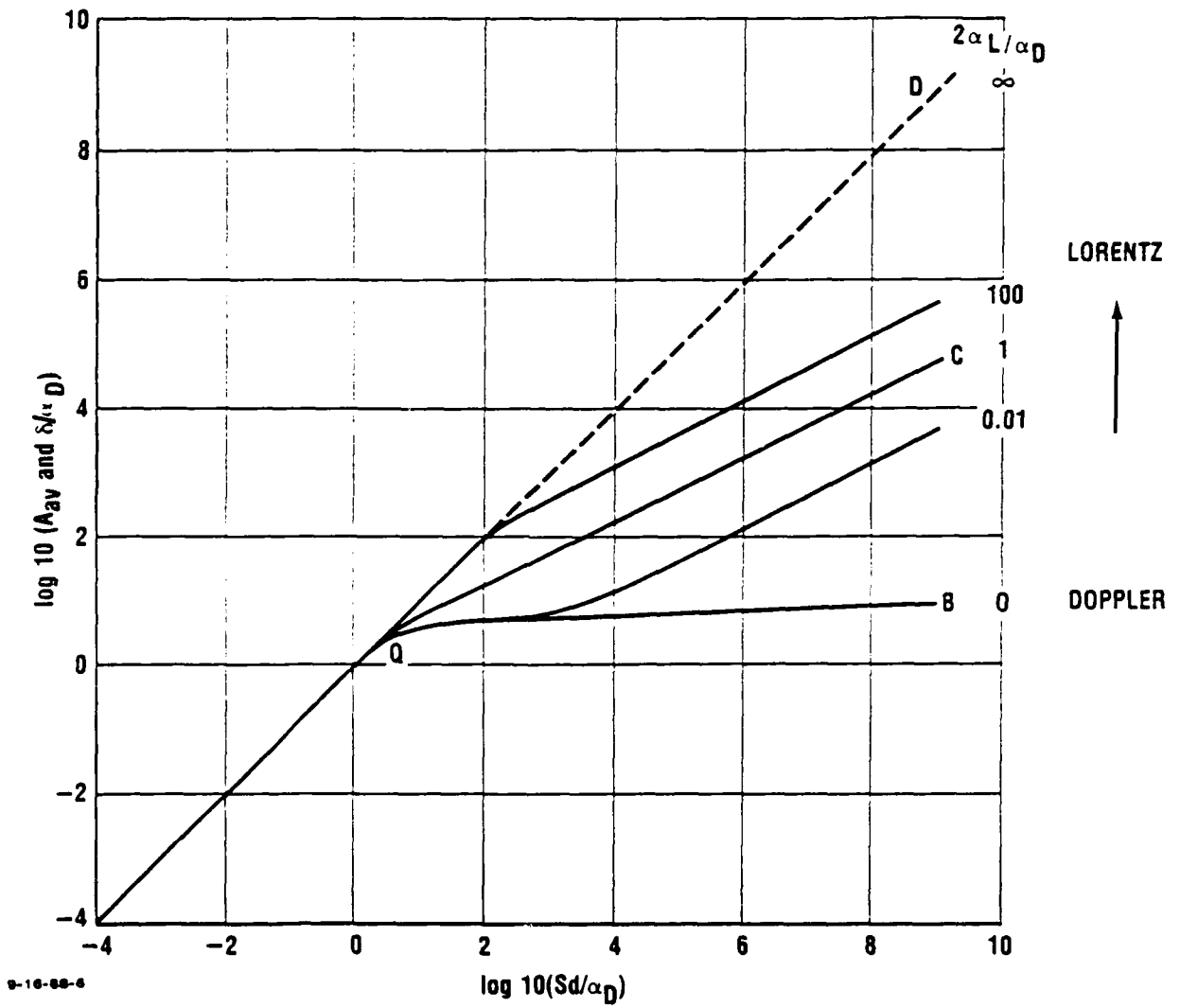


Figure 3-5. Curves of Growth of Spectral Lines for Combined Doppler and Lorentz Broadening.

### 3.5 MOLECULAR BAND RADIATION

In contrast to atomic spectral lines, which correspond to the transition between two electronic states, each of (fairly) sharply defined energy  $E_U$  and  $E_L$  so that there is a line of frequency

$$\nu(u,l) = (1/h) (E_U - E_L) \quad , \quad (3.42)$$

an electronic state for a molecule is characterized by vibrational quantum number  $v$  and rotational quantum number  $J$  as well as by the quantum numbers and symmetry factors that characterize the electronic state. Because the nuclear mass is so much larger than the electronic mass, the motions of electrons and nuclei can be decoupled--the electrons are treated as moving in the field of temporarily stationary nuclei, while the nuclei move in the smeared-out field of the electrons. This is called the *Born-Oppenheimer approximation*. The wave function is written as the product of electronic and vibrational/rotational wave functions. One application of this is provided by Gilmore's potential energy curves for the air molecules (see Figs. 2-5 to 2-7). The energy of a given molecular state can be written as the sum of electronic, vibrational, and rotational contributions

$$E(\text{mol}) = E(\text{electronic}) + \omega_e (v + 1/2) + B_e J(J+1) \quad , \quad (3.43)$$

where typically  $E(\text{electronic}) \sim 1-5 \text{ eV}$ ,  $\omega_e \sim 2000 \text{ cm}^{-1}$  ( $\sim 0.25 \text{ eV}$ ),  $B_e \sim 1 \text{ cm}^{-1}$  to  $2 \text{ cm}^{-1}$  ( $1.2 \times 10^{-4} - 2.4 \times 10^{-4} \text{ eV}$ ). The vibrational states differ by  $\sim 2000 \text{ cm}^{-1}$  and have rotational structure ( $\Delta J = 0, 1, 2, \dots$ ) with spacing  $2 B_e \sim 1-5 \text{ cm}^{-1}$ . It follows from this that since a given molecular electronic state corresponds to numerous vibrational and rotational levels, a transition between two molecular electronic states involves very many spectral lines characterized by the vibrational and rotational quantum numbers of upper and lower electronic states. Typically, the population of highly vibrationally excited states will be small, but the population of highly rotationally excited states (with rotational quantum numbers up to 30) will be large. Thus, we recognize that a molecular electronic transition is not characterized by a single spectral line, but by an array involving thousands of spectral lines of varying strength and width. In fact, there is a great deal of structure to these arrays, which are described as spectral bands.

Some excellent photographs of molecular electronic band spectra are given in Herzberg, 1950, Ch. II. They show a great richness of phenomena and both coarse and fine spectral structure. The coarse, banded structure ( $\sim 2000 \text{ cm}^{-1}$ ) is due to molecular vibrations, while the fine structure due to molecular rotational lines has lines spaced  $1 \text{ cm}^{-1}$

to  $5 \text{ cm}^{-1}$  apart. In general, the vibrational structure has a "sawtooth" character, falling off rapidly towards one side (either toward higher or lower frequency) while its rate of decline toward the other side is much slower. A typical electronic band system covers perhaps  $10,000\text{-}20,000 \text{ cm}^{-1}$  ( $\sim 100 \text{ nm}$  in the visible), so that it has  $\sim 10,000$  individual lines, of varying spacing and strength. From the discussion of Section 3.4 we see that in the lower atmosphere (below  $10 \text{ km}$  to  $40 \text{ km}$ ) most spectral lines are collision broadened with a typical line width  $\sim 0.01\text{-}0.1 \text{ cm}^{-1}$  (see Goody, 1964, p. 99).

In the IR there are molecular vibration-rotation bands due to molecules such as NO, CO,  $\text{CO}_2$ ,  $\text{H}_2\text{O}$ ,  $\text{O}_3$ , etc. The systems typically cover  $1000 \text{ cm}^{-1}$ , so that they have perhaps 1000 or less important lines each, but because of the differing symmetry of these various molecules, and more particularly because of the applications of interest, it is often desirable or necessary to treat the lines in real detail.

To compute the transition probability for a molecular transition, one again uses the Born-Oppenheimer separation of electronic and nuclear motions, in which the molecular wave function is described as the product of an electronic and a vibrational wave function.<sup>46</sup> For an *electronic* transition, the transition probability is represented in terms of the transition dipole matrix element  $(u|r|l)$  where  $r$  = electronic coordinate [see Eq. (3.30a)] as

$$\text{Transition probability} \sim f_{lu} q_{vv'} \quad , \quad (3.44)$$

where  $f_{lu}$  is an *electronic*  $f$ -number and  $q_{vv'}$ , the *Franck-Condon factor*, is the mean squared overlap of *vibrational* wave functions between initial and final states. This satisfies the conditions

$$\sum_v q_{vv'} = \sum_{v'} q_{vv'} = 1 \quad . \quad (3.45)$$

If the mean internuclear separation of a molecule in its initial and final electronic states is very similar, the vibrational overlap or Franck-Condon factor  $q_{vv'}$  is largest if  $\Delta v = 0$ , with transitions with  $\Delta v = 1, 2$ , having successively smaller Franck-Condon factors. However, as  $v$  increases, the overlap for  $\Delta v = 0$  decreases and so does the transition probability and intensity of the appropriate spectral lines. All this structure is implicit in the energy expression of Eq. (3.43) and the Born-Oppenheimer separation, and it gives rise to the structure of molecular bands. In analogy to the definition of an atomic

---

<sup>46</sup> From the correspondence principle, the rotational quantum numbers are so large that the rotation can be treated classically, except for  $\text{H}_2$ , HD, and  $\text{D}_2$  at low temperatures.

line strength  $S_{lu}$  of Eq. (3.34a), the transition probability for a band system is normally described in terms of the integrated band intensity  $S_{lu}$

$$S_{lu} = \int k(\nu) d\nu \text{ (cm}^{-2} \text{ atm}^{-1}) \text{ ,} \quad (3.46)$$

or equivalently, a band f-number, which is related to the band strength by the relation

$$S_{lu} = 2.3795 \times 10^7 f_{lu} \text{ .} \quad (3.47)$$

Appendix C presents the numerical factors in terms of fundamental constants and ties the various parameters together in a schematic way.

As in the case of an atomic transition, there are selection rules for molecular transitions, but these are naturally more complex because there are so many more quantum numbers and other symmetries involved.

For *electronic* transitions of diatomic molecules, we have the selection rules<sup>47</sup>:

$$\Delta\Lambda = 0, \pm 1 \text{ (}\Sigma \rightarrow \Sigma; \Sigma \rightarrow \Pi; \Pi \rightarrow \Pi, \text{ but not } \Sigma \rightarrow \Delta) \quad (3.48)$$

$$\Delta S = 0 \text{ (}n\Lambda \rightarrow n'\Lambda' \text{ only if } n' = n) \quad (3.49)$$

$$+ \Leftrightarrow -, \text{ not } + \Rightarrow +; - \Rightarrow - \quad (3.50)$$

$$g \Leftrightarrow u, \text{ not } g \Rightarrow g, u \Rightarrow u \text{ .} \quad (3.51)$$

For *vibrational* transitions within a given electronic state, things are quite different. A homogeneous diatomic molecule like  $N_2$  or  $O_2$  has no dipole moment, so that there are no transitions between different vibrational levels. For a heteronuclear diatomic molecule like  $NO$ , the selection rule  $\Delta v = \pm 1$  is only weakly obeyed because molecules do not behave completely like harmonic oscillators for which this selection rule holds rigorously.

For *rotational* transitions in homonuclear diatomic molecules, the selection rule  $\Delta J = \pm 1$  is strictly obeyed.<sup>48</sup>

Table 3-3(a) lists characteristics for some important electronic transitions in diatomic air molecules which are mainly in the UV and visible, and Table 3-3(b) lists similar characteristics for vibrational transitions, which are always in the IR. Table 3-3(a) presents a minimal characterization of six electronic band systems used for an approximate

<sup>47</sup> See Appendix A for a discussion of the various quantum numbers and other symmetry parameters.

<sup>48</sup> Pure rotational transitions are normally in the millimeter wave spectral region which is not normally of interest here, but rotational structure occurs in vibrational and electronic band systems.

Table 3-3. Some Characteristics of Important Molecular Band Systems of Air<sup>49</sup>

(a) Electronic Transitions

Band System	Wavelength ( $\mu\text{m}$ )	$S_{\text{band}}(\text{cm}^{-2} \text{atm}^{-1})$	$f_{\text{IU}}$
$\text{N}_2$ (First Positive, $\text{B}^3\Pi \rightarrow \text{A}^3\Sigma$ )	0.52-1.1	$6.7 \times 10^4$	0.0028
$\text{N}_2$ (Second Positive, $\text{C}^3\Pi \rightarrow \text{B}^3\Pi$ )	0.30-0.47	$1.0 \times 10^6$	0.043
$\text{N}_2^+$ (First Negative, $\text{B}^2\Sigma \rightarrow \text{X}^2\Sigma$ )	0.34-0.52	$8.3 \times 10^5$	0.035
$\text{O}_2$ (Schumann-Runge, $\text{B}^3\Sigma \rightarrow \text{X}^3\Sigma$ )	0.19-0.43	$(6 \times 10^6)$	0.17-0.34 $\lambda$
NO (Beta, $\text{B}^2\Pi \rightarrow \text{X}^2\Pi$ )	0.21-0.52	$1.3 \times 10^5$	0.0053
NO (Gamma, $\text{A}^2\Sigma \rightarrow \text{X}^2\Pi$ )	0.19-0.28	$5.9 \times 10^4$	0.0025

Note:

- the wavelength range is representative only
- $S_{\text{band}}$  (which is sometimes called  $S_{\text{IU}}$ ) has some temperature dependence.
- $f_{\text{IU}}$  is sometimes described as absorption f-number,  $f_{\text{abs}}$ , to distinguish it from the emission f-number  $f_{\text{U}}$  [see Appendix C, Eq. (C.10)].
- Note that the f-number for the  $\text{O}_2$  Schumann-Runge band has a strong wavelength dependence ( $\lambda$ -values in  $\mu\text{m}$ ):

$$f_{\text{IU}} = 0.10 \text{ at } \lambda = 0.2 \mu\text{m}$$

$$f_{\text{IU}} = 0.034 \text{ at } \lambda = 0.4 \mu\text{m}.$$

<sup>49</sup> These data are compiled from various sources and should be considered as representative only. For more up-to-date values of electronic transitions (Part (a)) see Kuz'menko et al, 1979; and for vibrational transitions (Part (b)), see Kennealy & Del Greco, 1983.

Table 3-3. (continued)

(b) Vibrational Transitions

Molecule	v -> v'	Wavelength ( $\mu\text{m}$ )	S <sub>band</sub> ( $\text{cm}^{-2} \text{atm}^{-1}$ )	f <sub>lu</sub>
CO	0-> 1	4.67	260	$1.09 \times 10^{-5}$
	0-> 2	2.34	1.79	$7.5 \times 10^{-8}$
NO	0-> 1	5.33	110	$4.7 \times 10^{-6}$
	0-> 2	2.69	1.3	$5.4 \times 10^{-8}$
OH	0-> 1	2.8	100	$4.0 \times 10^{-6}$
	0-> 2	1.4	4.0	$1.7 \times 10^{-7}$
CO <sub>2</sub>	000-> 010	15	187	$7.9 \times 10^{-6}$
	000-> 001	4.3	2700	$1.14 \times 10^{-4}$
	000-> 101	2.69	39	$1.6 \times 10^{-6}$
	000-> 201	2.0	1.0	$4.0 \times 10^{-8}$
H <sub>2</sub> O	000-> 010	6.27	300	$1.3 \times 10^{-5}$
	000-> 001	2.66	100	$4.5 \times 10^{-6}$
	000-> 011	1.88	30	$1.3 \times 10^{-6}$
	000-> 101	1.38	20	$8.0 \times 10^{-7}$
	000-> 111	1.14	0.6	$2.5 \times 10^{-8}$
O <sub>3</sub>	000-> 001	9.6	260	$1.1 \times 10^{-5}$

description of the radiation from high-temperature air. These (electronic) f-numbers are quite small ( $10^{-2}$ - $10^{-1}$ ) compared to the f-numbers for the Na-D or H-Ly- $\alpha$  lines, but they are in the general range of the allowed atomic transitions shown in Table 3-2(a).<sup>50</sup> Note that while five of the six band systems in Table 3-3(a) are relatively well-behaved, the O<sub>2</sub> Schumann-Runge system is anomalous, covering a very wide spectral range and having both a wavelength-dependent f-number and a very non-diagonal Franck-Condon array. The reason for this is that the internuclear separation of the O<sub>2</sub> B and X states is quite different (1.60 and 1.21 Å respectively)--see Herzberg, 1950, p. 560, and also Fig. 2-7.

Because of their symmetry, homonuclear diatomic molecules like N<sub>2</sub> and O<sub>2</sub> do not have IR active vibration-rotation transitions,<sup>51</sup> but NO and the triatomic species CO<sub>2</sub>, H<sub>2</sub>O, O<sub>3</sub>, N<sub>2</sub>O, and NO<sub>2</sub> are important radiators in the infrared which are indicated in Table 3-3(b). Note that the transition probabilities (f-numbers) for the vibration-rotation bands are significantly smaller than those for electronic bands.

How the band structure of a given molecular transition in a specified spectral range is treated depends on the particular application. Thus, if one asks for the emission from high-temperature gases at low spectral resolution, very little detail is necessary. In particular, for an optically thin situation when self-absorption and scattering are unimportant so that a Planck-type mean [see Eq. (3.27)] is all that one needs, the total integrated intensity suffices. Thus, the description in terms of electronic system f-numbers with vibrational structure analyzed in terms of a Franck-Condon factor is satisfactory for determining the total radiation from air or combustion products at high temperatures.

However, if one asks for the atmospheric transmittance through 1 km to 10 km path lengths (or through the whole atmosphere in vertical viewing), especially at high spectral resolution in the IR, where there are numerous absorption regions alternating with "windows," much more detail is needed. One example of this is when one views not a gray body through a long atmospheric path, but rather a rocket plume or other array of hot CO<sub>2</sub> and H<sub>2</sub>O gas viewed through the atmosphere containing cold H<sub>2</sub>O and CO<sub>2</sub> gas, or for laser transmission at very high spectral resolution.

---

<sup>50</sup> The reason why these f-numbers for given transitions are small is that the upper states radiate into a large number of lower-lying states over a wide spectral range: it is unusual for upper states such as Na (3<sup>2</sup>P) to radiate into just one lower state (here 3<sup>2</sup>S).

<sup>51</sup> But they do have Raman spectra, which, however, are not discussed here.

During the 1950s and 1960s a number of *Band Models* were devised and tested against experiment. These models use lines of equal or random spacing, of uniform or varying strength, sometimes with a configuration like the "Q-Branch" of a band [see, e.g., Herzberg (1950), p. 48, etc.]. Two limits are the weak- and strong-line approximations. In the *weak-line limit* the line is optically thin, even at the line center, so that the emission or absorption is proportional to the number of molecules in the path [ $A_{av} \sim (Nfd)$ --see Eq. (3.41a) or branch AQ of Fig. 3-5]. By contrast, in the *strong-line limit* the line is optically thick at the center, so that increasing the number of molecules in the path simply increases the emission or absorption in the line wings, and of course this gives a different variation of absorption  $A_{av}$  with  $Nfd$ , depending on the line shape (Doppler, Lorentz, or Voigt, see Fig. 3-5); the strong-line approximation traditionally corresponds to the Lorentz-line limit  $A_{av} \sim (Nfd)^{1/2}$  [cf. Eq. (3.41c), or branch QC in Fig. 3.5]. For a review of band models, see, e.g., Goody, 1964, Ludwig et al., 1973.

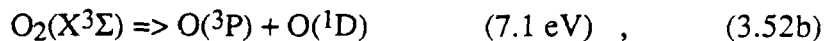
With the great increase in computer power over the last 20 years, it has become feasible to describe vibration-rotation bands in the IR by a line-by-line analysis, rather than by using band models. Note, however:

- (a) For electronic transitions, it is still frequently convenient to use band models rather than line-by-line descriptions, e.g., in the AFGL FASCODE transmission code, because of the very large number of spectral lines.
- (b) For many applications, it is convenient to describe vibration-rotation bands by band models rather than by line-by-line analyses, partly because it is quicker and partly because the detailed input data needed for line-by-line treatments is not available. Thus, in the 1970s an Atlas of Spectral Lines was developed at AFGL. By now this Atlas (Rothman et al., 1987) contains in excess of 350,000 individual lines, and in the IR line-by-line calculations can now be carried through for computations which could not have been considered 20 years ago, by using the FASCODE computer program. However, this HITRAN listing is quantitatively correct only up to  $\sim 600$  K; at higher temperatures there are many more spectral lines of importance. Thus, while FASCODE may give reasonable-appearing results for high-temperature air and other species, yet some important collections of lines will be missing. The HITEMP compilation consisting of  $\text{CO}_2$  and  $\text{H}_2\text{O}$  lines in selected absorption bands for temperatures up to 1000 K to 1500 K is being prepared at AFGL, but has not yet been published.

Let us now present some figures for the absorption cross sections of various molecules. Figure 3-6 shows the O<sub>2</sub> absorption coefficient in the far UV spectrum. O<sub>2</sub> can dissociate into two ground state (<sup>3</sup>P) oxygen atoms:

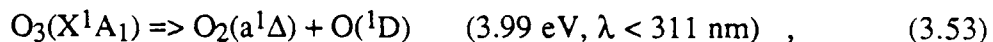


for  $\lambda < 242$  nm (5.1 eV = O<sub>2</sub> dissociation energy) and the weak Herzberg continuum is found there. The Schumann-Runge (SR) bands fall generally from 175 nm to 195 nm: below 175 nm (7.1 eV) there is the strong Schumann-Runge continuum:



and below ~ 130 nm the O<sub>2</sub>(X<sup>3</sup>Σ) molecule can dissociate into O(<sup>3</sup>P) + O(<sup>1</sup>S). Figure 3-6 shows the short wavelength portion of the SR band system (for  $\lambda > 175$  nm) and the SR continuum (140 nm to 175 nm). For  $\lambda < 125$  nm there is evidently at least one more band system, but this is not important for our purposes. At longer wavelengths the cross sections become smaller with a threshold ( for the Schumann-Runge B → X transition) at 242 nm.

Figure 3-7 shows the ozone spectral absorption in the visible and the near UV. The strongest system is the Hartley system which includes the photodissociation of the non-linear ozone molecule



which is very important for the absorption of solar UV in the earth's atmosphere. Figure 3-7(a) shows the cross section of O<sub>3</sub> in the near-UV; the strong Hartley system lies below  $\lambda = 300$  nm, while the longer-wave tail (i.e.,  $\lambda > 300$  nm) is known as the (weak) Huggins system (C-X). Ozone also absorbs in the orange/red portion of the visible: the weak Chappuis (B-X) absorption cross section is shown in Fig. 3-7(b).

By comparing the maximum absorption cross section in Figs. 3-6 and 3-7, we see that a strong absorption corresponds to a cross section of 10<sup>-18</sup> to 10<sup>-17</sup> cm<sup>2</sup>, while a weak absorption is down by perhaps a factor 10 to 100.

### 3.6 ATOMIC RADIATION IN GENERAL: FREE-FREE, FREE-BOUND, BOUND-BOUND

We have given a rather careful and detailed discussion of the effective spectral absorption arising from a single atomic spectral line, and from the electronic band system of a diatomic molecule, which is an array of separate lines. Individual atomic lines are not

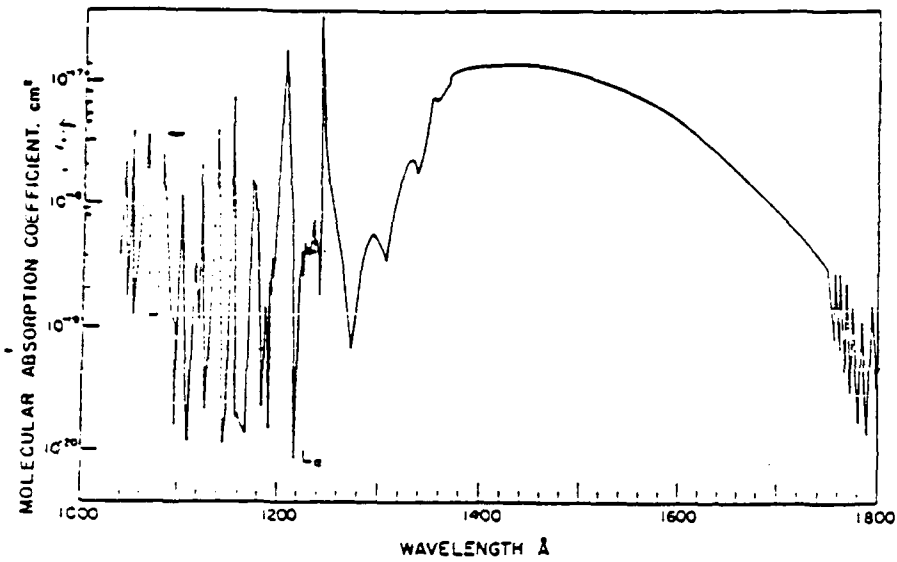
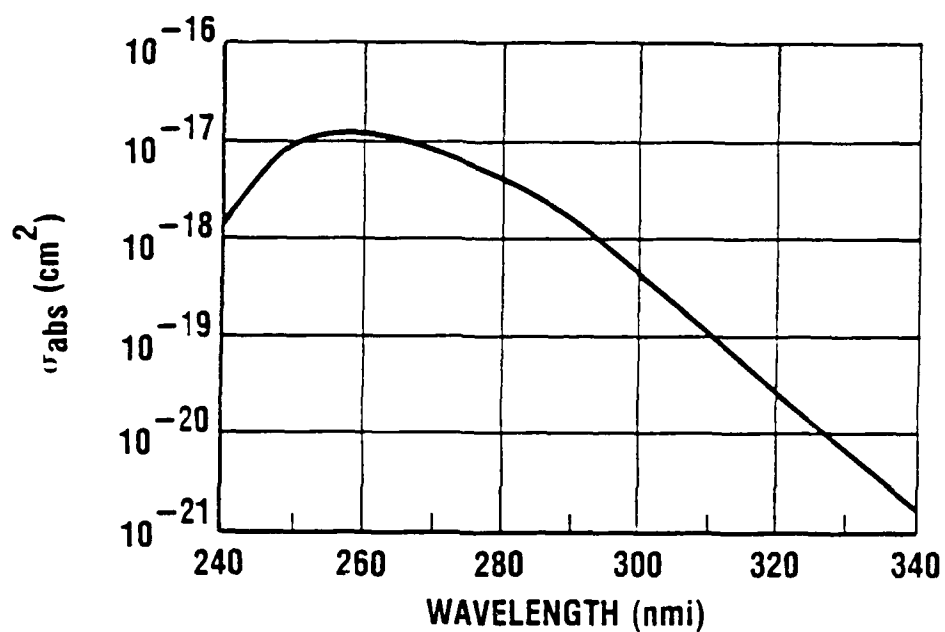
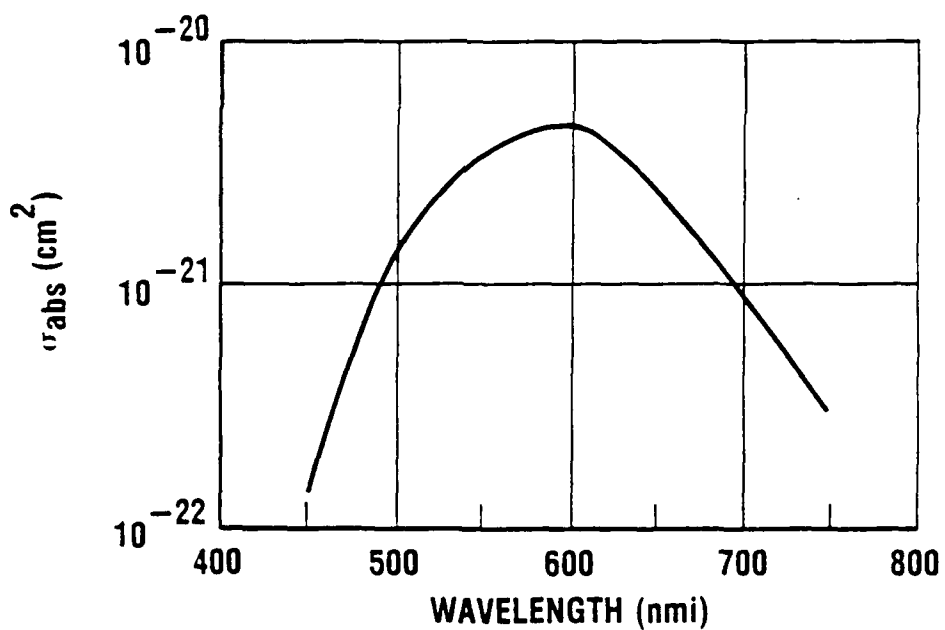


Figure 3-6. O<sub>2</sub> Absorption Cross Section in the UV.  
(Source: Watanabe, 1958)



(a)



(b)

3-16-88-8

Figure 3-7. O<sub>3</sub> Absorption Cross Section:  
 (a) UV (conventionally one speaks of the Hartley system below 300 nm and the Huggins system at longer wavelengths);  
 (b) Chappuis system in the Visible.  
 (Source: Vigroux, 1953--see also Goody, 1964)

particularly important from the standpoint of energy transfer involving blackbody radiation because a line is so narrow that the total energy carried within its width is a small fraction of the total Planck spectrum, and, further, it takes very few atoms to saturate a spectral line.<sup>52</sup> However, at temperatures above 6000 K, the N and O (and other) atoms have a sufficiently large number of lines and continua that their radiation is important.

From the standpoint of the overall thermal radiation from high-temperature air, one is most interested in absorbers covering a wide spectral interval, either arrays of individual spectral lines (such as molecular band spectra, which have been discussed in Section 3.5) or in continua, which are discussed here. The cross sections involved here are typically very small, but the large available column densities of potential absorbers more than make up for the narrow spectral interval covered by atomic resonance lines.

A typical atomic energy level diagram is shown in Fig. 3-8. Note that there are a number of discrete levels 0,1,2,3,... which cluster towards an ionization limit J and which make up the discrete spectrum D: transitions "a" and "b" belong to the discrete spectrum, and may be called *bound-bound transitions*. Above the ionization limit J all energy values are allowed, giving the continuous spectrum C.<sup>53,54</sup> Transitions involving at least one state in the continuum are not characterized by sharp spectral lines, because all energy values in the continuum are available. We distinguish between transitions involving one bound state and one free state, such as "c", which is a *free-bound transition*, and transitions whose initial and final states are both in the continuum, such as the *free-free transition* "d".

What is the physical meaning of these transitions? The free-bound transition "c" corresponds to a radiative ionization/deionization process:



<sup>52</sup> For instance, consider the Na-D line, actually a doublet at 589.0-589.6 nm. At STP, the collision line width is given by Eq. (3.36) as  $\alpha_{\text{Coll}} \sim 10^9$  Hz, and thus from Eq. (3.34b) we have  $\sigma_{\text{abs}} \sim 10^{-11}$  cm<sup>2</sup> within a line of 0.001 nm of both 589.0 and 589.6 nm. Now, if the number density of Na is just  $10^{-6}$  times ambient, then the line is optically thick already in a path length of 4 cm. Molecular and continuum cross sections are in the range  $10^{-20}$  to  $10^{-18}$  cm<sup>2</sup>, but this is clearly quite sufficient for the line center to be optically thick for a path going through a significant fraction of the atmosphere.

<sup>53</sup> Notice the narrow region K just below the ionization limit J. Here there are closely-spaced discrete (i.e., bound) levels, but at sufficiently large density or high temperature where the levels are broadened sufficiently so that the level width is greater than the level spacing gives rise to a quasi-continuous spectrum or an effective reduction in the ionization potential.

<sup>54</sup> There are also auto-ionizing discrete states which have structure above the ionization limit.

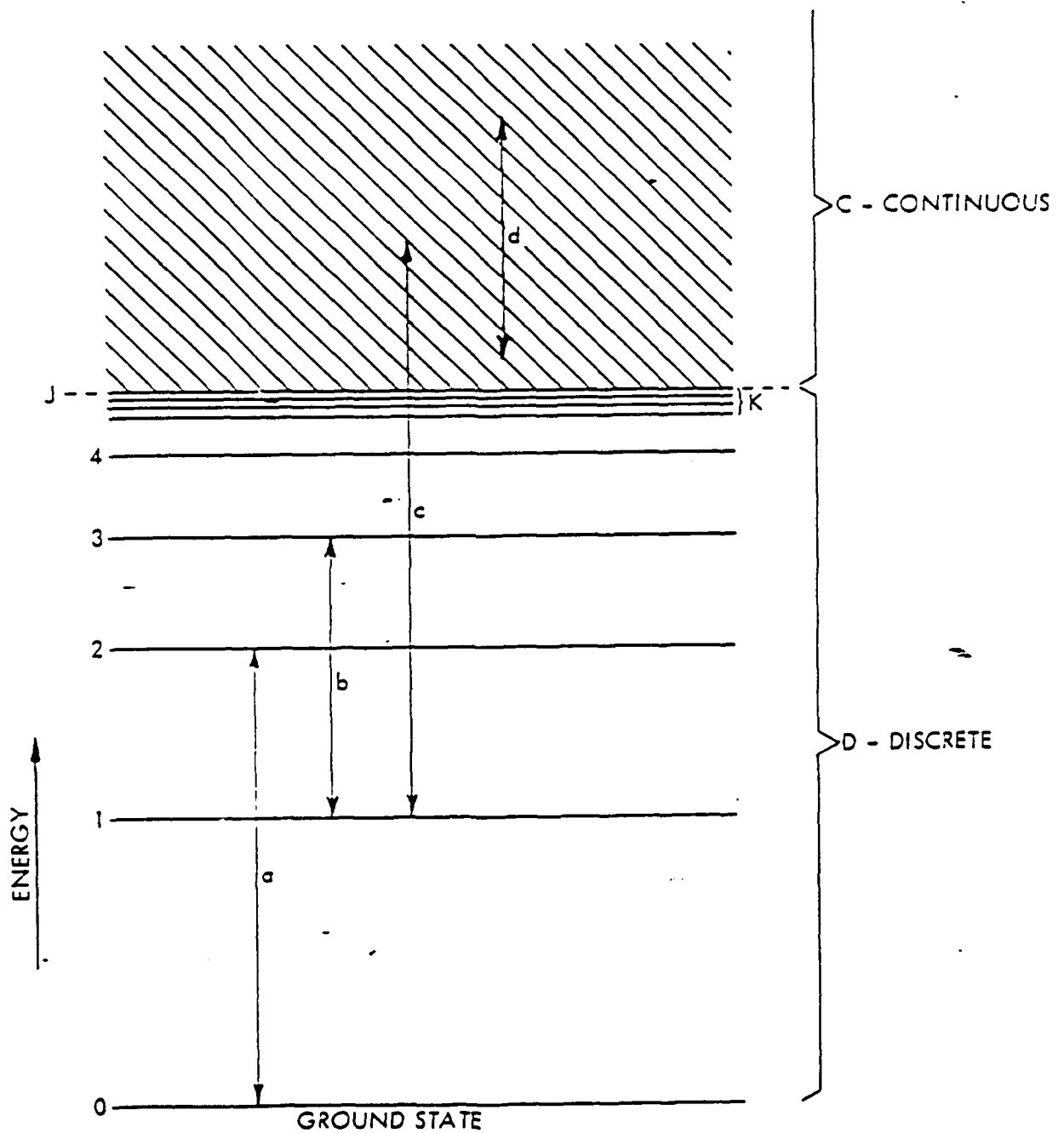
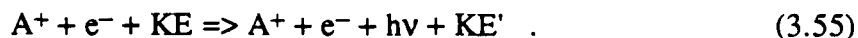


Figure 3-8. Continuous and Discrete Levels in an Atomic Spectrum.

while a free-free transition corresponds to the interaction of a free electron with an  $A^+$  ion, in which the electron is decelerated in the field of the ion, radiating its excess energy as a light quantum:

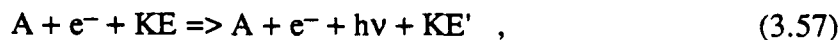


This *Bremsstrahlung* is of considerable importance in the context of air opacity, especially since the effect is observed also for an electron in the field of a neutral atom with which it interacts by polarization or other shorter-range interactions.

In practice, one treats all these continuum terms together--the free-free, free-bound as well as the closely spaced lines corresponding to the series limit region K, and for the case of a hydrogen-like atom (which has one electron outside a nucleus of charge  $+Ze$ ) the expression for the total radiance  $L(\lambda, T)$  due to all these three terms has a simple form:

$$L(\lambda, T) = C^* Z^2 n_e n_i / (kT)^{1/2}; \quad C^* = 6.36 \times 10^{-47} \text{ cgs} \quad (3.56)$$

for  $L(\lambda, T)$  of Eq. (3.56) in appropriate cgs (not MKS) units.<sup>55</sup> For a singly ionized atom, the effective charge  $Z = 1$ ; and for the neutral free-free, etc., continuum, such as the reaction



one can still use the expression (3.56), but with an appropriate numerical value

$$Z_{\text{eff}}^2 = Z_{\text{eff}}^2(\lambda, T) \quad (3.58)$$

Thus for  $T \sim 10,000$  K in air,  $Z_{\text{eff}}^2 \sim 1$  in the visible and  $\sim 0.1$  in the near infrared.<sup>56</sup> For the case of electron-neutral *Bremsstrahlung* one puts  $n_e n_{\text{tot}}$  in Eq. (3.56) instead of  $n_e n_i$  (where  $n_i$  = ion number density,  $n_{\text{tot}}$  = total number density), and thus for a sufficiently small degree of ionization, this neutral free-free, etc., radiation is actually more important than that from the ionized continuum.<sup>57</sup>

### 3.7 ABSORPTION COEFFICIENT OF HIGH-TEMPERATURE AIR

The absorption coefficient of high-temperature air has often been treated as due to the canonical six electronic band systems listed in Table 3-3(a), plus the NO vibration-

<sup>55</sup> Here the number densities  $n_e$  and  $n_i$  are listed per  $\text{cm}^3$ .

<sup>56</sup> See, for example, Morris et al., 1969, and Zeldovich and Raizer, 1966, Vol. I, p. 255 ff.

<sup>57</sup> This explains why the H to  $H^-$  continuum predominates over  $H^+$  to H in the solar photospheric emission.

rotation bands and a number of continua. Table 3-4 lists the continuous contributors that are important at relative density  $\rho/\rho_0 = 10^{-3}$  in the computations of Landshoff and Magee, 1969 (who also include the  $N_2$  Birge-Hopfield  $b^1\Sigma_u^+ - X^1\Sigma_g^+$  electronic band system in their calculations).

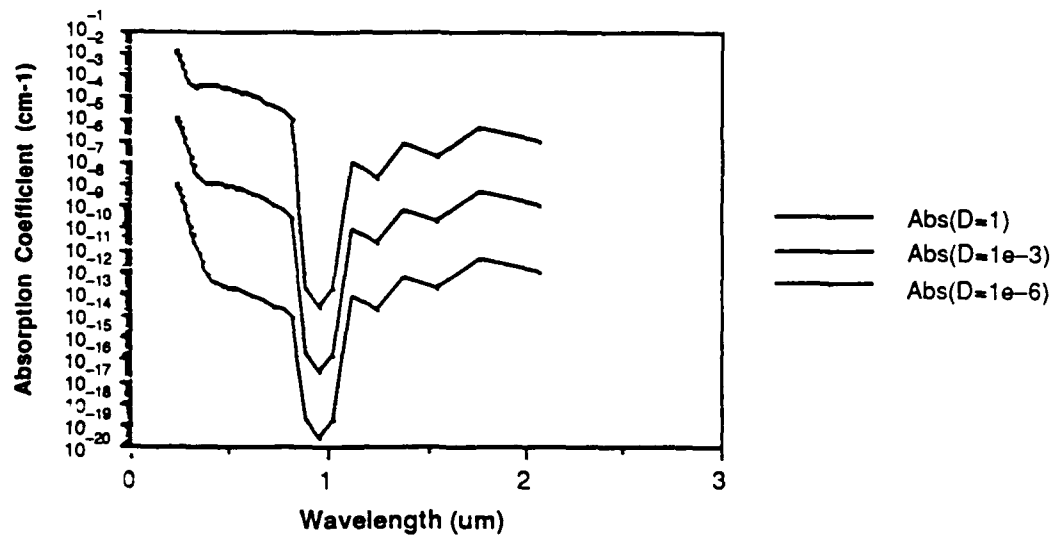
**Table 3-4. Continuous Contributors for the Absorption Coefficient of High-Temperature Air (Source: Landshoff and Magee, 1969)**

System	Spectral Region of Importance		Temperature Region (K)
	$\lambda$ (nm)	Energy (eV)	
$O_2$ Schumann-Runge Continuum	130-175	7.1-9.5	1000-10000
$NO_2$	240-1130	~1.1-5.1	1000-5000
$O^-$ photodetachment	120-830	~1.5-10.7	> 3000
N photoionization	Entire range of calculation		> 7000
O photoionization	Entire range of calculation		> 7000
Free-free in presence of ions	> 1600 Wider range at higher temperatures	< 0.8	> 6000

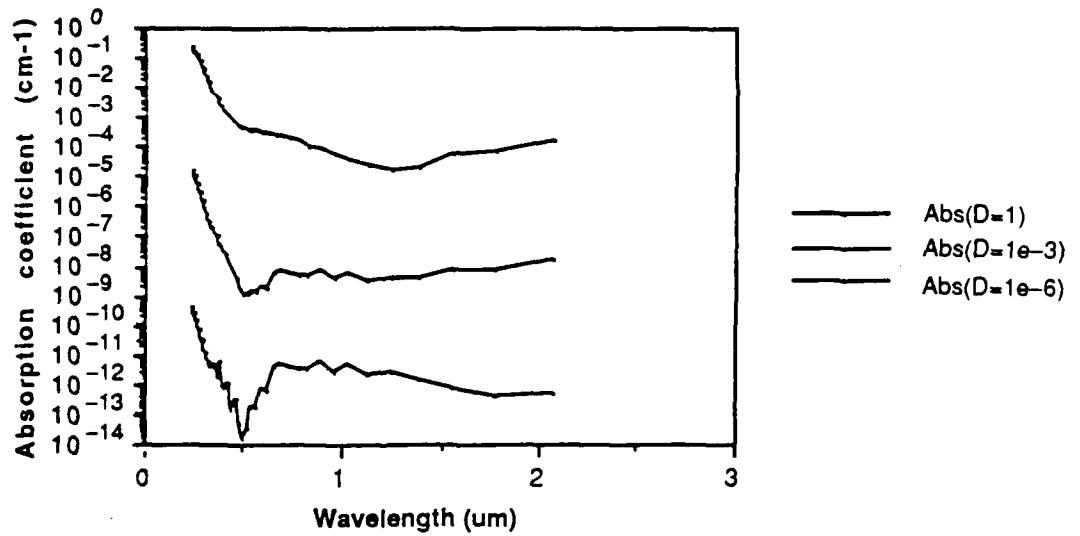
The computation is quite straightforward, if laborious. First one determines the equilibrium chemical composition of the material, then identifies the appropriate radiating systems and computes the spectral absorption coefficient  $k_\lambda$  at moderately low resolution, using an appropriate band model. In Fig.3-9 we show the spectral absorption coefficient for various density ratios  $D = \rho/\rho_0$  at temperatures  $T = 2000, 4000, 6000, 9000,$  and  $12000$  K from the results listed in Landshoff and Magee, 1969.

The following points should be noted:

1. In an optically thin medium, the absorption coefficient  $k_\lambda$  is proportional to  $p$  or  $\rho$ , as a measure of the number of absorbing or emitting molecules.
2. The temperature dependence is largely determined by the species that radiate. At intermediate temperatures there are more metastable molecules (such as  $NO, CN, OH,$  etc.) which tend to be effective radiators than either at low

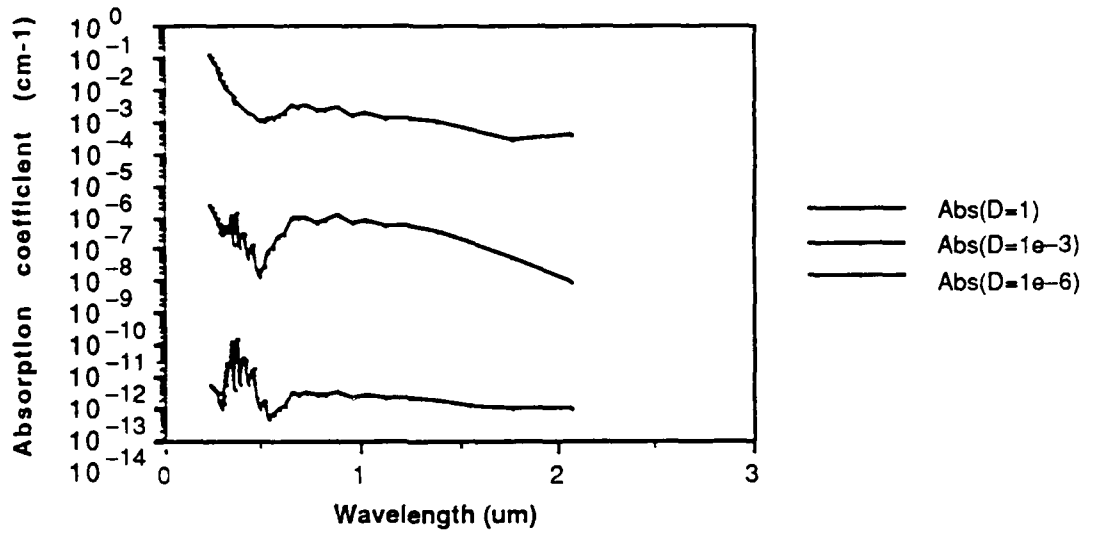


(a)  $T = 2000 \text{ K}$

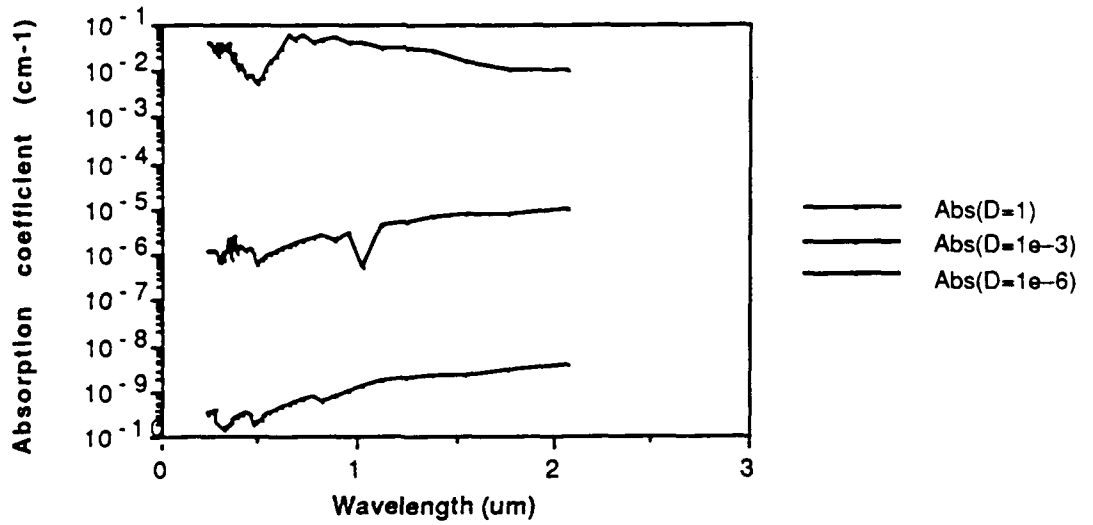


(b)  $T = 4000 \text{ K}$

Figure 3-9. Absorption Coefficient of High-Temperature Air.  
(Source: Landshoff and Magee, 1969)

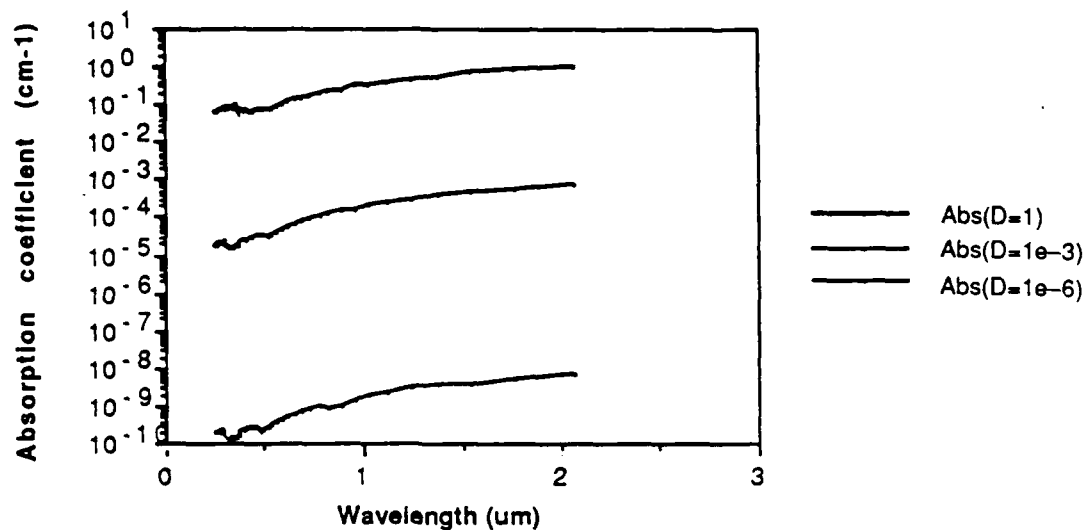


(c) T = 6000 K



(d) T = 9000 K

Figure 3-9. (continued)



(e)  $T = 12,000 \text{ K}$

Figure 3-9. (continued)

- temperatures (below  $\sim 1000 \text{ K}$ ), where there are few reactive molecules, or at high temperatures where there are few molecules left. (See, e.g., Fig. 2-3 in Chapter 2).
3. At the highest temperatures all the molecules dissociate, giving rise to a spectrally rather uniform absorption coefficient due to free-free and free-bound continua. [See, e.g., Fig. 3-9(e): at 12,000 K there are very few molecules left.]
  4. In addition to various continua, a large number of molecular band systems contribute over the temperature range considered here. Thus, the later computations of Johnston et al., 1977, use 21 electronic band systems in addition to the NO vibration and a number of continua, including those of Table 3-4 and some others. Note, however, that older air calculations using just 6 band systems agree fairly well (factor of two) with the observations, because the f-numbers are obtained from measurements of the radiation from high-temperature air.

### 3.8 RADIATION FROM HIGH-TEMPERATURE AIR

Figure 3-10 gives the energy radiated from hot air as a function of temperature and density. For ICBM or spacecraft reentry, peak heating typically occurs in the altitude range 15 km to 50 km, or  $\rho/\rho_0 \sim 0.16$  to  $0.00084$ , so that the  $\rho/\rho_0$  values  $10^{-3}$  to  $10^{-1}$  are most relevant to flight conditions. Kivel, 1961, points out that radiative heating will be important as compared to aerodynamic heating for high velocities ( $> 9$  km/sec) and low altitudes ( $< 45$  km). For the case of vehicles with ablative heat shields, radiation may become important at lower velocities and possibly at higher altitudes because of the production of small particles (e.g., soot) which are much more effective radiators than air molecules.<sup>58</sup> In Fig. 3-10 we also show the black-body radiation per unit area ( $\text{W}/\text{cm}^2$ ) which is, of course, only comparable with radiative gas heating in  $\text{W}/\text{cm}^3$  if we refer to a 1-cm thick layer of air. Since the shock layer (or boundary layer) is roughly 1 cm thick, the comparison is not inappropriate, but can in any case be used for scaling purposes. Since stagnation temperatures for satellite or ICBM reentry lie in the range 6000 K to 8000 K, we see that, indeed, radiative heating due to air is quite small compared to blackbody radiation from the surface.

---

<sup>58</sup> Ablative heat shields such as are used in many reentry vehicles can have quite different radiative properties from pure air. Thus, at 1 atmosphere pressure and 5000 K, the Planck mean absorption coefficient of a gaseous 50 percent carbon/50 percent air equilibrium mixture is 2500 times as large as that of pure air, while if the carbon is present as small soot particles, the Planck mean is larger still by another factor of 15 (see Main and Bauer, 1966, 1967). Therefore, a 1-cm thick soot layer would radiate like a blackbody.

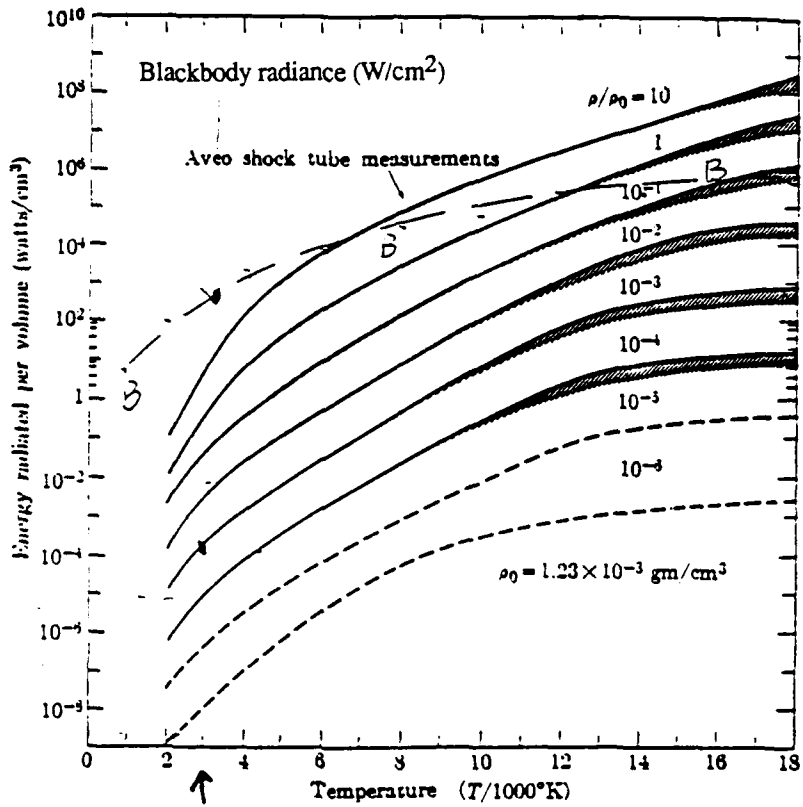


Figure 3-10. Energy Radiated from Hot Air (Source: Kivel, 1961).  
 The line B-B-B corresponds to the blackbody radiation (W/cm<sup>2</sup>)  
 at the appropriate temperature, which is only comparable  
 with the scale for a 1-cm thick air layer.

## 4. SOME HEATING MECHANISMS

### 4.1 INTRODUCTION

Chapter 2 examines the composition of high-temperature air in Local Thermodynamic Equilibrium (LTE), and Chapter 3 considers the radiation from high-temperature air, in effect in Radiative Steady State (RSS). These are limits which may not be attained in practice, but which are useful for specific applications. Here we present several different applications. For each one we ask how energy is transferred into the system and hence how adequately or rapidly is LTE (or RSS) approached.

The following topics are addressed here:

- Reentry heating, which is due to aerodynamic (shock and boundary layer) heating, is treated in Section 4.2.
- Nuclear fireball: this entails heating by keV X-rays, and is discussed in Section 4.3.
- Upper atmosphere-photodissociation of O<sub>2</sub> and O<sub>3</sub> by solar UV is discussed in Section 4.4. Unlike the nuclear and reentry cases, this is clearly a non-LTE situation

Light propagation effects are not considered here, but they can involve processes which are very far from LTE, in particular for the case of high-energy lasers.

All these examples demonstrate how the energy of excitation moves towards LTE. The details of the equilibration process are highly specific for each particular example, proceeding through some particular inelastic collisions and rate processes. It is generally appropriate to introduce a characteristic time for energy transfer

$$\tau_{\text{char}} \sim 1/(nk) \quad (4.1)$$

where  $n$  (cm<sup>-3</sup>) is the number density of colliding particles ( $\sim 2.5 \times 10^{19}$  cm<sup>-3</sup> at 1 atmosphere pressure--see Table 2-4 on p. 2-22), while the rate constant  $k$  (cm<sup>3</sup>/sec) refers to a specific rate-limiting step and is the product of the reaction cross section  $\sigma$  (cm<sup>2</sup>) and of the molecular collisional velocity  $v$  (cm/sec). Typically  $\sigma \sim 10^{-20} - 10^{-15}$  cm<sup>2</sup> and  $v \sim 10^5$  cm/sec, so that  $k = \sigma v \sim 10^{-15} - 10^{-10}$  cm<sup>3</sup>/sec.

If the critical species is present to 1 part per million, so that  $n \sim 10^{13} \text{ cm}^{-3}$ , then the characteristic time  $\tau_{\text{char}}$  is in the range 1 msec-100 sec, but the actual range is often much larger. In general, the system attains LTE in times much greater than  $\tau_{\text{char}}$ .

## 4.2 REENTRY HEATING

An ICBM or low-earth-orbiting satellite travels in space at a speed on the order of 7 km/sec. As the vehicle enters the earth's atmosphere, it is slowed down by collision with air molecules whose mean thermal speed is  $\sim 10^5 \text{ cm/sec} = 1 \text{ km/sec}$ . This leads both to a hypersonic shock wave<sup>59</sup> that stands off in front of the vehicle and also a boundary layer<sup>60</sup> on the vehicle. Figure 4-1 sketches how the initial kinetic energy of motion of the vehicle is converted into heat. Figure 4-1(a) shows schematically how the atmospheric density  $\rho$  and the vehicle velocity  $u$ , deceleration<sup>61</sup> and heating rate<sup>62</sup> change with altitude, and Fig. 4-1(b) presents the energy conversion from kinetic energy into heat in semi-quantitative form. It shows that fraction of the kinetic energy of the vehicle which reaches the surface as heat. As the vehicle comes down below 100 km where the gas-kinetic mean free path is 16 cm, a bow shock gradually builds up,<sup>63</sup> and through this shock (and the boundary layer which develops on the surface of the vehicle) the kinetic energy of the vehicle is gradually converted into heat, some of which reaches the surface. Note that as the vehicle slows down, its energy conversion fraction decreases. At altitudes in the 30-km-altitude range, the flow along the body changes from laminar to turbulent, with a significantly greater heat transfer rate. For reentry velocities of approximately 7 km/sec,<sup>64</sup> radiative heating is low because at temperatures below  $\sim 12,000 \text{ K}$  the radiation from hot

---

59 When a vehicle travels through the atmosphere faster than the local sound speed (which is  $\sim 0.3 \text{ km/sec}$  at 100 km altitude), a shock wave develops because the atmosphere cannot accommodate to the motion in a less drastic fashion. As the vehicle speed increases, the shock wave, which initially is almost perpendicular to the direction of motion of the vehicle, turns so as to make successively smaller angles to the velocity vector. At hypersonic conditions the shock 'wraps around' the front of the body.

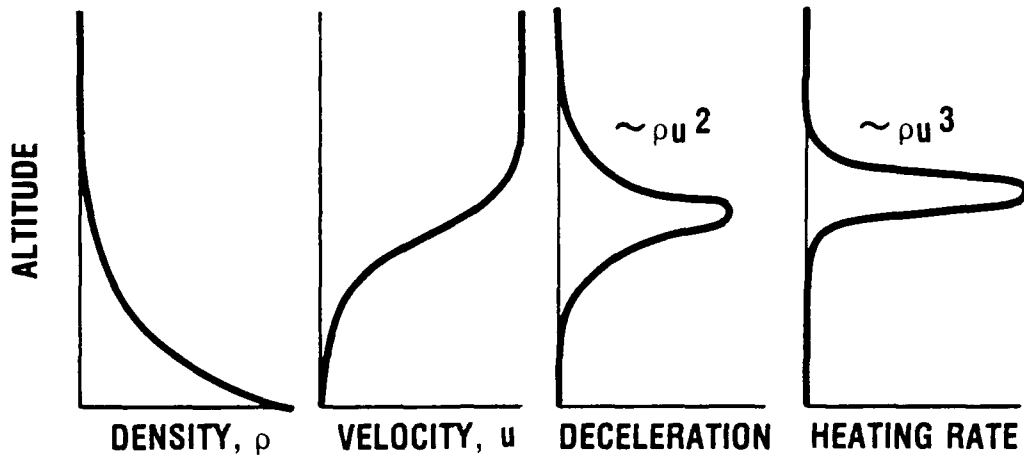
60 The boundary layer is a region of a supersonic flow close to a solid surface in which most of the interaction between the surface and the flow occurs. Thus the flow here is subsonic and non-ideal gas effects such as viscous dissipation and ablation occur in the boundary layer.

61 The deceleration is proportional to  $u^2$ .

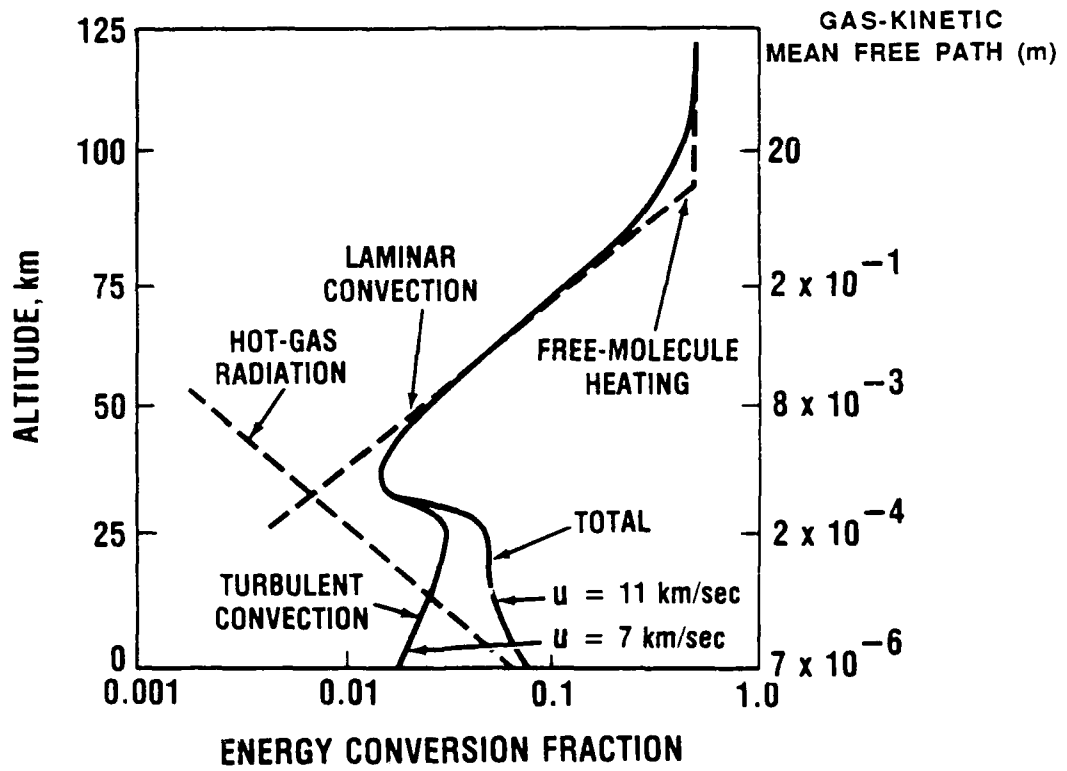
62 The heating rate is proportional to  $u^3$ .

63 At higher altitudes where the vehicle size is smaller than the mean free path, the presence of the vehicle does not affect the air flow and so no shock develops.

64 This corresponds to reentry from low earth orbit or to ICBM entry.



(a)



(b)

1-23-89-1

Figure 4-1. Energy Transfer on Reentry.  
 (a) Schematic of Slowing-Down and Heating-Up as Function of Altitude,  
 (b) Energy Conversion for Reentry at Different Velocities.

air is small--see Fig. 3-10 on p. 3-41. However, at higher entry velocities--such as 11 km/sec, as is illustrated in Fig. 4-1(b)--radiation from the hot gases becomes significant for altitudes below 25-30 km.<sup>65</sup>

Figure 4-2 gives more details of the flow over a reentry vehicle. Figure 4-2(a) shows the shock wave on the vehicle, indicating the stagnation region<sup>66</sup> near the blunt, rounded nose where the heating rate is greatest. To survive this high heating rate, a reentry vehicle typically has a heat shield composed of special material which ablates, i.e., decomposes while dissipating the large energy input. Downstream from the stagnation region the shock is oblique, i.e., weaker, and the boundary layer along the vehicle gradually thickens; we show schematically the transition from laminar to turbulent flow in the boundary layer, which typically occurs between 30 and 20 km altitude. For a typical reentry vehicle with an ablative heat shield the stagnation temperature is in the range 2500 K to 3000 K, while the boundary layer temperature is in the range 1000 K to 2000 K. Figure 4-2(b) indicates schematically how the velocity, temperature, pressure, and density vary as one goes in the stagnation region through the shock and to the vehicle wall "w." Note in particular the structure in temperature through the shock. This is determined by the transfer of energy from initial kinetic energy into various degrees of freedom, which is displayed in more detail in Fig. 4-2(c) which shows the effects of kinetics: translational and rotational equilibration occurs very rapidly, giving a high translational temperature immediately across the shock as all the directed energy of motion is transformed into random translational and rotational energy. Transfer into vibrational excitation takes longer and leads to a lower temperature as the energy is distributed among more degrees of freedom. Dissociation and electronic excitation takes longer still, giving yet a further reduction in kinetic temperature, while ionization is slower still, yielding the final equilibrium temperature. In this sketch, the energy distribution between different degrees of freedom corresponds to a normal shock in air at a velocity of 7 km/sec--see Table 4-1, which shows that here most of the energy goes into dissociation, a significant amount into vibrational excitation, and very little into ionization.<sup>67</sup>

---

<sup>65</sup> This radiation effect increases with increasing density because the vehicle boundary layer is evidently optically thin down to the lowest significant altitudes. This whole issue will be discussed in Part II, to be prepared later.

<sup>66</sup> The stagnation region is defined as that region in the flow where the ordered flow is brought to rest, so that all the ordered kinetic energy of motion must be transformed into thermal energy. Thus it is here that the temperature and hence the heating rate have their maximum values.

<sup>67</sup> By contrast, for a normal shock in Argon most of the energy goes into ionization.

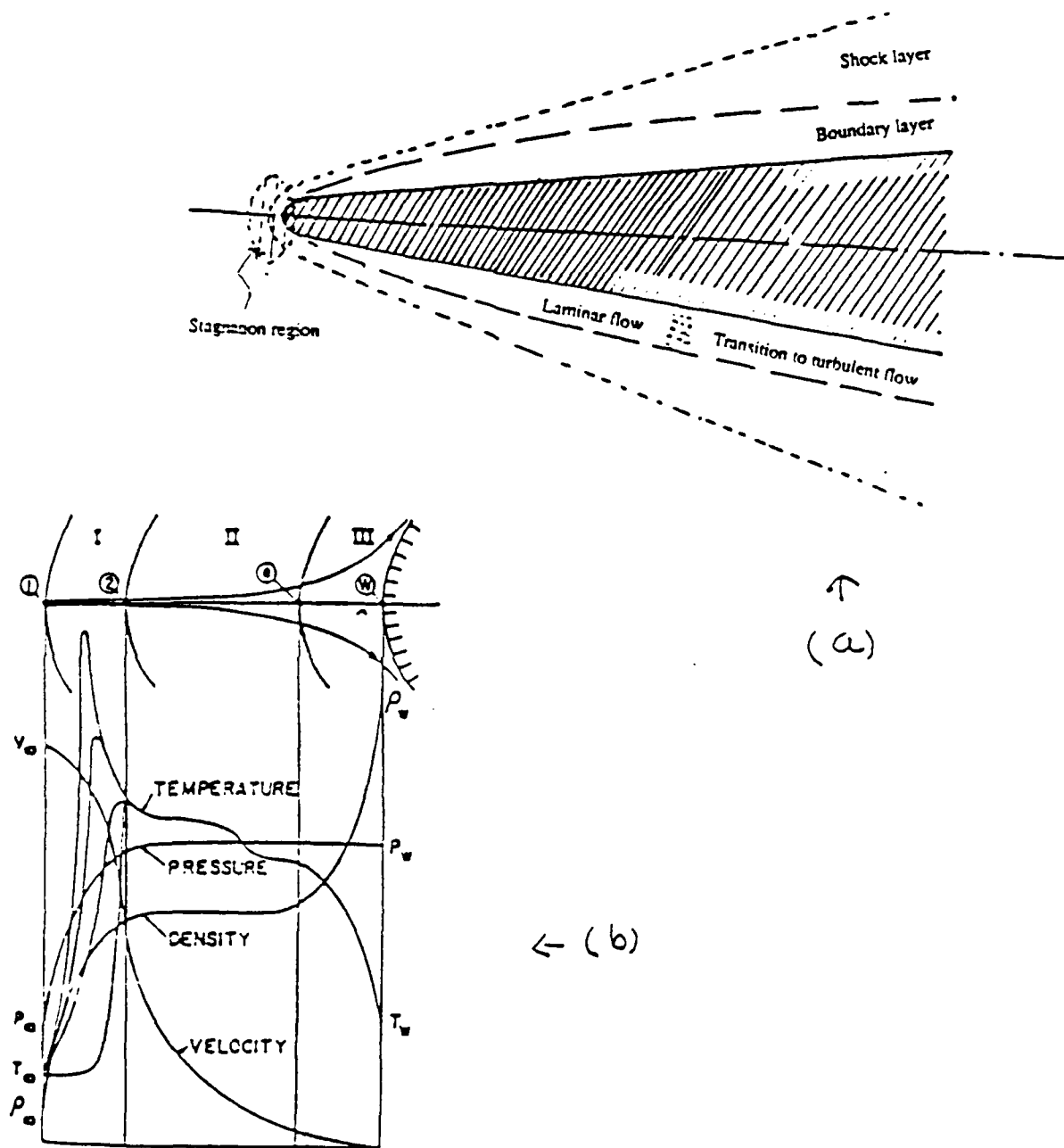


Figure 4-2. Schematic Air Flow on a Reentry Vehicle.  
 (a) Shock Wave and Boundary Layer on the Vehicle.  
 (b) Profile of temperature, density, velocity, and pressure through the Bow Shock. (Source: Murty, 1987--from OSC).  
 (c) Equilibration through Hypersonic Shock.

**Table 4-1. Energy Balance Behind a Normal Shock In Air (Source: Bauer, 1969)**

(A velocity of 5 km/sec corresponds to IRBM entry while 7 km/sec corresponds to ICBM entry.  
The ambient conditions are  $p_o = 0.01$  atm.,  $T_o = 294$  K,  
and energies are listed in eV/molecule or atom.)

$u_o$	5 km/sec	7 km/sec
Upstream of the shock		
Directed kinetic energy	3.76	7.3
Thermal enthalpy $c_p T$	0.006	0.006
Downstream of the shock		
Stagnation temperature (K)	5800 (~ 0.5 eV)	7500 (~ 0.65 eV)
Enthalpy of translation (3/2) kT	1.25	1.62
Rotational enthalpy, kT	0.5	0.65
Vibrational enthalpy	0.37	0.51
Dissociation energy	1.51	2.72
Electronic energy	0.011	0.075
Ionization energy	0.002	0.006
Chemical energy ( $N_2 + O_2 \rightleftharpoons 2NO$ )	-0.02	-0.01
Equilibrium composition downstream of the shock		
[N <sub>2</sub> ]	0.579	0.304
[NO]	0.0164	0.00615
[O <sub>2</sub> ]	0.000974	0.000124
[N]	0.0840	0.418
[O]	0.319	0.272
[e <sup>-</sup> ] = [NO <sup>+</sup> ]	0.000137	0.000630

### 4.3 NUCLEAR FIREBALL

A nuclear weapon emits a significant portion of its energy in the form of X-rays, which are absorbed in the atmosphere. The energy spectrum of these X-rays is normally continuous, having a Planck spectrum of temperature<sup>68</sup> 1-10 keV. Figure 4-3 gives the absorption and extinction (= absorption + scattering) coefficient of keV X-rays as a function of energy by "air," which is four parts of nitrogen to one part of oxygen.<sup>69</sup> Note that

- (a) The extinction coefficient falls off very rapidly with increasing energy, and scattering is only important at the highest energies.
- (b) A Planck blackbody spectrum of temperature  $T$  has its maximum energy density at frequency  $\nu_m$  such that<sup>70</sup>

$$h\nu_m/kT = 2.825 \quad . \quad (4.2)$$

For the extinction of X-rays in the atmosphere, one can define a dimensionless optical thickness  $X$

$$X = (\text{absorption coefficient}) \times (\text{column density}) \quad , \quad (4.3)$$

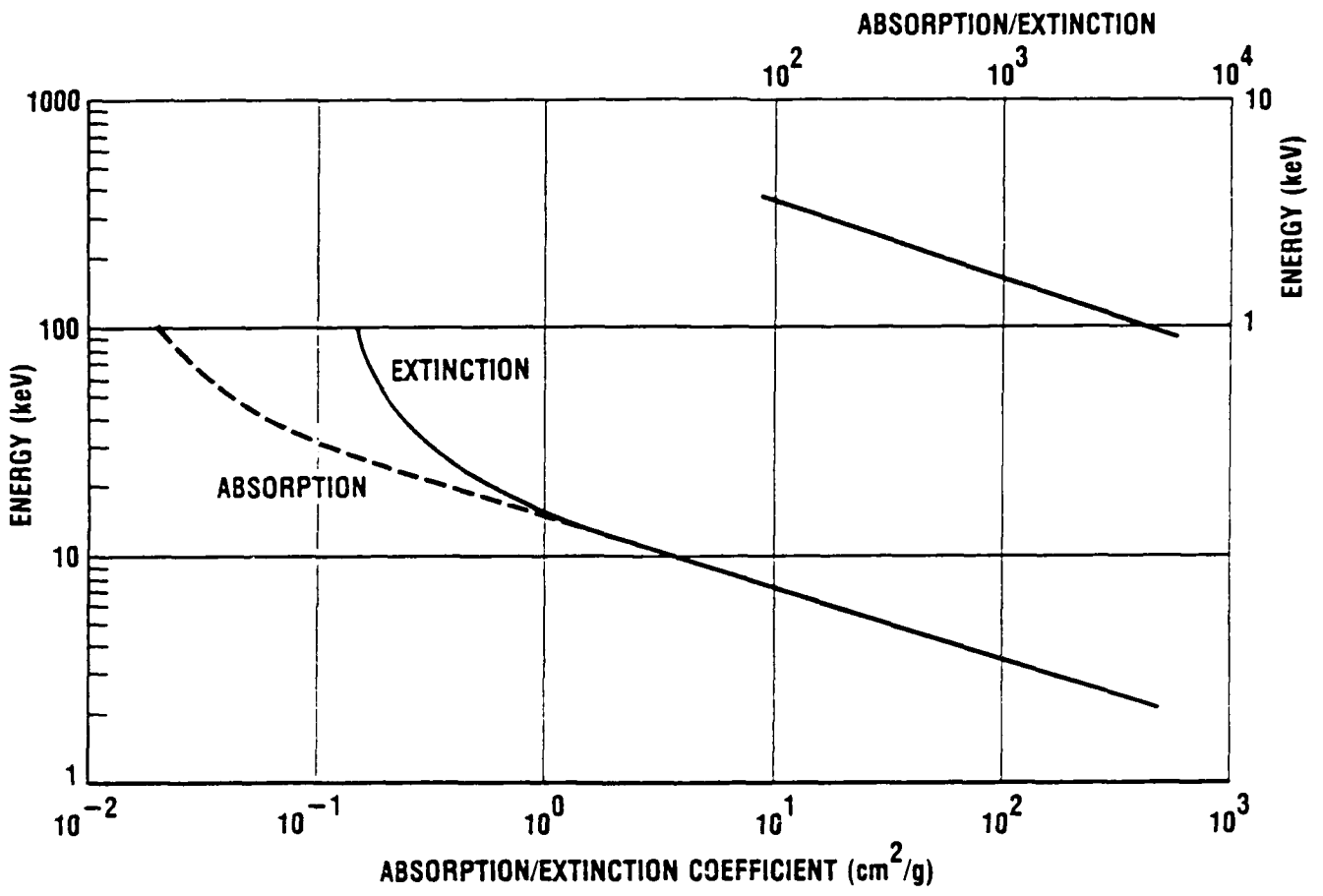
and if  $X \gg 1$ , the energy is absorbed in the relevant column. Table 4-2 gives the optical thickness  $X$  for 1 keV and 10 keV X-rays in a 10-km horizontal path in air at different altitudes. We see that at altitudes below 30 km to 50 km the X-ray energy is absorbed near the burst, giving rise to a well-confined fireball ( $\sim 1$ -10 km), but at altitudes above 70 km to 100 km the density is so low that energy deposition occurs over a very large atmospheric region ( $\sim 100$ -1000 km), giving rise to a very different sort of phenomenology.

---

<sup>68</sup> The notation is conventional but confusing, in that the temperature  $T$  of a black-body spectrum is normally measured as voltage  $V$  from the relation  $kT = eV$ . Note that the differential energy spectrum of a black body temperature 1 keV peaks at an energy of 2.8 keV--see Eq. (4.2)

<sup>69</sup> Note that the details of molecular structure are totally immaterial for incident X-rays in the keV energy range, because chemical binding energies--of 5 to 10 eV--are so much smaller than the X-ray energy.

<sup>70</sup> The spectrum as a function of wavelength has its maximum at  $\lambda_m$  where  $hc/\lambda_m kT = 4.965$ . This gives the well-known Wien's displacement law  $\lambda_m T = 0.290$  cm-K.



Source: Storm and Israel (1970).  
 9-16-68-7

Figure 4-3. keV X-Ray Absorption and Extinction Coefficients for Air  
 (Source: Storm and Israel, 1970)

**Table 4-2. Optical Thickness for keV X-rays in a Horizontal Path of 10-km Length in the Atmosphere at Different Altitudes. (Atmospheric data from USAF, 1965; absorption coefficient at 1 keV is  $4 \times 10^3$  cm<sup>2</sup>/g, at 10 keV it is 3 cm<sup>2</sup>/g)**

Altitude (km)	Density (kg/m <sup>3</sup> )	Mean free path (cm)	Optical Thickness for 10 km Path	
			(1 keV)	(10 keV)
0	1.23	$7 \times 10^{-6}$	$4.9 \times 10^6$	$3.7 \times 10^3$
10	0.41	$2 \times 10^{-5}$	$1.6 \times 10^6$	$1.2 \times 10^3$
20	0.089	$9 \times 10^{-5}$	$3.6 \times 10^5$	$2.7 \times 10^2$
40	0.0040	$2 \times 10^{-3}$	$1.6 \times 10^4$	12
70	$8.8 \times 10^{-5}$	$9 \times 10^{-2}$	$3.5 \times 10^2$	0.26
100	$5.0 \times 10^{-7}$	16	2.0	$1.5 \times 10^{-3}$

The following description of a low air burst (i.e., within the atmosphere) is taken verbatim from J. Zinn (LANL--see Barasch, 1979).<sup>71</sup>

"Within the first microsecond after detonation, the entire nuclear yield is deposited in the bomb materials, heating them to extremely high temperatures in the range  $10^7$  K. Some of this energy is immediately radiated away in the form of X-rays and extreme ultraviolet radiation, but this radiation is immediately reabsorbed in the air within the first few meters surrounding the device. The air is thereby heated to a very high temperature, in the range of  $10^6$  K, with a corresponding increase in pressure to several thousand atmospheres. This heated air and the hot bomb vapors (debris) in the interior constitute the initial fireball. The fireball subsequently expands through a combination of radiative and hydrodynamic processes. An intense shock wave (thin region of highly compressed air) is formed at the surface, which expands outward at a high velocity. Inside the shock, the energy is rapidly redistributed through emission and reabsorption of ultraviolet radiation.

The time variation of light emission during the first pulse of Fig. 4-4 is controlled by the radial growth of the shock. Although the shock surface is intensely luminous, the shock is opaque to visible light, thus concealing the air and bomb debris in its interior. As the shock expands, it engulfs cold air, causing its temperature to decrease, with a corresponding decrease in brightness. The optical energy emission rate (power) is proportional to the fireball brightness times the area of its surface. After detonation, the optical power first increases, because the increase in surface area outweighs the

<sup>71</sup> For a more detailed discussion, see Brode, 1968.

decrease in brightness. Later, it decreases, because the decrease in brightness is dominant.

During the early expansion and cooling of the fireball, the ultraviolet radiation in the interior decreases rapidly until it cannot effectively redistribute the energy. Thereafter, the shock temperature falls more rapidly than the temperature in the interior. As the expansion proceeds, the shock continues to cool, and as it does so, it becomes less and less opaque to visible light, while also becoming less luminous. A point is reached, corresponding to the minimum temperature region in Fig. 4-4, where the shock becomes sufficiently transparent to allow light from the hotter interior to begin to escape, causing the optical output to begin increasing again. Further growth of the shock results in increasing transparency and a further increase of the luminosity of the inner region.

As the expansion continues further, the temperature of the inner fireball decreases, due to the combined effects of hydrodynamic expansion and loss of energy by radiation. This cooling eventually results in the decrease in luminosity following the second maximum in Fig. 4-4. After the second maximum, the inner fireball gradually becomes transparent, revealing the bomb debris inside, whose brightness also decreases with time. The majority of the total energy radiated by the fireball comes from the second peak, which is not very different in its instantaneous brightness relative to the first peak, but lasts about 100 times longer. By the time this "thermal pulse" is over, the available energy has either been radiated away, trapped in the debris and entrained air of the fireball, or it is propagating in the shock wave, which is now well outside the visible fireball."

The fireball remains in the 1000 K to 10,000 K temperature range for times of 3 sec to 30 sec depending on bomb yield, so that its phenomenology is of considerable systems implication. For a discussion, see "The Effects of Nuclear Weapons"--referenced as ENW, 1964, Ch. 1 and 2, in particular pp. 87-100, or Zeldovich and Raizer, 1966, Vol.II, p. 611f for a description taken from the first (1957) edition of ENW.<sup>72</sup>

---

<sup>72</sup> Zeldovich & Raizer, 1966 describe the description of the evolution of a fireball in the first (1957) edition of ENW as better than that in the 1962/64 edition. There is now a third (1977) edition of ENW, which is poorer still from the standpoint of describing what actually was observed during a nuclear explosion, because by 1977 the observations of atmospheric nuclear tests of 1962 and earlier had been massaged to provide a homogenized but not necessarily more accurate description of what goes on.

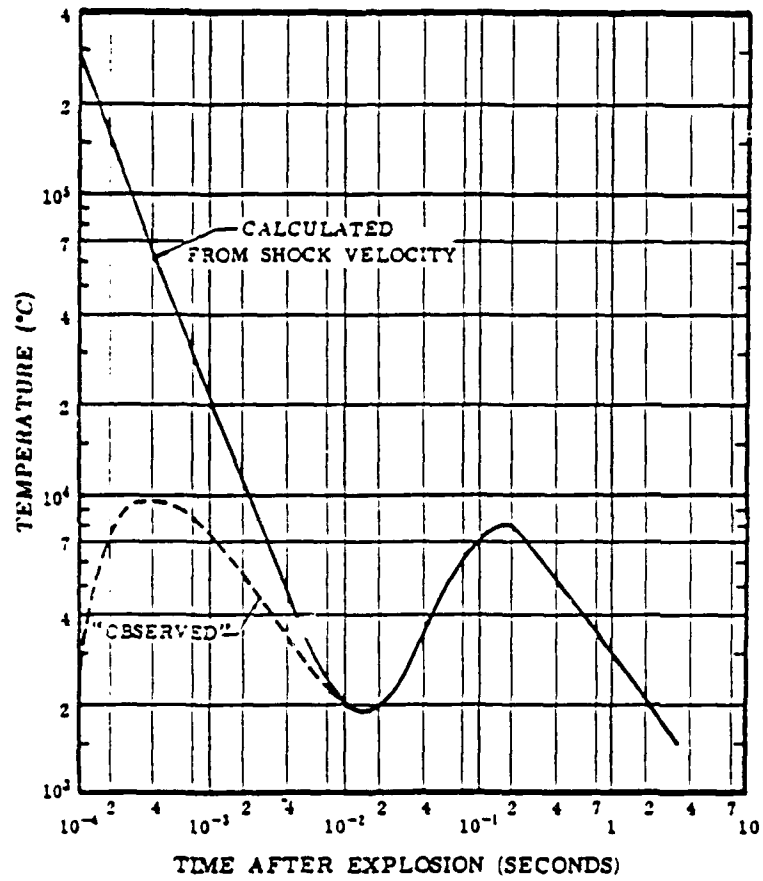


Figure 4-4. Variation of Apparent Fireball Surface Temperature with Time in a 20-kt Explosion. (Source: ENW, 1964, p. 75)

#### 4.4 UPPER ATMOSPHERE

Figure 4-5 shows the penetration of the solar radiation into the earth's atmosphere. The photodissociation of O<sub>2</sub> is responsible for the absorption of solar UV in the 150-nm to 180-nm (1500 to 1800 Å) range which occurs in the 100-km altitude range and provides the energy input which, in effect, drives the thermosphere, while the absorption of radiation in the 200-300 nm wavelength range by O<sub>3</sub> takes place at altitudes near 30 km to 50 km and is responsible for the stratospheric photochemistry. Figures 3-6 (p. 3-31) and 3-7 (p. 3-32) show the corresponding absorption cross section of the O<sub>2</sub> and O<sub>3</sub> molecules. Table 4-3 demonstrates that all this photochemistry is driven by a very small fraction of the solar irradiance; roughly half of the total solar irradiance penetrates the atmosphere, while only 0.015 of the earth's atmosphere is above 30-km altitude, and  $4 \times 10^{-7}$  above 100 km.

It is rather easy to demonstrate that O<sub>2</sub> dissociation in the thermosphere (80 km to 300 km, say) is not in LTE, but rather in Radiative Steady State (RSS). Table 4-4 lists temperature, density, O<sub>2</sub> and O densities and degree of dissociation defined as

$$\phi_{\text{diss}} = n_{\text{O}}/[n_{\text{O}} + n_{\text{O}_2}] \quad (4.4)$$

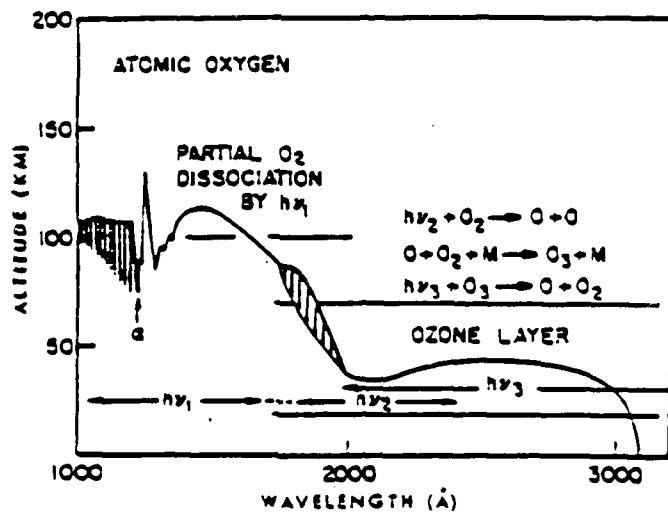
under representative mean conditions, and also the LTE degree of dissociation computed from the analysis of Section 2.2.2. This shows clearly that LTE simply cannot explain the degree of dissociation that is actually found.

A simple but often useful way to describe the non-LTE upper atmosphere without going to the full detail of individual species concentrations is to introduce population temperatures for different degrees of freedom, as is suggested in Section 2.5. Some representative population temperatures are listed in Table 4-5. It should be noted that--because the dissociation and ionization occurs through the direct absorption of solar radiation--the dissociation and ionization excitation temperatures are much larger than the kinetic temperatures of neutrals and electrons, and that different degrees of freedom (e.g., N<sub>2</sub> and O<sub>2</sub> dissociation) have different population temperatures because their excitation mechanisms differ.<sup>73,74</sup>

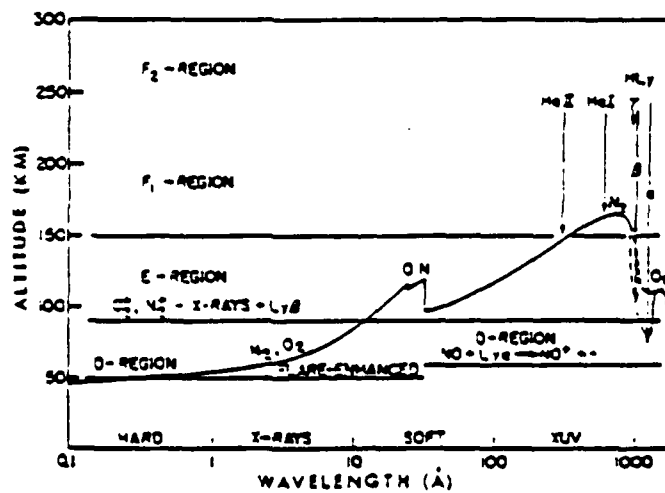
---

<sup>73</sup> Missing data normally indicate that the species are not important at the relevant altitudes.

<sup>74</sup> For a later version listing vibrational population temperatures of IR active molecules--O<sub>3</sub>, H<sub>2</sub>O, CO<sub>2</sub>, CO, NO--in the 60-km to 120-km altitude range--see Degges and Smith, 1977, and Degges and D'Agati, 1984; for a current version of this code, SHARC (Strategic High-Altitude Radiance Code) see Sharma et al., 1989.



(a) The depth to which 1/e of the incident solar intensity penetrates, for 1000 to 3000 Å.



(b) The depth to which 1/e of the incident solar intensity penetrates, for 0.1 to 1000 Å.

Figure 4-5. Penetration of Radiation into the Atmosphere  
(Source: R. Tousey, 1961)

**Table 4-3. Fraction of Solar Irradiance in Different Wavelength Intervals**  
(Source: USAF, 1965, p. 16-3)

Wavelength Interval	Fraction of Solar Spectral Irradiance
< 121.6 nm	$4.4 \times 10^{-6}$
121.6 nm (H Ly- $\alpha$ line)	$3.1 \times 10^{-6}$
121.6-180 nm	$2.3 \times 10^{-5}$
180-225 nm	$6.5 \times 10^{-4}$
225-300 nm	0.013
300-400 nm	0.079
400-700 nm	0.40
7000-1000 nm	0.22
1-2 $\mu\text{m}$	0.23
> 2 $\mu\text{m}$	0.059

**Table 4-4. O<sub>2</sub> Dissociation in the Thermosphere: Actual and LTE.**  
(Source of input data: Bortner and Kummler, 1969, and U.S. Standard Atmosphere, 1962)

h (km)	n(cm <sup>-3</sup> )	T (K)	n(O <sub>2</sub> )(cm <sup>-3</sup> )	n(O)(cm <sup>-3</sup> )	$\phi_{\text{diss}}^{\text{act}}$	K <sub>diss</sub> (T)*	$\phi_{\text{diss}}^{\text{LTE}}$
80	$3.8 \times 10^{14}$	181	$8.0 \times 10^{13}$	$8.5 \times 10^{10}$ **	$1.1 \times 10^{-3}$	$1.6 \times 10^{-117}$	$4.5 \times 10^{-66}$
100	$1.1 \times 10^{13}$	210	$2.0 \times 10^{12}$	$5.0 \times 10^{11}$	0.20	$6.0 \times 10^{-98}$	$1.6 \times 10^{-55}$
140	$9.5 \times 10^{10}$	714	$9.8 \times 10^9$	$2.2 \times 10^{10}$	0.70	$1.4 \times 10^{-11}$	$8.1 \times 10^{-12}$
200	$6.9 \times 10^9$	1236	$3.6 \times 10^8$	$3.2 \times 10^9$	0.90	$2.5 \times 10^4$	$3.4 \times 10^{-3}$
300	$6.7 \times 10^8$	1432	$1.1 \times 10^7$	$5.1 \times 10^8$	0.98	$1.8 \times 10^7$	0.13

\* K<sub>diss</sub>(T) is the O<sub>2</sub> dissociation equilibrium constant of Eq. (2.2).

\*\* At 80 km and below, the O-atom number density at night is less than in the day time, by a large factor. Daytime values are listed here.

**Table 4-5. Population Temperatures for Different Degrees of Freedom in the Upper Atmosphere (Source: Bauer, Kummler and Bortner, 1971)**

Altitude (km)	100	200	300
Kinetic temperature of neutrals (K)	185	930	1090
Kinetic temperature of electrons (K)	370	1570	1900
O <sub>2</sub> dissociation temperature (K)	1900	1870	1830
N <sub>2</sub> dissociation temperature (K)	1800	2800	(2400)
NO ionization temperature (K)	2560	2850	-
O <sub>2</sub> ionization temperature (K)	2630	3100	-
O( <sup>1</sup> D) excitation temperature (K)	1280	1870	-
O <sub>2</sub> (a <sup>1</sup> Δ) excitation temperature (K)	1000	-	-

The physics of the upper atmosphere will not be discussed in detail here. A discussion emphasizing the overall physics and simple but usable numbers is given in Bauer, 1972. There exist much more modern (and authoritative) treatments, our current understanding of the stratosphere is much better than it was in 1972 and also my discussion of meteorology as given there is bad. However, while we have much more data on the thermosphere--see e.g. U.S. National Report to IUGG, 1987--yet our understanding of the basic physics has changed very little, and modern books have a tendency to overwhelm the non-expert reader with details.

## 5. BIBLIOGRAPHY

- Allen, C.W., *Astrophysical Quantities*, Athlone Press, London, 2nd Ed., 1963.
- Aller, L.H., *Astrophysics; the Atmospheres of the Sun and Stars*, Ronald Press, 2nd Ed., 1963.
- AIP (American Inst. of Physics) Handbook*, D.E. Gray, Coordinating Editor, McGraw-Hill (2nd Ed. 1963, 3rd Ed. 1972).
- Anderson, G.P. et al, "AFGL Atmospheric Constituent Profiles (0-120 km)", AFGL-TR-86-0110, May 1986.
- Anderson, J.D., Jr., *Modern Compressible Flow: with Historical Perspective*, McGraw-Hill, 1982.
- Anderson, J.D., Jr., *Fundamentals of Aerodynamics*, McGraw-Hill, 1984.
- Anderson, J.D., Jr., "A Survey of Modern Research in Hypersonic Aerodynamics," AIAA paper 84-1578, June 1984.
- APS Study Group Participants, "Report to the APS of the Study Group on Science and Technology of Directed Energy Weapons," *Rev. Mod. Phys.*, 59, S1, 1987.
- Armstrong, B.H., et al., "Absorption Coefficients of Air" (title approximate), Report LMSD-5135, Lockheed Missiles and Space Division, Palo Alto, CA, August 1958.
- Armstrong, B.H., et al., *J. Quant. Spectrosc. Radiat. Transfer*, 1, 143, "Radiative Properties of High-Temperature Air," 1961.
- Arnold, J.O., et al., *J. Quant. Spectrosc. Radiat. Transfer*, 9, 775, "Line-by-Line Calculation of Spectra from Diatomic Molecules and Atoms, Assuming a Voigt Line Profile," 1969.
- Banks, P.M., and G. Kockarts, *Aeronomy (Parts A and B)*, Academic Press, New York, 1973.
- Barasch, G.E., "Light Flash Produced by an Atmospheric Nuclear Explosion," Los Alamos National Laboratory 79-84 (Mini-Review), November 1979.
- Bartky, C.D., "The Reflectance of Homogeneous Plane-parallel Clouds of Dust and Smoke," *J. Quant. Spectrosc. Radiat. Transfer*, 8, 51, 1968.
- Bartky, C.D., and E. Bauer, "Predicting the Emittance of a Homogeneous Plume Containing Alumina Particles," *J. Spacecr. & Rockets*, 3, 1523, 1966.

Bates, D.R., Ed., *Atomic and Molecular Processes* (see in particular Ch. 7 by Bates and Dalgarno, *Electronic Recombination*), Academic Press, 1962.

Bates, D.R., A.E. Kingston, and R.W.P. McWhirter, "Recombination between Electrons and Atomic Ions-1, Optically Thin Plasmas," *Proc. Roy. Soc. Lond.*, A267, 297; A270, 155, 1962.

Bauer, E., "Energy Transfer Mechanisms in Hypersonic Shocks," *J. Quant. Spectrosc. Radiat. Transfer*, 2, 499, 1969.

Bauer, E., "Physics of the Earth's Atmosphere: Lecture Notes," Institute for Defense Analyses Paper P-811, 1972.

Bauer, E., L.S. Bernstein, and G.M. Weyl, "Cirrus Clouds, Some Properties and Effects on Optical Systems: a Preliminary Examination," Institute for Defense Analyses Paper P-1743 (AD-B082 556), January 1984.

Bauer, E., and D.J. Carlson, *J. Quant. Spectrosc. Radiat. Transfer*, 4, 363, "Mie Scattering Calculations for Micron-size Alumina and Magnesia Spheres," 1964.

Bauer, E., R. Kummler, and M.H. Bortner, "Internal Energy Balance and Energy Transfer in the Lower Thermosphere," *Appl. Opt.*, 10, 1861, 1971.

Baulch, D.L., et al., *Evaluated Kinetic Data for High-Temperature Reactions*, Butterworths, London, 1972, 1973, 1976.

Baulch, D.L., et al., "Evaluated Kinetic and Photochemical Data for Atmospheric Chemistry: Supplements I, II," *J. Phys. Chem. Ref. Data*, 11 (2), 327, 1982 and 13 (4), 1259, 1984.

Blumer, H., "Radiation Diagrams of Small Dielectric Spheres," *Z. Phys.*, 119, 1925.

Bond, J.W., K.M. Watson, and J.A. Welch, *Atomic Theory of Gas Dynamics*, Addison-Wesley, Reading, MA, 1965.

Born, M.W., and E. Wolf, *Principles of Optics*, Pergamon, NY, 1959 (6th Ed., 1980).

Bortner, M., and R. Kummler, "The Chemical Kinetics and Composition of the Earth's Atmosphere," GE Report GE-9500-ECS-SR-1, July 1968.

Breene, R.G., Jr., and M.C. Nardone, "Radiant Emission from High-Temperature Equilibrium Air," *J. Quant. Spectrosc. Radiat. Transfer*, 2, 273, 1962.

Brode, H.L., "Review of Nuclear Weapons Effects," *Ann. Rev. Nucl. Sci.* 18, 153, 1968.

Chandrasekhar, S., *Radiative Transfer*, Dover, New York, 1960.

Chapman, S., and T.G. Cowling, *The Mathematical Theory of Non-Uniform Gases*, Cambridge University Press, 2nd Ed., 1952.

Clough, S.A., et al., "Atmospheric Radiance and Transmittance: FASCOD2," presented at 6th Conference on Atmospheric Radiation, Williamsburg, VA, May 1986.

Cohen, E.R., and B.N. Taylor, "The 1986 Adjustment of the Fundamental Physical Constants," *Rev. Mod. Phys.*, 59, 1121, 1987.

Condon, E.U., and G.H. Shortley, *Theory of Atomic Spectra*, Cambridge University Press, 1935.

*DNA Reaction Rate Handbook*, M. Bortner and T. Baurer, Eds., Defense Nuclear Agency DNA 1948H, 2nd Ed. 1972; Revision 8, 1979.

Degges, T.C., and A.P. D'Agati, "A User's Guide to the AFGL/Visidyne High Altitude Infrared Radiance Model Computer Program," AFGL-TR-85-0015 (AD-A161 432), Visidyne, Inc., October 1984.

Degges, T.C., and H.J.P. Smith, "High-Altitude Infrared Radiance Model," AFGL-TR-77-0271 (AD-A059 242), Visidyne, Inc., November 1977.

Defense Nuclear Agency, EM-1, *Nuclear Weapons Effects Manual 1*, EM-1, 1972 (revised edition in course of preparation)

ENW, *The Effects of Nuclear Weapons*, DOD and DOE, 2nd Ed., Glasstone, S., Editor, revised, 1964, 3rd Ed., S.Glasstone & P. Dolan, Editors, 1977.<sup>75</sup>

Fay, J.A., and F.R. Riddell, "Theory of Stagnation Point Heat Transfer in Dissociated Air," *J. Aero. Sci.*, 25, 73, 1958.

Flaud, J.M., and C. Camy-Peyret, "Vibrational-Rotational Intensities in H<sub>2</sub>O-Type Molecules," *J. Mol. Spectry*, 55, 278, 1975.

Fowler, R.H., and E.A. Guggenheim, *Statistical Thermodynamics*, Cambridge University Press, 1949.

Gazley, C., Jr., "Atmospheric Entry," Ch. 10 in H.H. Koelle, ed., *Handbook of Astronautical Engineering*, McGraw-Hill, 1961.

Gear, C.W., *Numerical Initial Value Problems in Ordinary Differential Equations*, Prentice-Hall, Englewood Cliffs, NJ, 1971.

Gebhardt, F.G., "High Power Laser Propagation," *Appl. Opt.*, 15, 1479, 1976.

Gilmore, F.R., "Equilibrium Composition and Thermodynamic Properties of Air to 24,000 K," RAND Report RM-1543 (AD-84052), 1955.

Gilmore, F.R., "Additional Values for the Equilibrium Composition and Thermodynamic Properties of Air," RAND Report RM-2328, 1959.

---

<sup>75</sup> Note: the 1964 reprint has additions to the 1962 revised editions; the 1977 (third) edition has been "improved" in a negative way from the standpoint of what was actually observed during the atmospheric nuclear tests.

Gilmore, F.R., "Potential Energy Curves for N<sub>2</sub>, NO, O<sub>2</sub> and Corresponding Ions," RAND Report RM-4034-PR, June 1964. See also *J. Quant. Spectrosc. Radiat. Transfer*, **5**, 369, 1965.

F.R. Gilmore, "The Contribution of Generally Neglected Band Systems and Continua to the Absorption Coefficient of High-Temperature Air," *J. Quant. Spectrosc. Radiat. Transfer*, **5**, 125, 1965.

Goody, R.M., *Atmospheric Radiation-I, Theoretical Basis*, Oxford University Press, 1964.

*HEL (High-Energy Laser) Propagation Handbook*, OptiMetrics for ASL, ASL-TR-0148, Vol. I, Phenomenological Basis (AD B106243), February 1984.

Herzberg, G., *Atomic Spectra and Atomic Structure*, Prentice-Hall, NJ, 1937.

Herzberg, G., *Molecular Spectra and Molecular Structure-II, IR and Raman Spectra of Polyatomic Molecules*, Van Nostrand, NJ, 1945.

Herzberg, G., *Molecular Spectra and Molecular Structure-I, Spectra of Diatomic Molecules*, Van Nostrand, NJ, (2nd Edition) 1950. See also Huber and Herzberg, 1979.

Herzberg, G., *Molecular Spectra and Molecular Structure-III, Electronic Spectra and Electronic Structure of Polyatomic Molecules*, Van Nostrand, NJ, 1966.

Hilsenrath, J., and M. Klein, "Tables of Thermodynamic Properties of Air in Chemical Equilibrium...from 1500 K to 15,000 K," Report AEDC-TDR--65-58, Arnold Engineering Development Center, National Bureau of Standards (AD612 301), 1965.

Hirschfelder, J.O., C.F. Curtiss, and R.B. Bird, *Molecular Theory of Gases and Liquids*, Wiley (1954, 1964).

Hochstim, A.R., "Theoretical Calculations of Thermodynamic Properties of Air," appendix in Hilsenrath and Klein, 1965, also Combustion Symposium, 1964.

Holland, D.H., et al., *Physics of High-Altitude Nuclear Burst Effects*, DNA 4501 F, Mission Research Corporation, December 1977.

Huber, K.P., and G. Herzberg, *Molecular Spectra and Molecular Structure-IV, Constants of Diatomic Molecules*, Van Nostrand Reinhold, 1979.

*IR Handbook*, W.L. Wolfe and G.J. Zissis, Eds., ERIM for the Office of Naval Research, Rev. Ed. 1985.

Jeans, J.S., *Dynamical Theory of Gases*, Cambridge University Press, 1925.

Jeans, J.S., *Introduction to the Kinetic Theory of Gases*, Cambridge University Press, 1982.

Johnston, R.R., R.K.M. Landshoff, and O.R. Platas, "Radiative Properties of High Temperature Air," Lockheed Palo Alto Research Laboratory Report LMSC D267205, Preliminary Draft, April 1972.

Johnston, R.R., and D.E. Stevenson, "Radiative Properties of High Temperature Air II," SAIC Report SAI-056-77-PA, June 1977.

Jursa, 1985. See USAF, 1985.

Keck, J.C., J. Camm, B. Kivel, and T. Wentink, "Radiation from Hot Air-2," *Ann. Phys. (NY)*, 7, 1, 1959.

Kennealy, J.P., and F.P. Del Greco, "The Kinetics of Atmospheric Radiative Processes in the Infrared," Ch. 11 in the DNA Reaction Rate Handbook, Revision 9, 1983.

Kivel, B., and K. Bailey, "Tables of Radiation from High Temperature Air," Report RR-21, AVCO-Everett Research Laboratory, Everett, MA, 1957.

Kivel, B., "Radiation from Hot Air and Its Effects on Stagnation-Point Heating," *J. Aero. Sci.*, 28, 96, 1961.

Kneizys, F., et al., "Atmospheric Transmittance/Radiance: Computer Code LOWTRAN-5," AFGL-TR-80-0067 (AD-A088 215), 1980.

Kneizys, F., et al., "Atmospheric Transmittance/Radiance: Computer Code LOWTRAN 6," AFGL-TR-83-0187, 1983.

Kondratyev, K. Ya., *Radiation in the Atmosphere*, Academic Press, NY, 1969.

Kuethe, A.M., *Foundations of Aerodynamics*, Wiley (2nd Ed. 1950, with J.D. Schetzer, 4th Ed. 1986, with C-Y Chow)

Kuz'menko, N.E., et al, "Electronic Transition Probabilities and Life Times of Electronically Excited States of Diatomic Molecules," *Sov. Phys. Uspekhi*, 22, #3, 160, 1979.

Landau, L.D., and E.M. Lifshitz, *Fluid Mechanics*, Pergamon, 1959.

Landau, L.D., and E.M. Lifshitz, *Statistical Physics*, Pergamon, 2nd Ed. 1969.

Landshoff, R.K.M., and J.L. Magee, Eds., *Thermal Radiation Phenomena, Vol. 1, Radiative Properties of Air*, and *Vol. 2, Excitation and Non-Equilibrium Phenomena in Air*, IFI/Plenum, New York, 1969.

Ludwig, C.B., et al., *Handbook of IR Radiation from Combustion Gases*, NASA-SP-3080, NASA/Marshall SFC, 1973.

Main, R.P., and E. Bauer, "Opacities of Carbon-Air Mixtures at Temperatures from 3000-10,000 K," *J. Quant. Spectrosc. Radiat. Transfer*, 6, 1, 1966.

Main, R.P., and E. Bauer, "Equilibrium Opacities and Emissivities of Hydrocarbon-Air Mixtures at High Temperatures," *J. Quant. Spectrosc. Radiat. Transfer*, 7, 527, 1967.

Martin, J.J., *Atmospheric Reentry*, Prentice-Hall, 1966.

McClatchey, R.A., et al., "Optical Properties of the Atmosphere (3rd Ed.)," AFCRL-72-0497 (AD-753075), 1972.

Minnaert, M.G.J., *The Nature of Light and Colour in the Open Air*, Dover Publications Inc., 1954.

Morris, J.C., et al., "Bremsstrahlung and Recombination Radiation of Neutral and Ionized Nitrogen," *Phys. Rev.* 180, 167, 1969.

Moss, J.N., and C.D. Scott, Eds., *Thermophysical Aspects of Reentry Flows*, AIAA Progress in Astronautics and Aeronautics, Vol. 103, 1985.

Murty, S.R., "Endo Heating Theory (RVTEMP)," unpublished briefing notes, Teledyne Brown Engineering, Huntsville, AL, August 1987.

Penner, S.S., *Quantitative Molecular Spectroscopy and Gas Emissivities*, Addison-Wesley, 1959.

Penner, S.S., and D.B. Olfe, *Radiation and Reentry*, Academic Press, 1968.

Predvoditelev, A.S., *High-Temperature Properties of Gases*, 1969.

Radzig, A.A., and B.M. Smirnov, *Reference Data on Atoms, Molecules, and Ions*, Springer 1985 (translated from Russian edition of 1980).

Rothman, L.S., et al., "The HITRAN Database: 1986 Edition", *Appl. Opt.* 26, 4058, 1987.

Schlichting, H., *Boundary Layer Theory*, McGraw-Hill, 7th Ed., 1979.

Sharma, R.D. et al., "SHARC: a Computer Model for Calculating Atmospheric Radiation under Non-Equilibrium Conditions", AFGL-TR-89-0083 (Also to be published in Proc. Feb. 1989 Meeting of the IRIS Specialty Group on Targets, Backgrounds, and Discrimination, ERIM, Ann Arbor, MI).

Slater, J.C., *Quantum Theory of Atomic Structure*, McGraw-Hill, 2 vols., 1960.

J.C. Slater, *Quantum Theory of Molecules and Solids, Vol. I, Electronic Structure of Molecules*, McGraw-Hill, 1963.

Smith, H.J.P., et al., "FASCODE-Fast Atmospheric Signature Code (Spectral Transmittance and Radiance)," Visidyne, Inc., Report AFGL-TR-78-0081, January 1978.

*Smithsonian Meteorological Tables*, R.J. List, Compiler, 6th Edition, 1949.

Storm, E., and H.I. Israel, "Photon Cross Sections from 1 keV to 100 MeV for Elements  $Z = 1$  to  $Z = 100$ ," *Nuclear Data Tables A7*, 565, 1970.

Tennekes, H., and J.L. Lumley, *A First Course in Turbulence*, MIT Press, 1972.

Tousey, R., "Ultraviolet Spectroscopy of the Sun," in *Space Astrophysics*, W. Liller, Ed., McGraw-Hill, 1961.

*USAF Handbook of Geophysics and the Space Environment*, 1965, S.L. Valley, Ed.; 1985, A.S. Jursa, Ed.

U.S. National Report to IUGG 1983-1986; Solar-Planetary Relations: Aeronomy, *Rev. Geophys.*, 25, No. 3, 417, April 1987.

*U.S. Standard Atmosphere*, 1962, p. K.3f, and USAF, 1965, p. 2-19f.

*U.S. Standard Atmosphere*, 1976, published by NOAA, NASA, USAF, October 1976.

Unsoeld, A., *Physik Sternatmosphaeren*, Springer, 2nd Ed., 1955.

Valley, 1965. See USAF, 1965.

Van de Hulst, H.C., *Light Scattering by Small Particles*, Wiley, NY 1957.

Veigele, William J., et al., "X-Ray Cross Section Compilation from 0.1 keV to 1 MeV. Input Data and Supplementary Results," Vol. II, Rev. 1, DNA 2433 F, July 1971.

Vigroux, E., "Contribution to the Experimental Study of Ozone Absorption," *Ann. Phys. (Paris)*, 8, 709, 1953.

Watanabe, K., "Ultraviolet Absorption Processes in the Upper Atmosphere," *Adv. Geophys.*, 2, 153, 1958.

Whitten, R.C. and W.W. Vaughan, "Guide to Reference and Standard Atmosphere Models", American Institute of Aeronautics and Astronautics Report AIAA-G-003-1988 (Review draft, June 1989).

Wolfe, W.L. and Zisis, G.J. ,1985. See *IR Handbook*, 1985.

Zeldovich, Ya. B., and Yu. P. Raizer, *Physics of Shock Waves and High-Temperature Hydrodynamic Phenomena*, Academic Press; 2 Vols., 1966, 1967.

**APPENDIX A**

**ELECTRONIC STRUCTURE OF SOME AIR ATOMS  
AND MOLECULES**

## APPENDIX A

### ELECTRONIC STRUCTURE OF SOME AIR ATOMS AND MOLECULES

This appendix presents a brief treatment of the quantum mechanical/spectroscopic structure of various air species.

#### A.1 ATOMS

The electronic structure of atoms is built up by filling electron shells subject to the Pauli exclusion principle, which says that for given principal quantum number  $n$  and orbital angular momentum quantum number  $l$  (where  $l < n$ ) one can have  $2(2l + 1)$  electrons.<sup>1</sup> The notation is odd but traditional<sup>2</sup>:

total orbital angular momentum ( $l$ or $L$ )	0	1	2	3	4	5
notation	s(or S)	p(or P)	d(or D)	f(or F)	g(or G)	...

where  $(nl)$  characterizes an individual electron wave function, while  $L$  is the orbital angular momentum of the atom. In other words, for given principal quantum number  $n$  we can have 2 s-electrons ( $l = 0$ ), 6 p-electrons ( $l = 1$ ), 10 d-electrons ( $l = 2$ ), etc.

Thus, the atoms in the periodic table are built up like this:

Z = 1	H:	(1s) <sup>2</sup> S (where 2 refers to a doublet, i.e., one electron of spin $s = 1/2$ , $2s + 1 = 2$ )
Z = 2	He:	(1s) <sup>2</sup> <sup>1</sup> S ("singlet S," <sup>1</sup> S, is a closed shell, two electrons of opposite spins)

---

<sup>1</sup> Each electron has four quantum numbers, which may be taken as the principal quantum number  $n$ , the orbital angular momentum quantum number  $l$ , the (integral) component  $l_z$  of  $l$  along some designated direction  $z$ , and the spin quantum number  $s_z$  corresponding to angular momentum  $\pm \hbar/2\pi$  along the designated  $z$ -direction. The exclusion principle says that no two electrons in an atom can have all four of  $(n, l, l_z, s_z)$  the same.

<sup>2</sup> S stands for "sharp," P for "principal," D for "diffuse," and F for "fundamental," empirical terms applied to the characters of spectral lines in the late 1890s as spectrographs were first used systematically to study atomic and molecular spectra.

Z = 3	Li	$(1s)^2(2s) \ ^2S$ [one (2s) electron outside a closed shell, i.e., doublet or unpaired electron]
Z = 4	Be	$(1s)^2(2s)^2 \ ^1S$ [two (2s) electrons of opposite spin, (2p) comes next, room for 6 of them]
Z = 5	B	$(1s)^2(2s)^2(2p) \ ^2P$
Z = 6	C	$(1s)^2(2s)^2(2p)^2 \ ^3P$ ("triplet P"--the two electron spins are parallel, $2s + 1 = 3$ if $s = 1$ )
Z = 7	N	$(1s)^2(2s)^2(2p)^3 \ ^4S$ ("quartet S," $s = 3/2$ . From $(2p)^3$ one can also make $^2D$ and $^2P$ configurations, which are, respectively, 2.38 eV and 3.58 eV above the $^4S$ ground state. Figure A-1, which shows the Potential Energy curves for $N_2$ , and Fig. A-2, which shows those for NO, indicate molecular states involving $N(^2D)$ and $N(^2P)$ , as well as those that dissociate into $N(^4S)$ )
Z = 8	O	$(1s)^2(2s)^2(2p)^4 \ ^3P$ (from $(2p)^4$ one can also make $^1D$ and $^1S$ configurations, which are, respectively, 1.97 and 4.19 eV above the $^3P$ ground state, where the triplet splitting is 0.02 and 0.04 eV. Figures A-2 for NO and A-3 for $O_2$ indicate molecular states involving $O(^1D)$ and $O(^1S)$ . They also show molecular negative ions dissociating into the atomic ion $O^- (^2P^o)$ which has 9 electrons outside the nucleus and is thus isoelectronic with Fluorine.
Z = 9	F	$(1s)^2(2s)^2(2p)^5 \ ^2P$ (one electron missing before a closed shell (halogen))
Z = 10	Ne	$(1s)^2(2s)^2(2p)^6 \ ^1S$ (closed shell--noble gas)
Z = 11	Na	$(1s)^2(2s)^2(2p)^6(3s) \ ^2S$ (next alkali, one electron outside a closed shell),

etc.

Atoms have electronically excited states, such as the Rydberg states of the H-atom, and of other atoms having just one electron outside a closed shell, but these states lie 10 eV or more above the ground state, so that transitions involving them lie in the far UV (10 eV corresponds to 1240 Å or 124 nm wavelength). For viewing through the atmosphere we are mainly interested in near-visible radiation, i.e.,  $\lambda \sim 300$  nm to 700 nm or energies of 4.1 eV to 1.8 eV. Important transitions in atomic oxygen correspond to the dipole-

forbidden 630 nm "red" ( $^1D \Rightarrow ^3P$ ) and 558 nm "green" ( $^1S \Rightarrow ^1D$ ) auroral lines, and to the atomic nitrogen  $^2P \Rightarrow ^2D$  (1040 nm) and  $^2D \Rightarrow ^4S$  (520 nm) lines. Figures A-1 to A-3 show that the air molecules  $N_2$ ,  $NO$ , and  $O_2$  have many low-lying states with important transitions between them, so let us now talk about molecular transitions.

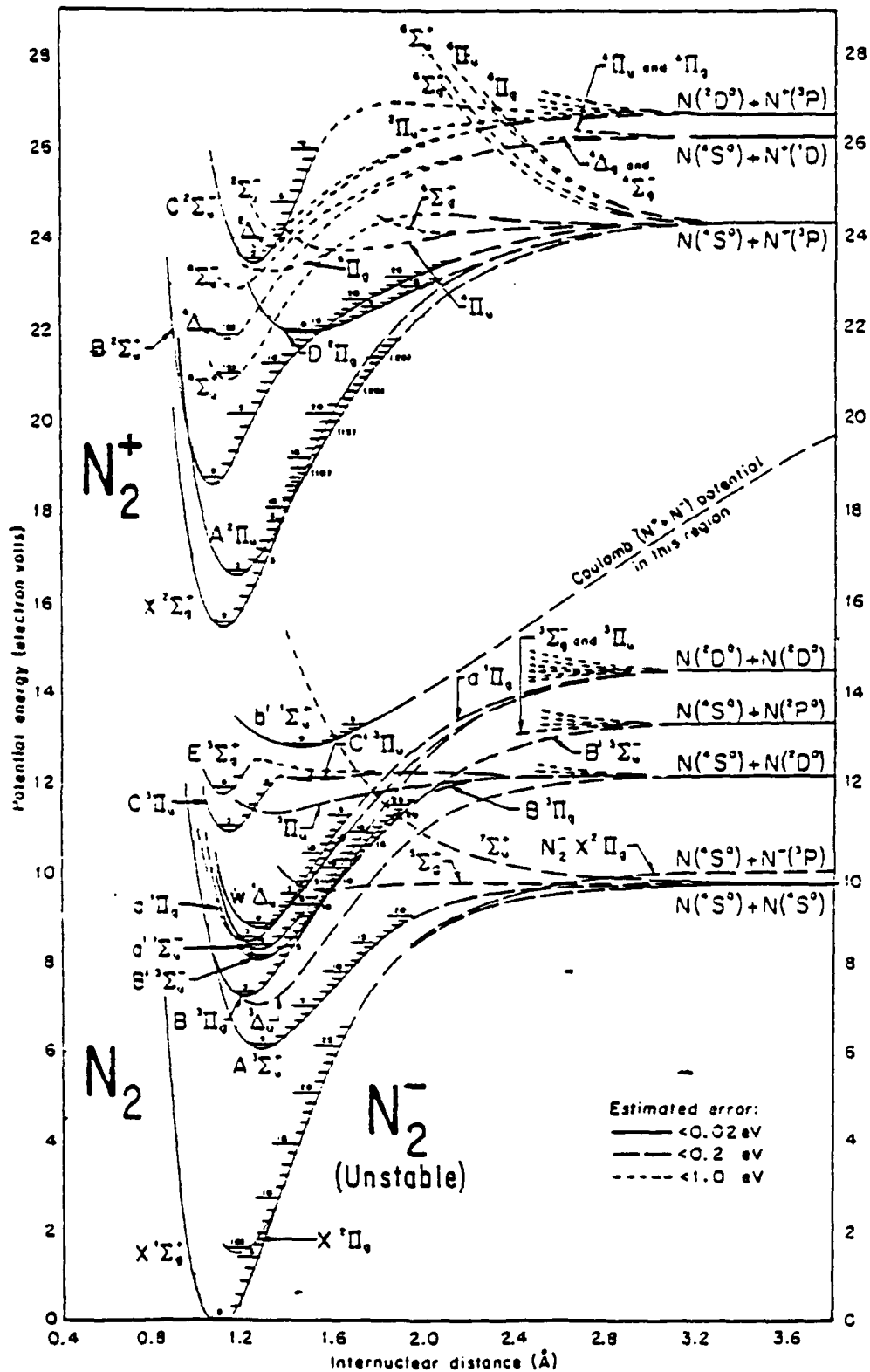


Figure A-1. Potential Energy Curves for  $N_2$  (Source: Gilmore, 1964. Note that the  $5\Sigma_g^+$  state is now thought to be bound more strongly than shown here.)

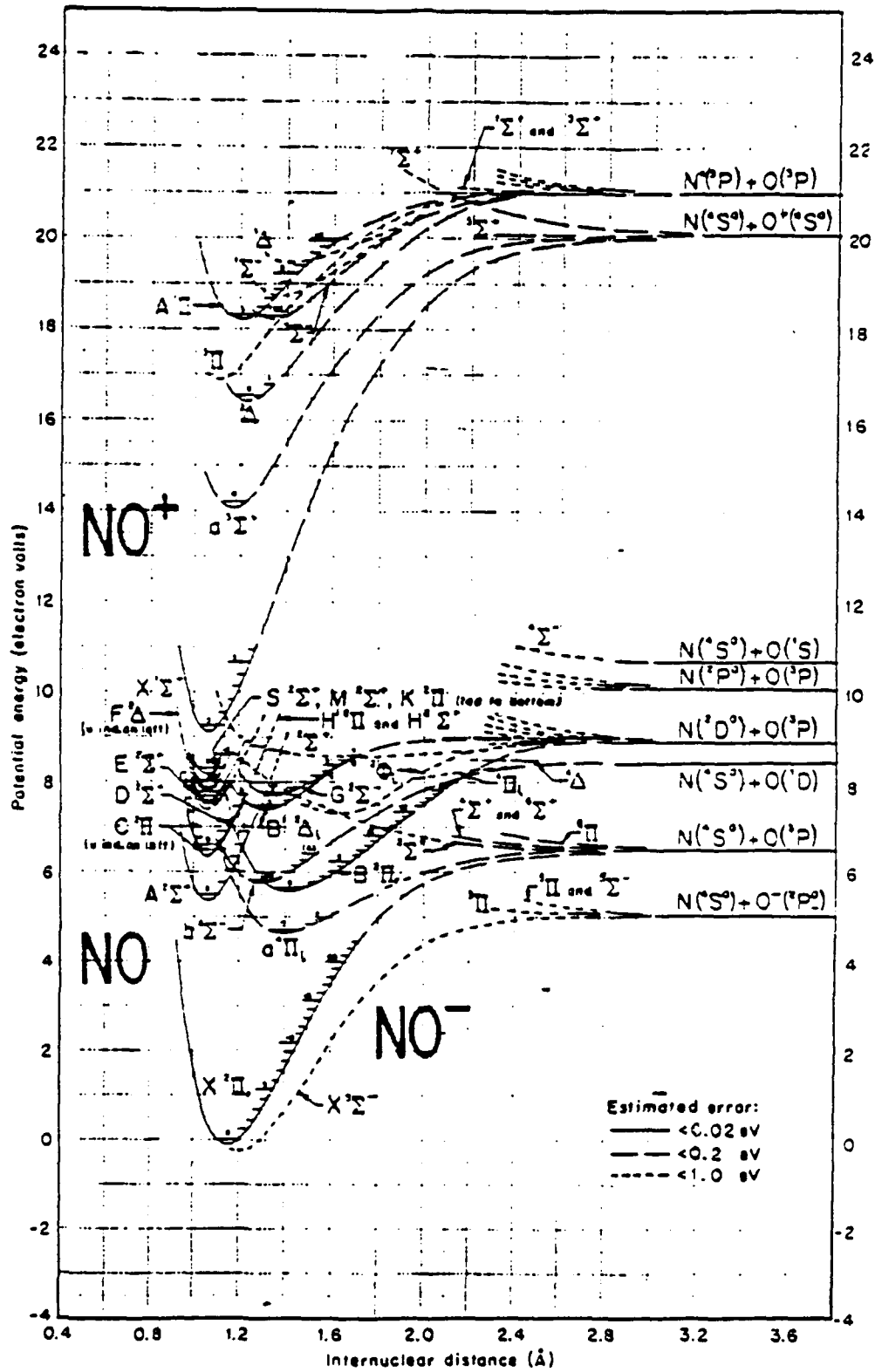


Figure A-2. Potential Energy Curves for NO (Source: Gilmore, 1964)

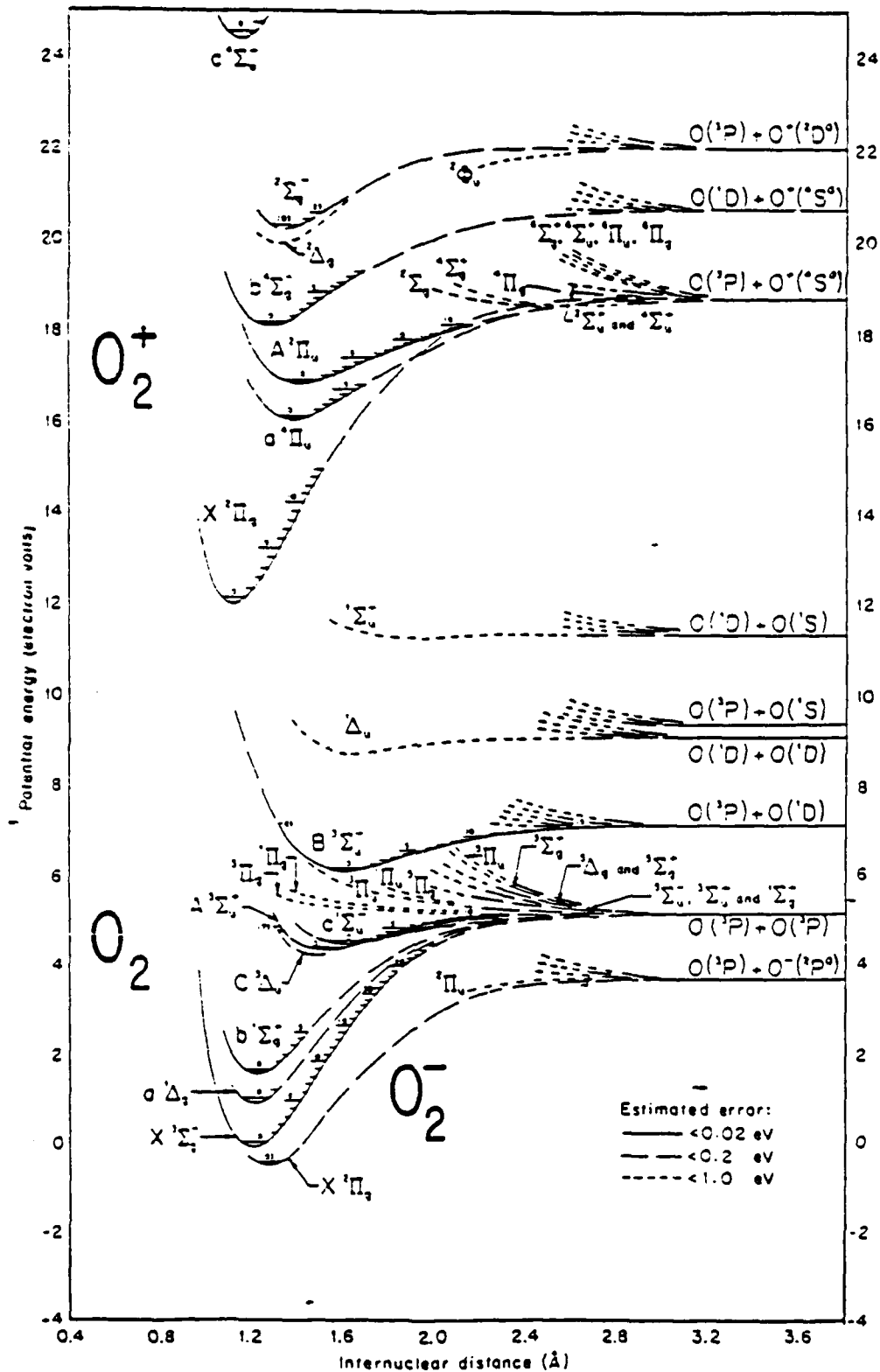


Figure A-3. Potential Energy Curves for  $O_2$  (Source: Gilmore, 1964)

## A.2 DIATOMIC MOLECULES

Here a key parameter is the angular momentum along the molecular axis:<sup>3</sup>

angular momentum:	0	1	2	3
notation:	$\Sigma$	$\Pi$	$\Delta$	$\Phi$

Another key parameter is the spin  $s$ , or equivalent multiplicity  $(2s+1)$ ; a molecular state is labeled  $^{2s+1} \Lambda$ . The (electronic) ground state of a molecule is always called "X," with excited states labeled A,B,... (in increasing energy<sup>4</sup>). The important air molecules  $N_2$ , NO, and  $O_2$  have very complex sets of electronically excited states;<sup>5</sup> which are shown in Figs. A-1 to A-3 respectively.

$H_2$ :  $H(1s^2S) H(1s^2S)$  gives a ground state  $X^1\Sigma$ .

$N_2$ : Ground state is  $X^1\Sigma_g^+$ .

Figure A-1 (from Gilmore, 1964) suggests that  $A^3\Sigma_u^+$  is the only other stable state that dissociates into  $N(^4S) + N(^4S)$ . However, current calculations and observations (Partridge et al., 1988) suggest that the  $^5\Sigma_g^+$  state is bound more strongly than suggested in Fig. A-1, and that in fact this A" state is the primary precursor state involved in the yellow Lewis-Rayleigh afterglow of  $N_2$ .

NO: Ground state  $X^2\Pi$ . See Fig. 2-6 [ $a^4\Pi_i$  also dissociates into  $N(^4S) + O(^3P)$ ]

$O_2$ : Ground state  $X^3\Sigma_g^-$ . See Fig. 2-7.

The other indexes correspond to different symmetries of the atom or molecule, which are important for radiative selection rules. In the case of an atom, if  $\Sigma_i l_i$  is odd or even the state is described as odd or even, respectively, while for a homonuclear diatomic molecule where the electronic wave function either remains the same or changes sign when it is reflected at the center of the interatomic line we describe the state as even (g) or odd (u).<sup>6</sup>

---

<sup>3</sup> The convention is the following:  $s,p,d,\dots$  applies to individual atomic electrons;  $S,P,D$  applies to (multi-electron) configurations in an atom;  $\sigma,\pi,\delta$  applies to single-electron states in a molecule, and  $\Sigma,\Pi,\Delta$  applies to (multi-electron) configurations in a molecule.

<sup>4</sup> Excited states of the same multiplicity (spin) as the ground state are labeled A,B, etc., while those of a different multiplicity are labeled a,b, etc.  $N_2$  is an exception; the convention is reversed due to a historical error.

<sup>5</sup> Principally because the ground states of the N and O atoms are not  $^1S$  but rather  $^4S$  and  $^3P$ , respectively.

<sup>6</sup> This property is called parity.

Further, in the case of a symmetric top (homonuclear diatomic molecule) there are two wave functions of different symmetry, labeled "+" and "-" respectively.<sup>7</sup>

As an example, reference to Fig. A-3 shows that two O(<sup>3</sup>P) atoms can come together along different potential energy curves to give a variety of different molecular states, both stable ones of different spin such as X<sup>3</sup>Σ<sub>g</sub><sup>-</sup>, C<sup>3</sup>Δ<sub>u</sub> and a<sup>1</sup>Δ<sub>g</sub>, b<sup>1</sup>Σ<sub>g</sub><sup>+</sup>, and also unstable (repulsive) states such as <sup>1,3</sup>Π<sub>u,g</sub>, etc. The important "Schumann-Runge" transition (discussed in Chapter III) is a transition B<sup>3</sup>Σ<sub>u</sub><sup>-</sup> => X<sup>3</sup>Σ<sub>g</sub><sup>-</sup> which demonstrates several selection rules:

- (i) spin remains constant (triplet to triplet)
- (ii) parity changes (u => g)
- (iii) inversion symmetry remains constant (- => -).

### A.3 TRIATOMIC MOLECULES

Things get more complicated. A triatomic molecule may be linear, like the CO<sub>2</sub> ground state (<sup>1</sup>Σ), or bent, e.g., NO<sub>2</sub>, O<sub>3</sub>, H<sub>2</sub>O. The ground and excited states are designated by <sup>-</sup>X', <sup>-</sup>A', <sup>-</sup>B', etc. For linear molecules the same state classification symbols (Σ, Π, etc.) are used as for diatomic molecules, while for nonlinear molecules the electronic symmetry is designated by the symbols A<sub>1</sub>, A<sub>2</sub>, B<sub>1</sub>, and B<sub>2</sub> for symmetric molecules like H<sub>2</sub>O and NO<sub>2</sub>, and the symbols A' and A'' for nonsymmetric molecules like HNO. A non-linear triatomic molecule has three fundamental vibration frequencies,<sup>8</sup> and different electronic states may be straight or bent differently from the ground state. For a discussion of the structure of these molecules, see Herzberg, 1966; for the applications discussed here it is sufficient to know that there are different types of states (electronic, vibrational, and rotational, with relatively weak coupling between them).

---

<sup>7</sup> Note that the statistical weight of a <sup>3</sup>D state is 15, while that of a <sup>3</sup>Δ state is 6. In each case the superscript 3 corresponds to spin 1, i.e., multiplicity 3, but D corresponds to L = 2, i.e., statistical weight (2L+1) = 5. By contrast, Δ (Λ.>0) corresponds to a symmetric top with doubly degenerate rotational levels--see, e.g., Herzberg, 1950, p. 128.

<sup>8</sup> See footnote 17 on p. 3-1 of the main text.

**APPENDIX B**

**PARTITION FUNCTION FOR THE DISSOCIATION OF A  
DIATOMIC MOLECULE**

## APPENDIX B

### PARTITION FUNCTION FOR THE DISSOCIATION OF A DIATOMIC MOLECULE

For the dissociation of a diatomic molecule, one may use the standard results--see any text on statistical mechanics, e.g., Fowler and Guggenheim, 1949, pp. 87, 96, 165:

$$f(J) = (2\pi M(J)kT/h^2)^{3/2} V g_J r_J \quad (J = A, B) \quad (\text{B.1a})$$

$$f(AB) = (2\pi M(AB)kT/h^2)^{3/2} V r(T) q(T) g_{AB} r_A r_B / \sigma_{AB} \quad (\text{B.1b})$$

$$r(T) = \text{rotational partition function}^1 = T/\Theta_R; \Theta_R = hcB_0/k \quad (\text{B.1c})$$

$$q(T) = \text{vibrational partition function}^2 = 1/[1-\exp(-\Theta_V/T)]; \Theta_V = hc\omega_0/k, \quad (\text{B.1d})$$

and

$g_J$  = electronic partition function (statistical weight)

$r_J$  = nuclear spin weight<sup>3</sup>

$\sigma_{AB}$  = symmetry number = 2 if A=B, otherwise, 1.

$B_0, \omega_0, T_0$ , etc., come from Huber and Herzberg, 1979, or equivalent and are measured in  $\text{cm}^{-1}$ .

Let us do calculations for the  $\text{O}_2$  molecule for which:

$$D = 5.116 \text{ eV, i.e., } \Theta_D = 59300 \text{ K}$$

$$\omega_0 = 1568 \text{ cm}^{-1}, \text{ i.e., } \Theta_V = (hc/k)\omega_0 = 1.439 \omega_0 = 2256 \text{ K}$$

$$B_0 = 1.438 \text{ cm}^{-1}, \Theta_R = (hc/k)B_0 = 2.07 \text{ K}$$

- 
- <sup>1</sup> This is an approximation good when the rotational level spacing is small compared to  $kT$ , which holds for molecules such as  $\text{N}_2$ ,  $\text{O}_2$ ,  $\text{NO}$ , etc. (not  $\text{H}_2$ !) at temperatures above  $\sim 200 \text{ K}$ .
  - <sup>2</sup> An approximation good for harmonic oscillators with vibrational spacing large compared with  $kT$ .
  - <sup>3</sup> For the dissociation of a diatomic molecule, the term  $r_{AB}/r_A r_B$  must equal unity because the nuclear spins do not change--see, e.g., Fowler and Guggenheim, 1949, p. 166.

$$g_{O_2}(T) = 3 + 2 \exp(-\Theta_E/T) ; \Theta_E = (hc/k)T_{el} = 11400 \text{ K (contribution from } ^1\Delta \text{ state)}$$

$$g_O = 3 .$$

Calculations for various values of number density ratios  $n/n_0$ , where  $n_0 = 2.687 \times \text{cm}^{-3}$ , respectively) are shown in Fig. 2-1, where we list a fractional dissociation defined as

$$\phi_{\text{diss}} = n_O / [n_O + n_{O_2}] . \quad (\text{B.2})$$

**APPENDIX C**

**EINSTEIN A- AND B-COEFFICIENTS, f-NUMBERS AND  
BAND STRENGTHS**

## APPENDIX C

### EINSTEIN A- AND B-COEFFICIENTS, f-NUMBERS AND BAND STRENGTHS

This appendix presents the relation between the various measures of band strength, following Einstein's derivation of the A (spontaneous) and B (stimulated) emission/absorption coefficients as presented by Penner, 1959--see also Ludwig et al, 1973. We use cgs units here because this is conventional.

Consider a transition from an upper state  $u$  to a lower state  $l$ , with  $N_j$  molecules in state  $j$  ( $= u, l$ ) per unit volume.  $A_{ul}$  and  $B_{ul}$  are emission coefficients (spontaneous and stimulated) and  $B_{lu}$  is the stimulated absorption coefficient. The spectral density of a black-body radiation field is:<sup>1</sup>

$$\rho(\nu) = (8\pi h\nu^3/c^3) (e^{h\nu/kT} - 1)^{-1} \quad , \quad (C.1)$$

whose units are erg sec/cm<sup>3</sup>, while  $B_{ij}$  is measured in cm<sup>3</sup>/erg sec<sup>2</sup> = cm/gm and  $A_{ij}$  is measured in sec<sup>-1</sup>.

In *Radiative Steady State*, defined as

$$\text{Absorption} = \text{Emission} \quad , \quad (C.2)$$

we have

$$N_l B_{lu} \rho(\nu_{lu}) = N_u [ A_{ul} + B_{ul} \rho(\nu_{lu}) ] \quad (C.3)$$

and

$$N_l/N_u = [ A_{ul} + B_{ul} \rho ] / B_{lu} \rho = (g_l/g_u) e^{h\nu/kT} \quad , \quad (C.4)$$

which gives the following relations between the A- and B-coefficients:

$$A_{ul} = (8\pi h\nu^3/c^3) B_{ul} \quad , \quad (C.5)$$

$$g_l B_{lu} = g_u B_{ul} \quad . \quad (C.6)$$

---

<sup>1</sup> In the notation of Section 3.2 of the main text, one should write  $B(\nu, T)$  instead of  $\rho(\nu)$ , but the use of  $\rho(\nu)$  is conventional here, and there would be confusion between blackbody radiance and the Einstein B-coefficient.

As in Eq.(3.34a) in the main text, we define a band strength

$$S'_{lu} = \int k_\nu [1 - \exp(-h\nu/kT)] d\nu = (c^2/8\pi\nu_{lu}^2) N_l A_{ul} (g_u/g_l) [1 - \exp(-h\nu_{lu}/kT)] \quad (C.7)$$

The factor  $[1 - \exp(-h\nu_{lu}/kT)]$  is a correction for stimulated emission, which arises because of the B-terms (stimulated emission and absorption). This term is often close to one at room temperature and can frequently be neglected, but it can be important here. The dimensions of band strength are

$$S'_{lu} = (\text{number density}) \times (\text{absorption cross section}) \quad (C.8)$$

and it is normally measured either in  $10\text{-}20 \text{ cm}^{-1}/(\text{molecules} \times \text{cm}^{-2})$  or in  $(\text{cm}^{-2} \text{ atm}^{-1})$ , where...

$$S(\text{cm}^{-2} \text{ atm}^{-1}) = 2.687 \times (T_0/T) S (\text{cm}^{-1}/\text{mol}.\text{cm}^{-2}) \quad (C.9)$$

with  $T_0 = 273.2 \text{ K}$  - see, e.g. Flaud & Camy-Peyret, 1975, p. 284. One may write

$$S_{lu}(\text{cm}^{-2} \text{ atm}^{-1}) = 3.21 \times 10^{28} A_{ul}/\nu_{ul}^2 \quad (C.10)$$

where  $A_{ul}$  is measured in  $\text{sec}^{-1}$  and  $\nu_{ul}$  in Hz.

One may also define a dimensionless absorption oscillator strength  $f_{lu} = f_{\text{abs}}$  by

$$S'_{lu} = (\pi e^2/mc) N_l f_{lu} [1 - \exp(-h\nu_{lu}/kT)] \quad (C.11)$$

or at Standard Temperature and Pressure (STP), if practically all the absorbing molecules are in the ground state  $l$ , provided that  $\exp(-h\nu_{lu}/kT) \ll 1$ ,

$$S_{lu} (\text{cm}^{-2} \text{ atm}^{-1}) = 2.3795 \times 10^7 f_{lu} \quad (C.12)$$

and an emission oscillator strength  $f_{ul}$  is related to the absorption oscillator strength  $f_{lu}$  by the relation

$$f_{ul} = (g_l/g_u) f_{lu} \quad (C.13)$$

From (C.10) and (C.12) we get

$$A_{ul} = 7.413 \times 10^{-22} \nu_{lu}^2 f_{lu} \quad (C.14)$$

Finally, the lifetime,  $\tau_u$ , of an excited state  $u$  is related to the A-coefficients of all lower-lying states by the relation

$$1/\tau_u = \sum_j A_{uj} + \sum_j B_{uj} \rho(\nu_{ju}) + \sum_{u'} B_{uu'} \rho(\nu_{uu'}) \quad (C.15)$$

**APPENDIX D**

**EXCERPTS FROM PHYSICAL CONSTANTS, USAF 1985  
AND  
U.S. STANDARD ATMOSPHERE, 1962**

**APPENDIX D**  
**EXCERPTS FROM PHYSICAL CONSTANTS, USAF 1985**  
**AND**  
**U.S. STANDARD ATMOSPHERE, 1962**

Physical Constants (from USAF, 1985, p. A-7\*) .....D-4  
U.S. Standard Atmosphere, 1962 ("USSA-62"\*\*) .....D-5

---

\* Agree to four figures or better with Cohen and Taylor (1987), which is the latest compilation of physical constants.

\*\* Note that USSA-62 corresponds to near-solar maximum conditions (the largest ever was in 1957, with Zurich Sunspot number 190); USSA-76 corresponds to near-solar minimum conditions, with a density smaller by perhaps a factor 3 at 500 km altitude. CIRA-72 has intermediate values. For a current listing of reference and standard atmospheres, see Whitten & Vaughan, 1989.

# UNITS, CONSTANTS, AND CONVERSION FACTORS

Quantity	Symbol (expression)	Value in SI (cgs) units	Error (ppm)
1 Speed of light in vacuum	$c$	$2.997\,924\,58 \times 10^8 \text{ m}\cdot\text{s}^{-1}$ ( $10^{10} \text{ cm}\cdot\text{sec}^{-1}$ )	0.004
2 Elementary charge	$e$	$1.602\,189\,2 \times 10^{-19} \text{ C}$ ( $10^{-20} \text{ emu}$ )	2.9
		$(4.803\,242 \times 10^{-10} \text{ esu})$	2.9
3 Planck's constant	$h$	$6.626\,176 \times 10^{-34} \text{ J}\cdot\text{s}$ ( $10^{-27} \text{ erg}\cdot\text{sec}$ )	5.4
	$\hbar = h/2\pi$	$1.054\,588\,7 \times 10^{-34} \text{ J}\cdot\text{s}$ ( $10^{-27} \text{ erg}\cdot\text{sec}$ )	5.4
4 Electron rest mass	$m_e$	$9.109\,53\,4 \times 10^{-31} \text{ kg}$ ( $10^{-27} \text{ gm}$ )	5.1
5 Avogadro constant	$N_A$	$6.022\,045 \times 10^{23} \text{ mol}^{-1}$ ( $10^{23} \text{ mol}^{-1}$ )	5.1
recent value		$6.022\,097\,8 \times 10^{23} \text{ mol}^{-1}$ ( $10^{23} \text{ mol}^{-1}$ )	1.0
6 Molar gas constant	$R$	$8.314\,471 \times 10^0 \text{ J}\cdot\text{mol}^{-1}\cdot\text{K}^{-1}$ ( $10^7 \text{ erg}\cdot\text{mol}^{-1}\cdot\text{K}^{-1}$ )	31
7 Boltzmann constant	$k = R/N_A$	$1.380\,662 \times 10^{-23} \text{ J}\cdot\text{K}^{-1}$ ( $10^{-16} \text{ erg}\cdot\text{K}^{-1}$ )	32
8 Gravitational constant	$G$	$6.672\,0 \times 10^{-11} \text{ N}\cdot\text{m}^2\cdot\text{kg}^{-2}$ ( $10^{-8} \text{ dyn}\cdot\text{cm}^2\cdot\text{gm}^{-2}$ )	615
9 Molar volume (273.15 °K, $p_0 = 1 \text{ atm}$ )	$V_m = RT_0/p_0$	$22.413\,83 \times 10^{-3} \text{ m}^3\cdot\text{mol}^{-1}$ ( $10^3 \text{ cm}^3\cdot\text{mol}^{-1}$ )	31
10 Faraday constant	$F = N_A e$	$9.648\,456 \times 10^4 \text{ C}\cdot\text{mol}^{-1}$ ( $10^3 \text{ emu}\cdot\text{mol}^{-1}$ )	2.8
11 Rydberg constant	$R_\infty = [4\pi\epsilon_0]^{-2}(m_e e^4/4\pi\hbar^3 c)$	$1.097\,373\,177 \times 10^7 \text{ m}^{-1}$ ( $10^5 \text{ cm}^{-1}$ )	0.07
recent value		$1.097\,373\,147\,6 \times 10^7 \text{ m}^{-1}$ ( $10^5 \text{ cm}^{-1}$ )	0.0003
12 Fine structure constant	$\alpha^{-1} = [4\pi\epsilon_0](\hbar c/e^2)$	137.036 04	0.11
recent value		137.035 963	
13 Classical electron radius	$r_e = [4\pi\epsilon_0]^{-1}(e^2/m_e c^2)$	$2.817\,938\,0 \times 10^{-15} \text{ m}$ ( $10^{-13} \text{ cm}$ )	2.5
14 Specific electron charge	$e/m_e$	$1.758\,804\,7 \times 10^{11} \text{ C}\cdot\text{kg}^{-1}$ ( $10^7 \text{ emu}\cdot\text{gm}^{-1}$ )	2.8
15 Electron Compton wavelength	$\lambda_c = \hbar/m_e c = \alpha^{-1} r_e$	$3.861\,590\,5 \times 10^{-13} \text{ m}$ ( $10^{-11} \text{ cm}$ )	1.6
16 Bohr radius	$a_0 = \alpha^{-2} r_e$	$0.529\,177\,06 \times 10^{-10} \text{ m}$ ( $10^{-8} \text{ cm}$ )	0.82
17 Magnetic flux quantum	$\Phi_0 = [c]^{-1}(\hbar c/2e)$	$2.067\,850\,6 \times 10^{-15} \text{ T}\cdot\text{m}^2$ ( $10^{-7} \text{ Gs}\cdot\text{cm}^2$ )	2.6
	$h/2m_e$	$4.135\,701 \times 10^{-15} \text{ J}\cdot\text{s}\cdot\text{C}^{-1}$ ( $10^{-7} \text{ erg}\cdot\text{sec}\cdot\text{emu}^{-1}$ )	2.6
18 Quantum of circulation	$h/2m_e$	$3.638\,945\,5 \times 10^{-4} \text{ J}\cdot\text{Hz}^{-1}\cdot\text{kg}^{-1}$ ( $10^0 \text{ erg}\cdot\text{sec}\cdot\text{gm}^{-1}$ )	1.6
19 Atomic mass unit	$1 \text{ u} = \text{gm}\cdot\text{mol}^{-1}/N_A$	$1.660\,565\,5 \times 10^{-27} \text{ kg}$ ( $10^{-24} \text{ gm}$ )	5.1
20 Proton rest mass	$m_p$	$1.672\,648\,5 \times 10^{-27} \text{ kg}$ ( $10^{-24} \text{ gm}$ )	5.1
		$1.007\,276\,470 \text{ u}$ (amu)	0.011
	$m_p/m_e$	1836.151 52	0.38
21 Neutron rest mass	$m_n$	$1.674\,954\,3 \times 10^{-27} \text{ kg}$ ( $10^{-24} \text{ gm}$ )	5.1
		$1.008\,665\,012 \text{ u}$ (amu)	0.037
22 Electron g factor	$g_e = \mu_e/\mu_B$	1.001 159 656 7	0.0035
recent value		1.001 159 652 200	0.0004
23 Bohr magneton	$\mu_B = [c](e\hbar/2m_e c)$	$9.274\,078 \times 10^{-24} \text{ J}\cdot\text{T}^{-1}$ ( $10^{-21} \text{ erg}\cdot\text{Gs}^{-1}$ )	3.9
24 Nuclear magneton	$\mu_N = [c](e\hbar/2m_p c)$	$5.050\,824 \times 10^{-27} \text{ J}\cdot\text{T}^{-1}$ ( $10^{-24} \text{ erg}\cdot\text{Gs}^{-1}$ )	3.9
25 Electron magnetic moment	$\mu_B$	$9.284\,832 \times 10^{-24} \text{ J}\cdot\text{T}^{-1}$ ( $10^{-21} \text{ erg}\cdot\text{Gs}^{-1}$ )	3.9
26 Proton magnetic moment	$\mu_p$	$1.410\,617\,1 \times 10^{-26} \text{ J}\cdot\text{T}^{-1}$ ( $10^{-23} \text{ erg}\cdot\text{Gs}^{-1}$ )	3.9
	$\mu_p/\mu_B$	658.210 688 0	0.010
27 Proton gyromagnetic ratio	$\gamma_p$	$2.675\,198\,7 \times 10^8 \text{ rad}\cdot\text{s}^{-1}\cdot\text{T}^{-1}$ ( $10^4 \text{ rad}\cdot\text{sec}^{-1}\cdot\text{Gs}^{-1}$ )	2.8
28 Stefan-Boltzmann constant	$\sigma = (\pi^2/60)k^4/\hbar^3 c^2$	$5.670\,32 \times 10^{-8} \text{ W}\cdot\text{m}^{-2}\cdot\text{K}^{-4}$ ( $10^{-5} \text{ erg}\cdot\text{sec}^{-1}\cdot\text{cm}^{-2}\cdot\text{K}^{-4}$ )	125
29 First radiation constant	$c_1 = 2\pi\hbar c^2$	$3.741\,832 \times 10^{-16} \text{ W}\cdot\text{m}^2$ ( $10^{-3} \text{ erg}\cdot\text{sec}^{-1}\cdot\text{cm}^2$ )	5.4
30 Second radiation constant	$c_2 = \hbar c/k$	$1.438\,786 \times 10^{-2} \text{ m}\cdot\text{K}$ ( $10^0 \text{ cm}\cdot\text{K}$ )	31

### Energy equivalents

Quantity	Symbol (expression)	Value	Error (ppm)
Atomic mass unit	$u$	931.501 6 MeV	2.8
Proton mass	$m_p$	938.279 6 MeV	2.8
Neutron mass	$m_n$	939.573 1 MeV	2.8
Electron mass	$m_e$	0.511 003 4 MeV	2.8
Electron volt	$1 \text{ eV}/k$	11 604.50 K	31
	$1 \text{ eV}/\hbar c$	$8\,065.479 \text{ cm}^{-1}$	2.6
	$1 \text{ eV}/h$	$2.417\,969\,6 \times 10^{14} \text{ Hz}$	2.6
	$1 \text{ eV}$	$1.602\,189\,2 \times 10^{-12} \text{ ergs}$	2.9
Planck's constant	$\hbar$	$6.582\,173 \times 10^{-22} \text{ MeV}\cdot\text{sec}$	2.6
	$\hbar c$	$1.973\,285\,8 \times 10^{-11} \text{ MeV}\cdot\text{cm}$	2.6
	$(\hbar c)^2$	$0.389\,385\,7 \text{ GeV}^2\cdot\text{mb}$	5.2
Rydberg constant	$R_\infty \hbar c$	13.605 804 eV	2.6
Voltage-wavelength product	$V\lambda$	12 398.520 eV·Å	2.6
Gas constant	$R$	1.987 19 cal·mol <sup>-1</sup> ·K <sup>-1</sup>	31

Properties of the U. S. Standard Atmosphere, 1962, condensed from the complete tables. Numbers following the plus or minus sign are the power of ten by which that entry and each following entry should be multiplied.

Geom Alt (m)	Temperature (°C)		Pressure (mb)	Density (kg m <sup>-3</sup> )	Particle Speed (m sec <sup>-1</sup> )	Collision Frequency (sec <sup>-1</sup> )	Mean Free Path (m)	Molecular Weight	Sound Speed (m sec <sup>-1</sup> )	Coefficient of Viscosity (kg m <sup>-1</sup> sec <sup>-1</sup> )	Kinematic Viscosity (m <sup>2</sup> sec <sup>-1</sup> )	Thermal Conductivity (K cal m <sup>-1</sup> sec <sup>-1</sup> )	
	(°K)	(°C)											
-5000	320.676	47.526	1.77762 +3	1.9311 -0	4.0153 +25	481.15	1.1507 +10	4.2675 -8	20.964	358.986	1.9122 -5	1.0058 -5	6.6515 -6
-4000	311.166	41.016	1.59598	1.7697	3.6798	479.22	1.0138	4.5912	20.964	355.324	1.9123	1.0096	6.5156
-3000	301.659	31.509	1.42973	1.6189	3.3662	471.21	9.4888 +9	5.0109	20.964	351.625	1.8020	1.1625	6.3161
-2000	301.154	28.004	1.27783	1.4782	3.0715	469.19	8.5356	5.1948	20.964	347.888	1.6515	1.2525	6.2958
-1000	291.651	21.501	1.13931	1.3370	2.8009	461.09	7.6949	6.0120	20.964	344.111	1.6206	1.3516	6.1718
0	288.150	15.000	1.01325 -1	1.2250 -0	2.5471 +25	458.91	6.9194 +9	6.6320 -8	20.964	340.291	1.7091 -5	1.4607 -5	6.0530 -6
1000	281.651	8.501	8.98762 +2	1.1117 -0	2.3015 +25	453.71	6.2079 +9	7.3090 -8	20.964	336.435	1.7579 -5	1.5813 -5	5.9405 -6
2000	275.154	2.001	7.95014	1.0066	2.0929	448.40	5.5558	8.0724	20.964	332.542	1.7240	1.7147	5.8073
3000	268.659	-4.491	7.01211	9.0925 -1	1.8906	443.15	4.9591	8.9161	20.964	328.583	1.6930	1.8628	5.6811
4000	262.166	-10.981	6.16601	8.1935	1.7037	437.76	4.3141	9.9166	20.964	324.589	1.6612	2.0275	5.5586
5000	255.676	-17.471	5.40182	7.3613	1.5313	432.31	3.9183	1.1033 -7	20.964	320.545	1.6282	2.2110	5.4311
6000	249.187	-23.963	4.72176 +2	6.6011 -1	1.3726 +25	426.79	3.4674 +9	1.2309 -7	20.964	316.452	1.5919 -5	2.4162 -5	5.3068 -6
7000	242.700	-30.450	4.11052	5.9002	1.2268	421.20	3.0586	1.3771	20.964	312.306	1.5612	2.6161	5.1798
8000	236.215	-36.935	3.56516	5.2579	1.0933	415.53	2.6809	1.5353	20.964	308.105	1.5271	2.9011	5.0520
9000	229.733	-43.417	3.08007	4.6706	9.7116 +24	409.79	2.3556	1.7196 -7	20.964	303.848	1.4926	3.1957	4.9235
10000	223.252	-49.898	2.64999	4.1351	8.5981	403.97	2.0559	1.9619	20.964	299.532	1.4577	3.5251	4.7942
11000	216.774	-56.376	2.26999 +2	3.6180 -1	7.5853 +24	398.07	1.7872 +9	2.2373 -7	20.964	295.154	1.4223 -5	3.8988 -5	4.6642 -6
12000	210.300	-62.850	1.91991	3.1191	6.4861	392.95	1.5278	2.4817	20.964	290.699	1.3216	4.5574	4.6617
13000	203.826	-69.324	1.65796	2.6660	5.5333	397.95	1.3057	3.0177	20.964	295.069	1.3216	5.3325	4.6617
14000	207.352	-75.798	1.41701	2.2786	4.7378	397.95	1.1160	3.5659	20.964	295.069	1.3216	6.2391	4.6617
15000	210.878	-82.272	1.21118	1.9175	4.0195	397.95	9.5386 +8	4.1720	20.964	295.069	1.3216	7.2995	4.6617
16000	214.404	-88.746	1.03528 +2	1.6647 -1	3.4614 +24	397.95	8.1533 +8	4.8008 -7	20.964	295.069	1.3216 -5	8.5397 -5	4.6617 -6
17000	217.930	-95.220	8.81971 +1	1.4230	2.9589	397.95	6.9696	5.7098	20.964	295.069	1.3216	9.9902	4.6617
18000	221.456	-101.694	7.56522	2.5291	2.5291	397.95	5.9580	6.6793	20.964	295.069	1.3216	1.1686 -4	4.6617
19000	224.982	-108.168	6.46748	2.1621	2.1621	397.95	5.0935	7.8130	20.964	295.069	1.3216	1.3670	4.6617
20000	228.508	-114.642	5.52930	1.8910 -2	1.8910	397.95	4.3516	9.1387	20.964	295.069	1.3216	1.5909	4.6617
21000	232.034	-121.116	4.72893 +1	1.6715 -2	1.5711 +24	391.01	3.7163 +8	1.0731 -6	20.964	295.069	1.3216 -5	1.8813 -4	4.6617 -6
22000	235.560	-127.590	4.01719	1.4510	1.3114	391.01	3.1735	1.2595	20.964	296.177	1.3222	2.2201	4.7001
23000	239.086	-134.064	3.36646	1.2306	1.1337	400.63	2.7121	1.4772	20.964	297.019	1.3376	2.6135	4.7203
24000	242.612	-140.538	2.81774	1.0100	9.7598 +23	400.63	2.3196	1.7410	20.964	297.720	1.4190	3.0713	4.7403
25000	246.138	-147.012	2.35922	8.3316	8.3316	402.43	1.9853	2.0270	20.964	298.389	1.4181	3.6135	4.7602
26000	249.664	-153.486	2.00017 +1	7.1230 +23	7.1230 +23	403.33	1.7005 +8	2.3719 -6	20.964	299.056	1.4538 -5	4.2139 -4	4.7800 -6
27000	253.190	-160.000	1.61619	5.2111	5.2111	405.12	1.2503	3.2002	20.964	300.306	1.4616	5.8105	4.8197
28000	256.716	-166.514	1.19703	3.8200	3.8200	406.91	9.2197 +7	4.4131	20.964	301.709	1.4753	8.0131	4.8593
29000	260.242	-173.028	8.89063 +0	2.8105	2.8105	408.68	6.8180	5.5912	20.964	303.025	1.4859	1.0962 -3	4.8988
30000	263.768	-179.542	6.63112	2.0559	2.0559	413.35	5.8300	8.2177	20.964	306.189	1.5160	1.5312	5.0031

(Continued)

Properties of the U. S. Standard Atmosphere, 1962, condensed from the complete tables. Numbers following the plus or minus sign are the power of ten by which that entry and each following entry should be multiplied. (Continued)

Geometric Altitude (m)	Temperature		Pressure (mb)	Density (kg m <sup>-3</sup> )	Particle Speed (m sec <sup>-1</sup> )	Collision Frequency (sec <sup>-1</sup> )	Mean Free Path (m)	Molecular Weight	Sound Speed (m sec <sup>-1</sup> )	Coefficient of Viscosity (kg m <sup>-1</sup> sec <sup>-1</sup> )	Kinematic Viscosity (m <sup>2</sup> sec <sup>-1</sup> )	Thermal Conductivity (K cal m <sup>-1</sup> sec <sup>-1</sup> )
	(°K)	(°C)										
30000	219.282	-318.648	4.96522 +0	7.2579 -3	1.5491 +23	418.22	3.7358 +7	1.1195 -5	28.964	310.099	1.5133 -5	5.1125 -6
30000	211.818	-28.312	3.77138	5.3666	1.1159	421.03	2.7911	1.5110	28.964	313.665	1.5723	5.2213
40000	250.350	-22.800	2.87183	3.9957	8.3082 +22	422.78	2.1017	2.0135	28.964	317.189	1.6489	5.3265
42000	255.878	-17.272	2.19967	2.9918	6.2210	432.48	1.5910	2.7111	28.964	320.672	1.6291	5.4101
44000	261.103	-11.744	1.69196	2.2589	4.6968	437.13	1.2152	3.5970	28.964	324.116	1.6573	5.5138
46000	266.925	-6.225	1.31310 +0	1.7141 -3	3.5612 +22	441.72	9.3100 +6	4.7001 -6	28.964	327.521	1.6851 -6	6.6501 -6
48000	270.650	-2.500	1.02296	1.3167	2.7178	444.79	7.2079	6.1489	28.964	329.799	1.7017	6.7214
50000	270.650	-2.500	7.97790 -1	1.0269	2.1152	441.79	5.6214	7.9125	28.964	329.799	1.7017	6.7214
52000	270.650	-2.500	6.22283	8.0697 -4	1.6655	441.79	4.3817	1.0111 -4	28.964	329.799	1.7017	6.7214
54000	267.560	-5.590	4.81917	6.3137	1.3128	442.21	3.1365	1.2869	28.964	327.911	1.6883	5.6622
56000	263.628	-9.522	3.76572 -1	4.9762 -4	1.0317 +22	438.98	2.6885 +6	1.6328 -4	28.964	325.492	1.6686 -5	5.5867 -6
58000	259.699	-13.451	2.91373	3.9886	8.1271 +21	435.70	2.0959	2.0788	28.964	323.053	1.6187	5.5109
60000	255.772	-17.378	2.24606	3.0592	6.3610	432.39	1.6280	2.6287	28.964	320.706	1.6287	5.4319
62000	251.816	-22.101	1.72157	2.3931	4.9760	428.38	1.2617	3.3952	28.964	317.630	1.6015	5.3131
64000	247.202	-29.918	1.31501	1.8037	3.9168	421.63	9.7719 +5	4.3131	28.964	312.628	1.5638	5.1896
66000	235.363	-37.787	9.9067 -2	1.4713 -4	3.0591 +21	417.78	7.5111 +5	5.5223 -3	28.964	307.519	1.5226 -5	5.0352 -6
68000	227.529	-45.621	7.41183	1.1399	2.3701	407.82	5.7213	7.1218	28.964	302.387	1.4808	4.8796
70000	219.700	-53.450	5.52017	8.7535 -5	1.8201	400.74	4.3174	9.2021	28.964	297.139	1.4383	4.7230
72000	211.876	-61.274	4.05013	6.6593	1.3817	393.53	3.2254	1.2201 -3	28.964	291.800	1.3953	4.5654
74000	201.057	-69.093	2.93758	5.0151	1.0128	386.21	2.3838	1.6202	28.964	286.365	1.3515	4.4067
76000	196.24	-76.91	2.1015 -2	3.736 -5	7.768 +20	378.7	1.741 -5	2.175 -3	28.964	280.83	1.307 -5	4.247 -6
78000	188.13	-81.72	1.4877	2.750	5.719	371.1	1.256	2.951	28.964	275.18	1.262	4.086
80000	180.65	-92.50	1.0366	1.999	4.157	363.4	8.910 +4	4.065	28.964	269.41	1.216	3.925
85000	180.65	-92.50	4.1250 -3	7.955 -6	1.651 +20	363.4	3.558 +4	1.021 -2	28.964	269.41	1.216 -5	3.925 -6
90000	180.65	-92.50	1.6138	3.170	6.591 +19	363.4	1.418	2.563	28.96	269.41	1.216	3.925
95000	195.51	-77.61	6.8012 -4	1.211	2.520	378.2	5.610 +3	6.705	28.91	269.41	1.216	3.925
100000	210.02	-63.13	3.0075	4.971 -7	1.037	392.4	2.409	1.629 -1	28.88	269.41	1.216	3.925
105000	233.90	-39.25	1.4318	2.117	4.431 +18	415.0	1.089	3.810	28.75	269.41	1.216	3.925
110000	257.00	-16.15	7.3541 -5	9.829 -8	2.073 +18	436.5	5.356 +2	8.150 -1	28.56	269.41	1.216	3.925
115000	303.78	30.63	4.1221	4.623	9.830 +17	476.5	2.773	1.719 -10	28.32	269.41	1.216	3.925
120000	349.49	76.31	2.5217	2.436	5.226	513.4	1.588	3.233	28.07	269.41	1.216	3.925
125000	412.35	169.20	1.6863	1.278	2.761	580.3	9.181 +1	6.118	27.81	269.41	1.216	3.925
130000	533.80	260.65	1.2214	7.589 -9	1.657	610.2	6.280	1.019 +1	27.58	269.41	1.216	3.925
135000	621.30	351.15	9.3130 -6	4.921 -9	1.083 +17	619.9	4.353 +1	1.560 +1	27.37	269.41	1.216	3.925
140000	714.22	411.07	7.4101	3.391	7.516 +16	715.7	3.317	2.218	27.20	269.41	1.216	3.925
145000	803.74	530.59	6.0540	2.451	5.450	793.2	2.562	3.095	27.05	269.41	1.216	3.925
150000	892.79	619.61	5.0617	1.836	4.107	810.0	2.077	4.114	26.92	269.41	1.216	3.925
155000	957.91	681.79	4.2992	1.416	3.251	870.1	1.674	5.197	26.79	269.41	1.216	3.925

(Continued)

Properties of the U. S. Standard Atmosphere, 1962, condensed from the complete tabular data. Numbers following the plus or minus sign are the power of ten by which that entry and each following entry should be multiplied. (Continued)

Geometric Altitude (m)	Temperature		Pressure (mb)	Density (kg m <sup>-3</sup> )	Particle Speed (m sec <sup>-1</sup> )	Collision Frequency (sec <sup>-1</sup> )	Mean Free Path (m)	Molecular Weight	Sound Speed (m sec <sup>-1</sup> )	Coefficient of Viscosity (kg m <sup>-1</sup> sec <sup>-1</sup> )	Kinematic Viscosity (m <sup>2</sup> sec <sup>-1</sup> )	Thermal Conductivity (K cal m <sup>-1</sup> sec <sup>-1</sup> )		
	(°K)	(°C)												
160000	1022.23	749.08	3.6913	-6	1.159	-9	2.618	+16	901.0	1.396	-1	6.353	-11	26.66
165000	1062.74	789.59	3.2019	-10	9.611	-10	2.102		924.1	1.190		7.711		26.52
170000	1105.51	832.56	2.7926		8.036		1.640		910.7	1.019		9.211		26.35
175000	1150.97	857.82	2.4377		6.815		1.548		953.2	0.851	-1.0	1.070	+2	26.30
180000	1156.12	882.97	2.1536		5.838		1.419		967.5	7.722		1.332		26.15
185000	1180.97	907.82	1.9018	-6	5.036	-10	1.166	+16	980.7	6.771	-1.0	1.410	+2	26.00
190000	1205.50	932.35	1.6852		4.317		1.013		993.6	5.955		1.648		25.85
195000	1220.81	947.69	1.4976		3.792		0.866	+15	1002.8	5.274		1.901		25.70
200000	1235.95	962.80	1.3319		3.318		7.818		1011.8	4.682		2.161		25.56
210000	1265.49	992.31	1.0652	-6	2.550	-10	6.097	+15	1029.8	3.716	-1.0	2.771	+2	25.27
220000	1291.09								1017.3	2.976		3.519		21.90
230000	1321.70	1018.55	6.9601		1.564		3.815		1061.7	2.304		4.429		21.69
240000	1359.90	1046.75	5.6857		1.215		3.071		1078.3	1.962		5.196		21.40
250000	1357.28	1081.13	4.6706	-11	9.978	-11	2.493		1091.8	1.641		6.778		21.11
260000	1373.81	1108.69	3.8573	-7	8.013	-11	2.031	+15	1105.1	1.330	-1.0	8.307	+2	21.82
270000	1389.59	1116.41	3.2019		6.521		1.669		1118.2	1.105		1.012	+3	23.53
280000	1401.51	1131.39	2.6708		5.315		1.377		1131.2	9.223	-1	1.227		23.24
290000	1418.70	1145.55	2.2401		4.351		1.143		1144.1	7.738		1.178		22.95
300000	1432.11	1158.96	1.8838		3.585		9.528	+14	1156.8	6.521		1.773		22.66
310000	1439.40	1166.25	1.5919	-7	2.976	-11	8.031	+14	1167.2	5.531	-1	2.109	+3	22.37
320000	1446.15	1173.00	1.3498		2.479		6.761		1177.5	4.712		2.499		22.08
330000	1452.11	1179.26	1.1184		2.073		5.727		1187.7	4.026		2.950		21.80
340000	1458.23	1185.08	9.8011	-8	1.740		4.869		1197.8	3.452		3.470		21.52
350000	1463.67	1190.52	8.3915		1.465		4.154		1207.8	2.969		4.048		21.24
360000	1468.79	1195.61	7.2061	-8	1.237	-11	3.554	+14	1217.7	2.562	-1	4.751	+3	20.97
370000	1473.66	1200.51	6.2061		1.019		3.051		1227.6	2.217		5.538		20.70
380000	1478.33	1205.18	5.3599		8.914	-12	2.636		1237.4	1.921		6.433		20.41
390000	1482.88	1209.73	4.6117		7.489		2.267		1247.1	1.673		7.151		20.19
400000	1487.38	1214.23	4.0301		6.498		1.963		1256.7	1.468		8.607		19.91
410000	1487.12	1213.97	3.5077	-8	5.588	-12	1.709	+14	1261.3	1.279	-1	9.808	+3	19.70
420000	1487.05	1213.90	3.0391		4.816		1.490		1271.8	1.122		1.131	+3	19.37
430000	1487.22	1214.07	2.6731		4.164		1.302		1279.2	9.858	-2	1.298		19.21
440000	1487.70	1214.55	2.3105		3.480		1.110		1286.6	8.678		1.303		19.03
450000	1488.52	1215.37	2.0511		3.122		9.991	+13	1291.0	7.652		1.691		18.82
460000	1489.73	1216.58	1.8013	-8	2.713	-12	8.773	+13	1301.3	6.758	-2	1.926	+4	18.63
470000	1491.38	1218.23	1.5886		2.362		7.716		1308.6	5.976		2.190		18.44
480000	1493.49	1220.31	1.4012		2.061		6.796		1315.8	5.293		2.486		18.26
490000	1496.10	1222.95	1.2300		1.801		5.991		1323.0	4.691		2.819		18.10
500000	1499.22	1226.07	1.0957		1.577		5.291		1330.2	4.168		3.191		17.91

(Continued)